E-ISSN 2228-8082
Volume 78, Number 2, February 2026

PMAC
PRINCE MAHIDOL AWARD CONFERENCE 2026

SMJ

Siriraj Medical Journal

The world-leading biomedical science of Thailand

MONTHLY

ORIGINAL ARTICLE REVIEW ARTICLE

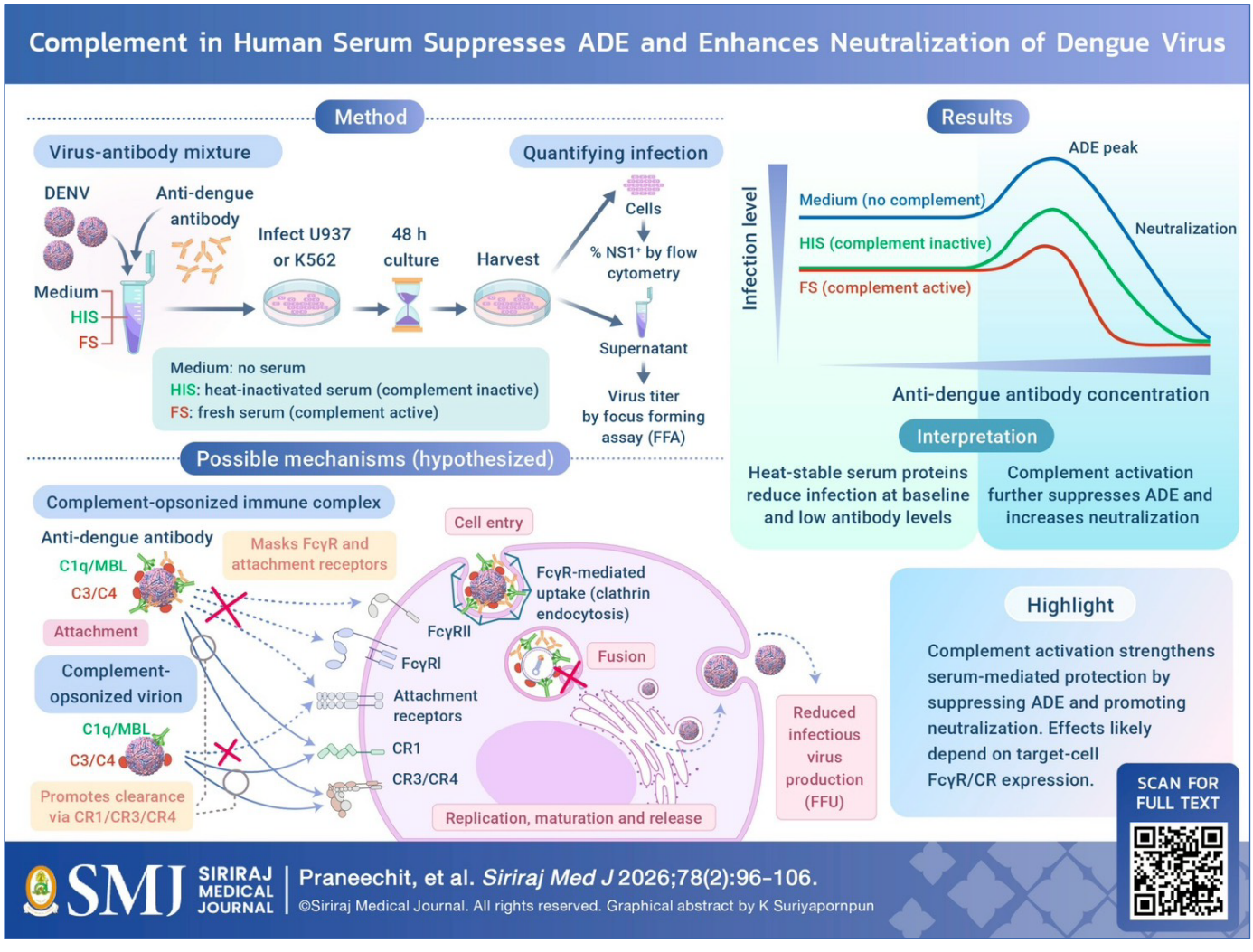

Indexed by

Scopus® DOAJ EBSCO

https://he02.tci-thaijo.org/index.php/sirirajmedj/index
E-mail: sijournal92@gmail.com

SMJ
Siriraj Medical Journal
The world-leading biomedical science of Thailand
Volume 78 Number 2
February 2026

ORIGINAL ARTICLE

REVIEW ARTICLE

SIRIRAJ MEDICAL JOURNAL

https://he02.tci-thaijo.org/index.php/sirirajmedj/index

Office: His Majesty the King's 80th Birthday Anniversary 5th December 2007 Building (SIMR), 2nd Fl., Room No.207
Faculty of Medicine Siriraj Hospital, Mahidol University, Bangkok 10700, Thailand
E-mail: sijournal92@gmail.com

Development and Evaluation of a Patient Education Booklet on Fall Prevention Exercises for Older Lower Limb Prosthesis Users

Prawina Sakulkosol, M.Sc.[1], Pieter U Dijkstra, Ph.D.[1], Kazuhiko Sasaki, Ph.D.[1], Gary Guerra, Ph.D.[2], Jutamanee Poonsiri, Ph.D.[1,*]

[1]Sirindhorn School of Prosthetics and Orthotics, Faculty of Medicine Siriraj Hospital, Mahidol University, Bangkok, Thailand, [2]Department of Exercise and Sport Science, St. Mary's University, San Antonio, Texas, USA.

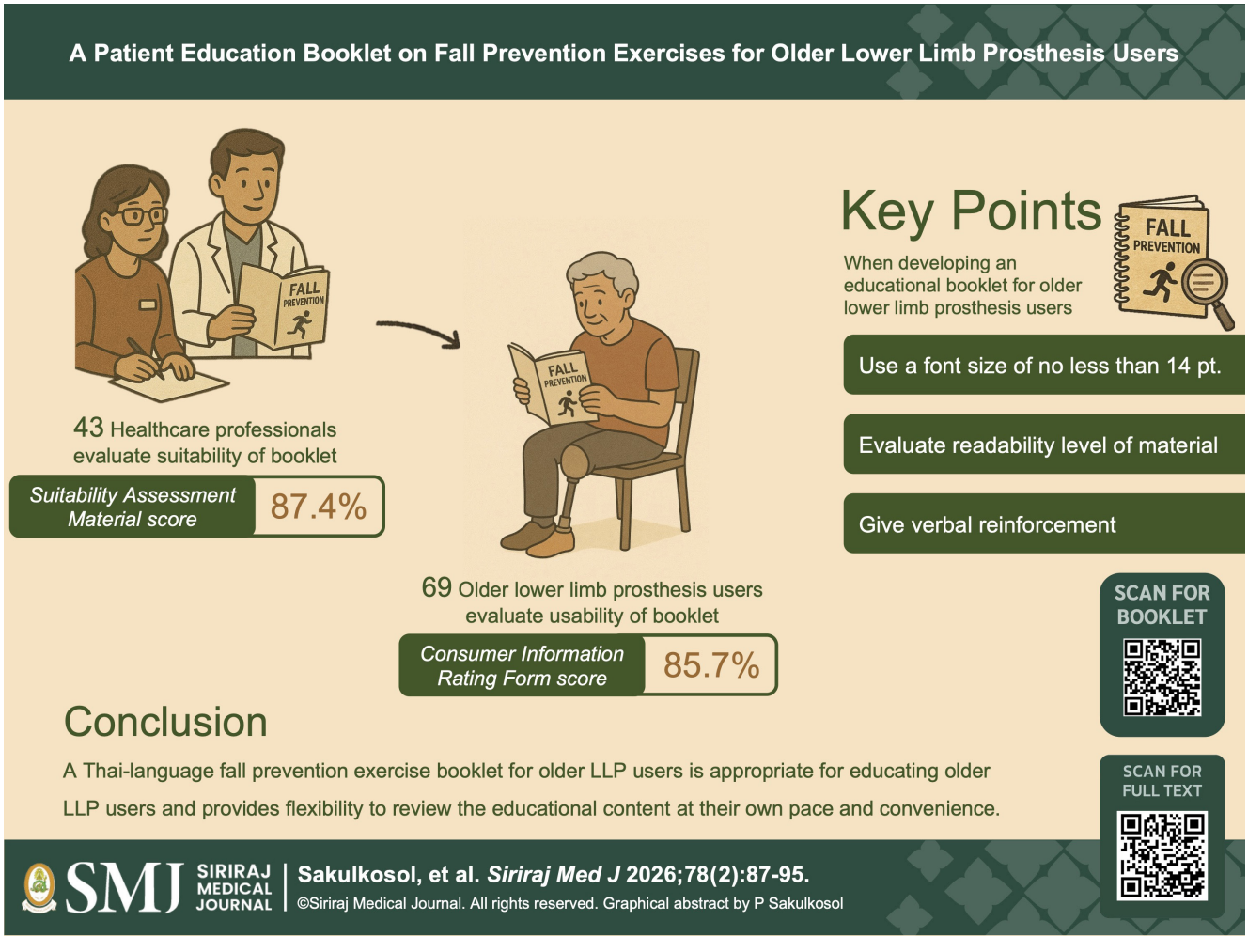

**Corresponding author: Jutamanee Poonsiri*
E-mail: jutamanee.poo@mahidol.ac.th
Received 14 October 2025 Revised 17 November 2025 Accepted 18 November 2025
ORCID ID:http://orcid.org/0000-0002-4957-0990
https://doi.org/10.33192/smj.v78i2.277785

ABSTRACT

Objective: To assess the suitability and usability of a patient education booklet on fall prevention exercises for older lower limb prosthesis (LLP) users.

Materials and Methods: A descriptive study was conducted from February 2024 to March 2025. A fall prevention exercise booklet was developed based on literature and clinical guidelines. The booklet covered the following domains: falls and fall prevention in older adults, benefits of exercises, exercise principles and precautions, and exercise descriptions. Healthcare professionals who care for LLP users assessed the educational booklet's suitability using the Suitability Assessment of Material (SAM) tool. Based on their feedback, the font size was increased from 12 to 14 points. Thereafter, older LLP users (over 60) assessed the educational booklet's usability using the Consumer Information Rating Form (CIRF).

Results: Suitability was assessed by 43 evaluators (30 prosthetists, six physical therapists, four nurses and three rehabilitation physicians). The median (IQR) SAM score was 88.1 (81.0; 95.2). Usability was assessed by 69 participants. The median (IQR) CIRF score was 86.9 (80.8; 90.9).

Conclusion: The results of the suitability and usability assessments indicate that the developed fall prevention exercise booklet is appropriate for educating older LLP users. The booklet provides a practical tool that enables LLP users to perform exercises safely at home and review educational content at their own pace.

Keywords: Fall prevention education; fall prevention exercise; older adult; amputee; prosthesis (Siriraj Med J 2026;78(2):87-95)

INTRODUCTION

The majority of falls among older adults result from a combination of age-related and disease-related factors, along with their interaction with the social and physical environment.[1] In 2003, about 20% of older adults living in urban areas of Thailand experienced a fall.[2] Falls are the most common cause of injury[3] among older adults and the sixth leading cause of death in this population.[4] Falls are also common among adults with lower limb amputation (LLA).[5] More than half of community-dwelling adults with an LLA experience at least one fall a year, and about one-third have multiple falls after completing rehabilitation.[6] Of these falls, 40-60% result in injuries such as fractures,[7] brain injury,[8] or stump injury,[9] often requiring a hospital stay. Approximately 13% of individuals with transfemoral amputation have fallen while wearing a prosthesis and required hospitalization.[10] The average six-month direct medical cost of fall-related hospitalization in individuals with transfemoral amputation is estimated at US$25,652, while emergency department visits cost about US$18,091.[10]

Fall prevention training has been shown to reduce falls and improve balance confidence in adults with an LLA.[11] Most previous studies on fall prevention education for people with LLA have adopted programs designed for older adults.[12] However, no studies to date have confirmed the effectiveness of these programs in reducing fall risk among older lower limb prosthesis (LLP) users.

In general, written materials are preferred when developing health educational material[13], as they can be reread when needed, which is especially useful for older adults who may experience cognitive difficulties. Older adults favor written materials that begin with a concise summary of relevant risk information, which helps capture attention and allows them to focus on information that is of priority.[14] Furthermore, older adults prefer materials specifically tailored to their needs.[14]

The personalized OTAGO exercise program has been shown to decrease fall rates from 80% to 27% among older patients at a Geriatric Rehabilitation Clinic.[15] The OTAGO exercise booklet tailored for older LLP users, a population at heightened risk of falls, may improve engagement, safety, and overall program effectiveness. Before using the booklet in patient education, it is important to validate the written content to ensure alignment with the intended educational objectives[16] and to confirm that the booklet is understandable to most individuals. Therefore, the objective of this study was to assess the suitability and usability of a patient education booklet on fall prevention exercises specifically developed for older LLP users.

MATERIALS AND METHODS

This descriptive study was approved by the Institutional Review Board of the Faculty of Medicine Siriraj Hospital, Mahidol University (COA no. Si 076/2024).

Booklet development

Based on the WHO Falls Prevention Model for Active Ageing, fall prevention material was developed for LLP users.[17] The model consists of three steps: increasing awareness through education, building capability through assessment, and providing training.[17] In this study, we focused on two components: increasing awareness and training.

Information on the importance of fall prevention was taken from posters developed by the Department of Disease Control, Ministry of Public Health, Thailand.[18] The exercise component was based on the OTAGO exercise program, which has been shown to have a positive effect on reducing fall rates among older adults over a period of one year (incidence rate ratio = 0.68, 95% CI: 0.56; 0.79).[19] The developed booklet includes 16 exercises — five strength and 11 balance exercises. The exercises were translated by researchers from English to Thai. An English linguist verified the accuracy of the translation, while a Thai linguist evaluated readability and comprehension. Based on their feedback, the Thai text was refined for clarity and accessibility. Illustrations were adapted to depict an older LLP user as the model. The final booklet was printed in color, using a standard A5 format (14.8 x 21.0 cm). (See additional material).

Suitability assessment

Participants

Healthcare professionals assessed the suitability of the booklet. They were included if they were a prosthetist, physical therapist, rehabilitation nurse, rehabilitation physician or geriatric medicine physician and had published work related to LLP care, elderly care, falls, or fall prevention.

Data were collected from February to July 2024. Healthcare professionals were recruited using the snowball sampling technique, starting with a small number of initial contacts who met the inclusion criteria.[20] The researcher first contacted the head officers of each involved profession at the Faculty of Medicine Siriraj Hospital to suggest professionals who met inclusion criteria. These professionals subsequently referred additional potential participants.[20] The researchers mailed hard copies of participant information sheet, consent form, booklet, Suitability Assessment of Materials (SAM), and forms to suggest other potential participants to the professionals. The booklet was provided to participants in hard copy so the participants could examine the book's size, color, and quality. Healthcare professionals who agreed to participate in the study provided written informed consent, evaluated the booklet, and sent it back to the researcher. Based on a previous study, it was estimated that a sample of 45 professionals would be adequate for assessing suitability.[21]

Measures

The fall prevention exercise booklet was assessed using the SAM tool. SAM consists of 22 items categorized into six domains: content, literacy demand, graphics, layout and typography, learning stimulation and motivation, and cultural appropriateness.[22] The item related to interaction was excluded as it was not applicable to exercise materials for older LLP users. Each item was rated, 0 indicating unsuitable, 1 indicating adequate, and 2 indicating superior suitability.[22] The overall suitability score was calculated as a percentage of the maximum score; (Sum of the item ratings/ 21*2) * 100. For cases with missing data, the formula was (Sum of the valid item ratings/ $n_{\text{valid answers}}$*2) * 100. Scores of 70–100% indicated superior materials, 40–69% adequate material, and 0–39% unsuitable material.[22]

Before conducting the usability assessment among older LLP users, minor revisions were made based on the professionals' feedback, including increasing the font size from 12 to 14.

Usability assessment

Participants

Older LLP users evaluated the usability of the booklet. Inclusion criteria were: age of at least 60 years, use of a prosthesis for more than one year, ability to walk every day with a prosthesis either with or without a gait aid for at least eight hours a day[23] without pain, and ability to speak and read Thai. Exclusion criteria included: cognitive impairment or a history of severe depression or other mental disorders. Cognitive impairment was screened using the Montreal Cognitive Assessment (MoCA); participants scoring below 26 were excluded.[24]

Data were collected from November 2024 to March 2025. Potential participants contacted the researcher after viewing invitation posters at the Sirindhorn School of Prosthetics and Orthotics. The researcher provided an information sheet and explained the study's purpose and procedures to the participants. Participants who agreed to participate in the study provided written informed consent. Convenience sampling was applied. The sample size was calculated with nQuery Advisor software using the formula for confidence intervals for proportions with normal approximation, assuming an expected proportion of 80% and standard error of 8%. With power set at 80% and the significance level at 0.05, the required sample size was 62 participants. Allowing for a 10% dropout rate, the target sample size was 69 LLP users.

Measures

Participant characteristics were recorded, including age, gender, underlying diseases, medication use, cause and level of amputation, and level of education. After that, participants read the fall prevention exercise booklet and assessed its usability using the Consumer Information Rating Form (CIRF). The CIRF was developed and validated to assess written medication information (WMI).[25] The Thai version of the CIRF used in this study demonstrated acceptable construct validity through principal component analysis, known-group validity, and internal consistency (Cronbach's alpha = 0.904).[26] The Thai CIRF includes four domains: comprehensibility, future use, utility, and design quality. The five comprehensibility items, rated on a 5-point Likert scale (1: very hard, to 5: very easy), assess how easy it is to read, understand, seek information, remember, and retain for future reference. The three future use items, also rated on a 5-point Likert scale (1: very unlikely to 5: very likely), assess future use of the information received. To assess the perceived usefulness and quantity of the WMI, six utility items, rated on a 3-point Likert scale (1: = not so useful to 3: very useful) and one additional question assessing the adequacy of the information quantity (0: too little or too much information, 1: right amount of information), were used. The seven design quality items, rated on a 5-point Likert scale (1: low quality, 5: high quality), assess opinions regarding the information's design, layout, and tone. The overall score was calculated as a percentage of the maximum score. A score of 80% or more indicated acceptable usability for patients.[27]

Data analysis

Descriptive statistics were used to summarize participant characteristics and the suitability and usability scores of the developed booklet. As the SAM and CIRF results were not normally distributed, the median and interquartile range (IQR) were reported. For comparison with studies reporting mean values, mean scores were also presented in the discussion section.

RESULTS

Suitability assessment of materials

A total of 43 healthcares participated in the study, including 30 prosthetists, six physical therapists, four nurses and three rehabilitation physicians. The median (IQR) SAM score was 88.1 (81.0; 95.2). Overall, 93% of professionals (40 of 43) gave an overall suitability score of 70% or higher.

Frequencies of item scores for each SAM domain are presented in Fig 1. More than half of the healthcare professionals rated most items as "superior", with the exception of the Reading level item (superior; 40%, adequate; 37%, unsuitable; 16%, missing; 7%). Nine percent of evaluators did not rate the Typography item (superior; 84%, adequate; 7%, missing; 9%).

Usability assessment of material

In total, 69 older LLP users (median (IQR) 65 (62; 70) years, 63 males) participated (Fig 2 and Table 1).

The median (IQR) CIRF score was 86.9 (80.8; 90.9). In total, 77% of older LLP users (53 of 69) gave an overall usability score of 80% or higher. Frequencies of item scores for each domain are presented in Fig 3.

Within the Comprehensibility domain, more than half of the participants rated three of the five items as "very easy" (Read, Understand and Keep for future use). However, the Remember and Locate information items received lower ratings: 46% of participants rated the Remember item as "very hard and pretty hard" and 41% rated the Locate information item as "very hard and pretty hard."

Within the Future use, the Data quantity and the Design quality domain, more than half of the participants rated all items as "very likely", "right amount", and "very high", respectively.

In the Data utility domain, over half of the participants rated four of the six items (Storage, Precautions, Directions, and Benefits) as "very useful". Adverse effects and the Contraindications items were rated "not so useful." by 14% and 12% of participants, respectively.

DISCUSSION

This study evaluated the suitability and usability of a fall prevention exercise booklet for older LLP users. The findings support its use in clinical settings, with over 90% of healthcare professionals rating the booklet's suitability at 70% or higher. The mean SAM scores across the six domains was 87.4%, which is comparable to the 86.8% SAM score reported in a Spanish study evaluating an educational booklet promoting healthy lifestyles in sedentary adults with cardiometabolic risk factors. [28]

More than half of the healthcare professionals rated most SAM items as "superior", except for the Reading level item. A possible explanation is the lack of standardized tools to assess reading grade levels in Thai. While such tools are well-established for English, they may not be directly applicable to Thai, a syllabic-alphabetic language.[29] Unlike English, Thai lacks word segmentation, capital letters, sentence endings or explicit word boundary delimiters.[30] The meaning of a Thai word can vary depending on the context, functioning as a full sentence

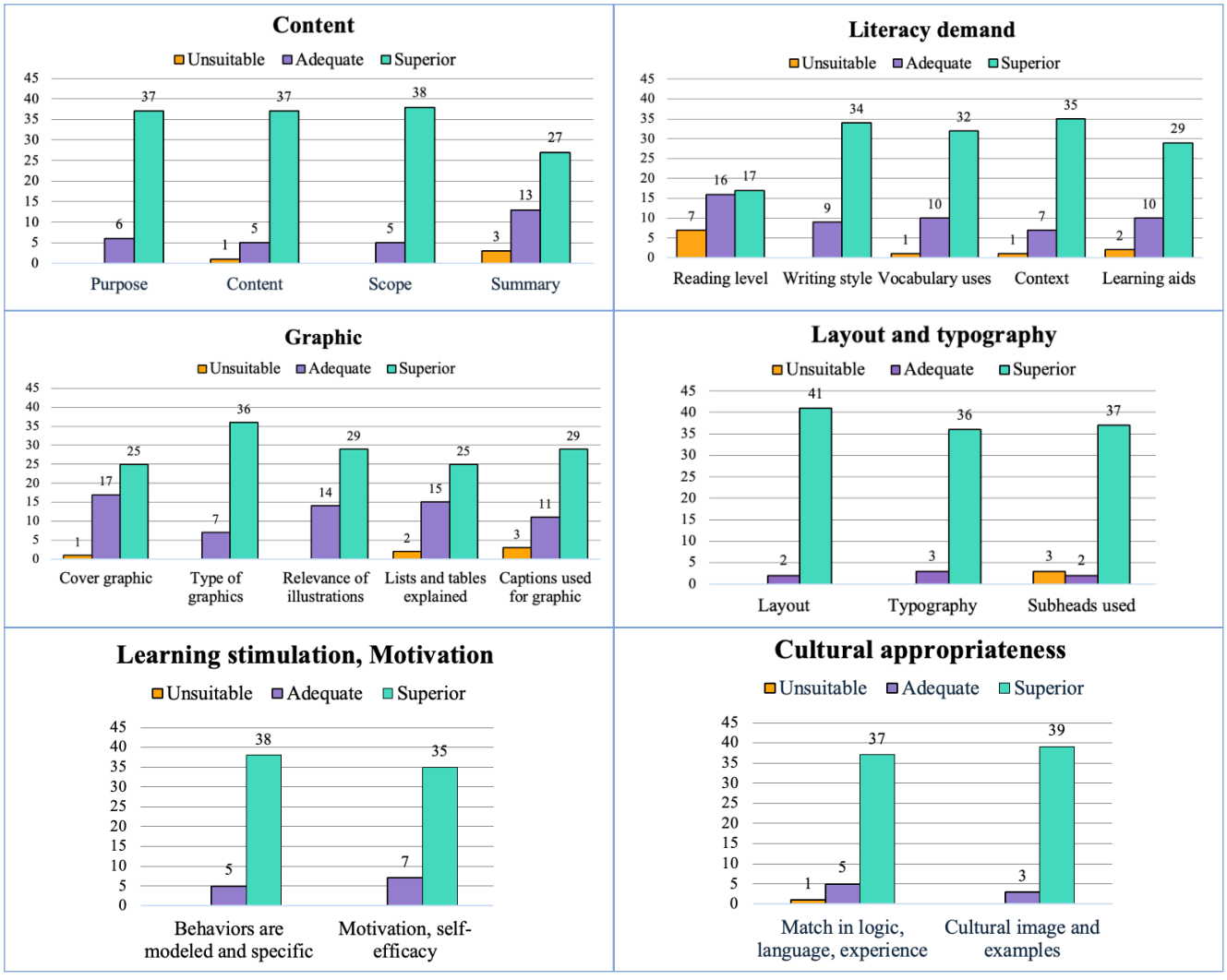

Fig 1. Frequencies of item scores across each domain of the Suitability Assessment of Materials tool (n=43).

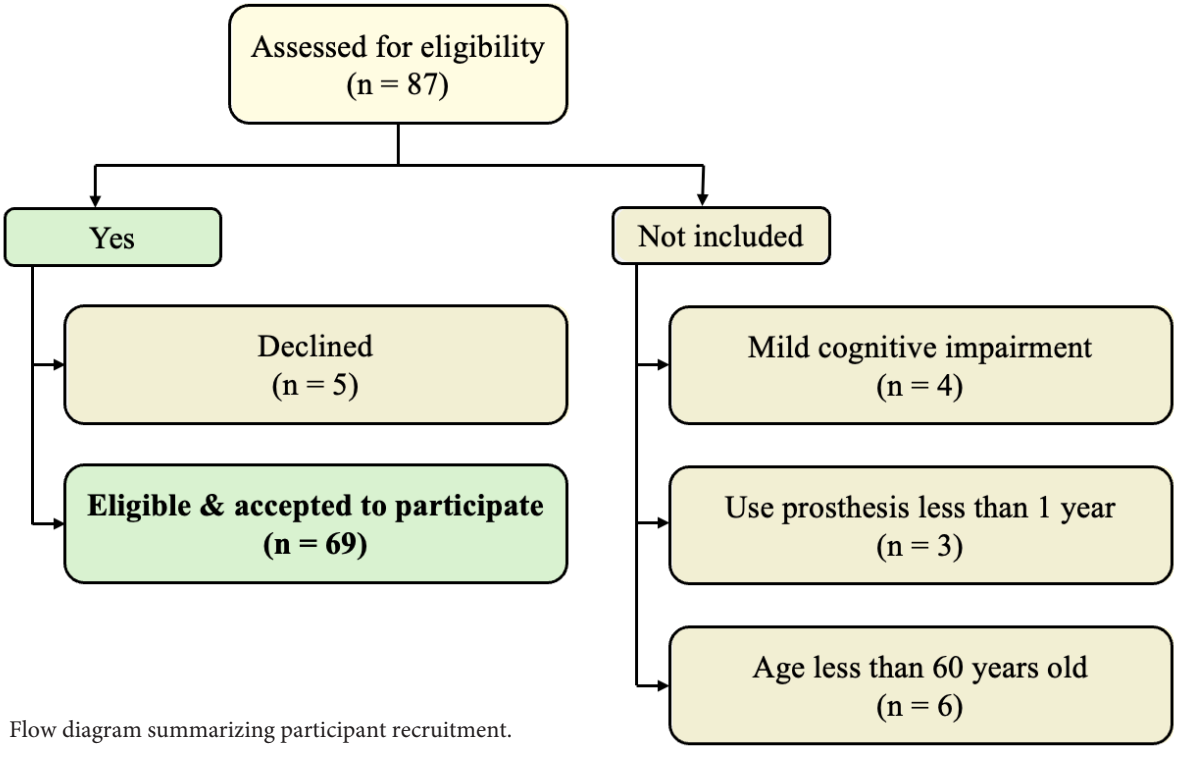

Fig 2. Flow diagram summarizing participant recruitment.

TABLE 1. Participant characteristics in the usability assessment (n=69).

Characteristic	Median	IQR
Age (years)	65	62; 70
n	%	
Gender		
Male	63	91%
Level of amputation		
TF	16	23%
KD	3	4%
TT	48	70%
AD	2	3%
Cause of amputation*		
Accident	62	90%
Diabetes	3	4%
Tumor	2	3%
Congenital	1	1%
Snake bite	1	1%
Education		
Primary	36	52%
Secondary	18	26%
College	4	6%
Bachelor	9	13%
Master	2	3%

* The sum of percentages isn't equal to 100 because of rounding.

Abbreviations: IQR = interquartile range, TF = transfemoral, KD = knee disarticulation, TT = transtibial, AD = ankle disarticulation

or compound noun.[30] Developing suitable educational material for individuals with lower limb amputation is particularly challenging since 44% reportedly did not complete high school.[31] In our study 52% of participants had completed only primary education. Healthcare professionals must therefore recognize the importance of tailoring education material to the reading ability of users with low health literacy to enhance comprehension and health outcomes.[32] Another possible explanation for the lower scores on the Reading level item is that many healthcare professionals who treat LLP users may not have specific training in educational material design or in assessing the readability of texts. Moreover, the SAM criteria may not align well with the structure of the Thai education system, which consists of pre-primary (ages 3-5), primary (6 years), lower secondary (3 years), and upper secondary (3 years) levels.

Similarly, 9% of evaluators did not rate the Typography item (superior; 84%, adequate; 7%, missing; 9%). The SAM criteria for typography, such as "no all caps for long headers or running text" and "uppercase and lowercase serif or sans serif" do not apply directly to Thai script. A study from Saudi Arabia evaluating health education brochures reported similar issues when using the SAM.[33]

Initially, we printed the developed booklet using a 12-point font size, following design guidelines for written patient education materials.[34] However, one-third of the suitability evaluators provided open-ended feedback, suggesting that font size was too small. In response, we increased the font size to 14 points, consistent with recommendations from a recent scoping review advising that patient education materials use a minimum font size of 14 points.[14]

In this study, the target population of older LLP

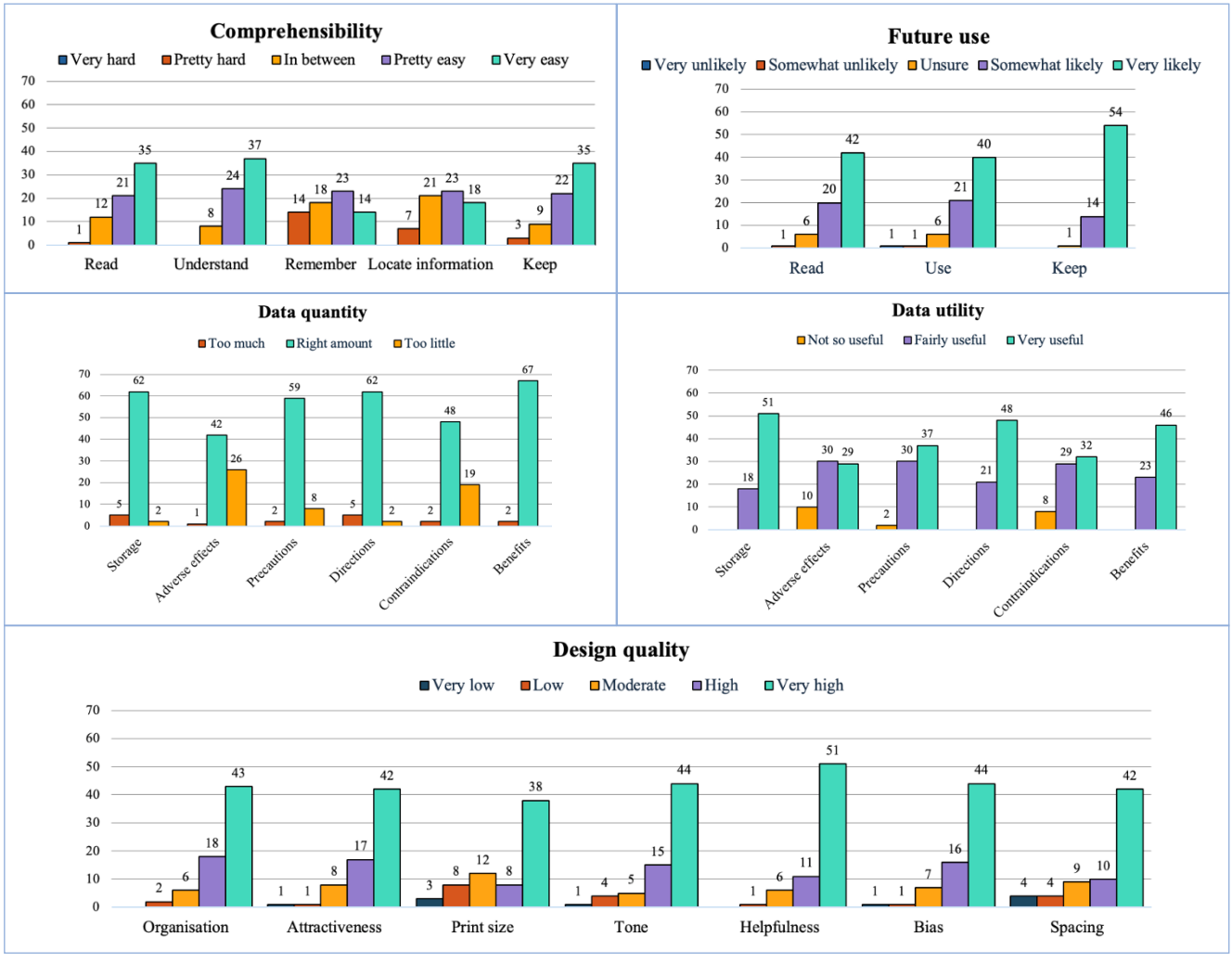

Fig 3. Frequencies of item scores across each domain of the Consumer Information Rating Form.

users evaluated the usability of the developed booklet, allowing for authentic feedback from actual end users regarding its clarity and usefulness. Overall, 77% of older LLP users rated the booklet with a usability score of 80% or higher, indicating that it is suitable for use among older LLP users. The mean CIRF scores across the four domains was 85.7%, which closely aligns with findings from a previous study assessing a pictographic action plan for individuals with low literacy and adrenal insufficiency (85.2%).[35]

In the Comprehensibility domain, more than half of the participants rated the booklet as "very easy" to read and understand, and they would keep it for future use. But about 65% reported difficulty locating specific information and 74% reported difficulty remembering information. These difficulties likely reflect characteristics of the study sample. More than half of the participants had only primary-level education, which may affect their ability to navigate written materials and retain new information. Additionally, many participants were not accustomed to receiving written instructions for home exercises, which could contribute to challenges in retrieving information. Cognitive decline and lower education levels have been associated with reduced recall[36,37] and information-seeking ability among older adults.[38] Therefore, a prior study recommended that healthcare professionals should review the booklet together with patients and provide verbal reinforcement when introducing the exercise.[21] Structured follow-up sessions may further support older LLP users who experience difficulty remembering instructions over time.

In the data quantity domain, older LLP users rated the adverse effects and contraindications items as providing "too little" information. These ratings may affect the overall rating of the utility domain. When older LLP users experience that little information was available, they may rate these items as "not so useful".

The findings underscore the importance of tailored educational materials for older LLP users, a population at particularly high risk for falls. The developed

booklet demonstrates promise as a practical tool for promoting fall prevention when used alongside clinical guidance. Additionally, the strong alignment between professional and older LLP users' usability evaluations supports its broader implementation in rehabilitation care settings.

Some limitations of this study must be noted. Although the study aimed to include five different categories of healthcare professionals, only four were ultimately represented. The absence of a geriatric physician is unlikely to have substantially influenced the suitability assessments much because the included rehabilitation physicians had extensive experience in caring for older LLP users. The booklet was designed specifically for older LLP users, with an age cut-off of 60 years, consistent with the definition of older adults by the Thai Ministry of Social Development and Human Security.[39] However, definitions of elderly individuals vary across contexts and may reflect chronological age, or declines in social roles, and or decline in functional capacities.[40] Given the heterogeneous nature of aging, where the degree and onset of age-related decline varies among individuals, our chosen age threshold may limit the generalizability of findings to the broader population of older LLP users. Furthermore, most participants were male with a transtibial amputation with a traumatic cause, which is consistent with findings from previous studies conducted in Thailand.[41] Therefore, while the sample may not be representative for the global population of LLP users it is representative for lower limb amputees in Thailand.[42]

Future research should assess the memory retention and comprehension of the educational content after they have read the fall prevention educational booklet to make sure the content is understandable and memorable. In addition, future research should evaluate the effectiveness of the fall prevention educational booklet in reducing fall incidence among older LLP users in real-world settings.

CONCLUSION

This study developed and evaluated the suitability and usability of a Thai-language fall prevention exercise booklet for older LLP users. The booklet is appropriate for educating older LLP users and provides flexibility to review the educational content at their own pace and convenience.

Data availability statement

Data supporting the findings of this study are available in the supplementary material. Additional details can be obtained from the first author upon request.

ACKNOWLEDGEMENTS

The authors would like to thank the evaluators and participants for their valuable contributions to this study. Additionally, the authors express their gratitude to undergraduate students Ekarin Fuengniem, Jutharat Khamjeak, and Thitphichaphon Wanthanaphithak for their assistance in collecting pilot data for the suitability assessment.

DECLARATIONS

Grants and Funding Information

This research was supported by the Faculty of Medicine Siriraj Hospital, Mahidol University, Grant number (IO) R016731031.

Conflict of Interest

The authors declare no conflicts of interest.

Author Contributions

Conceptualization and methodology, P.S., P.U.D., K.S., G.G., and J.P. ; Investigation, P.S. and J.P. ; Formal analysis, P.S. and J.P. ; Visualization, P.S. ; Writing – original draft, P.S., P.U.D., and J.P. ; Writing – review and editing, P.S., P.U.D., K.S., G.G., and J.P. ; Funding acquisition, P.S. and J.P. ; Supervision, P.U.D., K.S., G.G., and J.P. All authors have read and agreed to the final version of the manuscript.

Use of Artificial Intelligence

The authors declare no use of artificial intelligence.

REFERENCES

1. Rubenstein LZ. Falls in older people: epidemiology, risk factors and strategies for prevention. Age Ageing. 2006;35(Suppl_2):ii37–ii41.
2. Assantachai P, Praditsuwan R, Chatthanawaree W, Pisalsarakij D, Thamlikitkul V. Risk factors for falls in the Thai elderly in an urban community. J Med Assoc Thai. 2003;86(2):124–30.
3. World Health Organization. Ageing And Life Course Unit, Université De Genève. Centre Interfacultaire De Gérontologie. A global response to elder abuse and neglect: building primary health care capacity to deal with the problem worldwide. Geneva: World Health Organization; 2008.
4. Zalewski CK. Aging of the human vestibular system. Semin Hear 2015;36(3):175–96.
5. Hunter SW, Batchelor F, Hill KD, Hill A-M, Mackintosh S, Payne M. Risk factors for falls in people with a lower limb amputation: a systematic review. PM R. 2017;9(2):170–80. e1.
6. Miller WC, Speechley M, Deathe B. The prevalence and risk factors of falling and fear of falling among lower extremity amputees. Arch Phys Med Rehabil. 2001;82(8):1031–7.
7. Lewallen R, Johnson Jr E. Fractures in amputation stumps: review of treatment of 16 fractures. Mayo Clin Proc. 1981;56(1):22-6.

8. Kulkarni J, Wright S, Toole C, Morris J, Hirons R. Falls in patients with lower limb amputations: prevalence and contributing factors. Physiotherapy. 1996;82(2):130–6.
9. Behar T, Burnham S, Johnson Jr G. Major stump trauma following below-knee amputation. Outcome and recommendations for therapy. J Cardiovasc Surg (Torino). 1991;32(6):753–6.
10. Mundell B, Maradit Kremers H, Visscher S, Hoppe K, Kaufman K. Direct medical costs of accidental falls for adults with transfemoral amputations. Prosthet Orthot Int. 2017;41(6):564–70.
11. Kaufman KR, Miller EJ, Deml CM, Sheehan RC, Grabiner MD, Wyatt M, et al. Fall prevention training for service members with an amputation or limb salvage following lower extremity trauma. Mil Med. 2024;189(5-6):980–7.
12. Clemens S, Doerger C, Lee S-P. Current and emerging trends in the management of fall risk in people with lower limb amputation. Curr Geriatr Rep. 2020;9(3):134–41.
13. Smith JA, Kindo CC, Kurian S, Whitaker LM, Burke C, Wachel B, et al. Evaluation of patient chemotherapy education in a gynecology oncology center. Support Care Cancer. 2004;12(8): 577–83.
14. Goodman C, Lambert K. Scoping review of the preferences of older adults for patient education materials. Patient Educ Couns. 2023;108:107591.
15. Dajpratham P, Thitisakulchai P, Pongratanakul R, Prapavanond R, Haridravedh S, Muangpaisan W. Effectiveness of personalized multifactorial fall risk assessment and intervention in reducing fall rates among older adults: a retrospective study. Siriraj Med J. 2025;77(1):64–72.
16. Pantera E, Pourtier-Piotte C, Bensoussan L, Coudeyre E. Patient education after amputation: systematic review and experts' opinions. Ann Phys Rehabil Med. 2014;57(3):143–58.
17. World Health Organization. WHO global report on falls prevention in older age. Geneva: World Health Organization; 2007.
18. Division of noncommunicable diseases [Internet]. Nonthaburi: The division; 2021. Fall prevention for the elderly; [cited 2025 July 1]; [about 2 screens]. Available from: http://ftp.thaincd.com/2016/media.php?gid=1-015-009
19. Thomas S, Mackintosh S, Halbert J. Does the 'Otago exercise programme'reduce mortality and falls in older adults? a systematic review and meta-analysis. Age Ageing. 2010;39(6):681–7.
20. Parker C, Scott S, Geddes A. Snowball sampling. SAGE research methods foundations. 2019.
21. Ximenes MAM, Fontenele NÂO, Bastos IB, Macêdo TS, Galindo NM, Caetano JÁ, et al. Construction and validation of educational booklet content for fall prevention in hospitals. Acta Paul Enferm. 2019;32:433–41.
22. Doak C, Doak L, Root J, editors. Assessing suitability of materials. Teaching patients with low literacy skills. Philadelphia: Lippincott; 1996:41–60. Available form: https://catalog.nlm.nih.gov/discovery/fulldisplay/alma995897153406676/01NLM_INST:01NLM_INST
23. Klute GK, Berge JS, Orendurff MS, Williams RM, Czerniecki JM. Prosthetic intervention effects on activity of lower-extremity amputees. Arch Phys Med Rehabil. 2006;87(5):717–22.
24. Nasreddine ZS, Phillips NA, Bédirian V, Charbonneau S, Whitehead V, Collin I, et al. The Montreal Cognitive Assessment, MoCA: a brief screening tool for mild cognitive impairment. J Am Geriatr Soc. 2005;53(4):695–9.
25. Krass I, Svarstad BL, Bultman D. Using alternative methodologies for evaluating patient medication leaflets. Patient Educ Couns. 2002;47(1):29–35.
26. Wongtaweepkij K, Krska J, Pongwecharak J, Pongpunna S, Jarernsiripornkul N. Development and psychometric validation for evaluating written medicine information in Thailand: the consumer information rating form. BMJ Open. 2021;11(10):e053740.
27. Reeves PT, Kenny TM, Mulreany LT, McCown MY, Jacknewitz-Woolard JE, Rogers PL, et al. Development and assessment of a low literacy, pictographic asthma action plan with clinical automation to enhance guideline-concordant care for children with asthma. J Asthma. 2023;60(4):655–72.
28. Espigares-Tribo G, Ensenyat A. Assessing an educational booklet for promotion of healthy lifestyles in sedentary adults with cardiometabolic risk factors. Patient Educ Couns. 2021;104(1):201–6.
29. Tongtep N, Coenen F, Theeramunkong T. Content-based readability assessment: a study using a syllabic alphabetic language (Thai). In: Pham DN, Park SB, editors. Artificial Intelligence. PRICAI 2014: Proceeding of the 13th Pacific Rim International Conference on Artificial Intelligence; 2014 Dec 1-5; Gold Coast, Australia. Switzerland: Springer; 2014. p. 863–70.
30. Chen Y-H, Daowadung P. Assessing readability of Thai text using support vector machines. Maejo Int J Sci Technol. 2015;9(3):355–69.
31. Corey MR, Julien JS, Miller C, Fisher B, Cederstrand SL, Nylander WA, et al. Patient education level affects functionality and long term mortality after major lower extremity amputation. Am J Surg. 2012;204(5):626–30.
32. Sudore RL, Schillinger D. Interventions to improve care for patients with limited health literacy. J Clin Outcomes Manag. 2009;16(1):20–9.
33. Jahan S, Al-Saigul AM, Alharbi AM, Abdelgadir MH. Suitability assessment of health education brochures in Qassim province, Kingdom of Saudi Arabia. J Family Community Med. 2014;21(3): 186–92.
34. Dreeben-Irimia O. Patient education in rehabilitation: Jones & Bartlett Learning; 2010.
35. Reeves PT, Packett AC, Burklow CS, Echelmeyer S, Larson NS. Development and assessment of a low-health-literacy, pictographic adrenal insufficiency action plan. J Pediatr Endocrinol Metab. 2022;35(2):205–15.
36. Vinkers DJ, Gussekloo J, Stek ML, Westendorp RG, Van Der Mast RC. Temporal relation between depression and cognitive impairment in old age: prospective population based study. BMJ. 2004;329(7471):881.
37. Rastall M, Brooks B, Klarneta M, Moylan N, McCloud W, Tracey S. An investigation into younger and older adults'memory for physiotherapy exercises. Physiotherapy. 1999;85(3):122–8.
38. Peterson DJ, Gargya S, Kopeikin KS, Naveh-Benjamin M. The impact of level of education on age-related deficits in associative memory: Behavioral and neuropsychological perspectives. Cortex. 2017;91:9–24.
39. Nanasilp P. Gerontological nursing's core knowledge: Who are the older persons, determinant by age or other factors. J Nurs. 2015;42:156–62.
40. Sabharwal S, Wilson H, Reilly P, Gupte CM. Heterogeneity of the definition of elderly age in current orthopaedic research. Springerplus. 2015;4:1–7.
41. Thirapatarapong W, Dajpratham P. Prosthetic usage among the Thai lower limb amputees. Siriraj Med J. 2017;61(4):185–8.
42. Godlwana L, Nadasan T, Puckree T. Global trends in incidence of lower limb amputation: a review of the literature. S Afr J Physiother. 2008;64(1):8–12.

Complement in Human Serum Suppresses Antibody-Dependent Enhancement and Potentiates Neutralization of Dengue Virus

Hansa Praneechit, B.Sc.[1,5], Somchai Thiemmeca, Ph.D.[1,2], Nuntaya Punyadee, Ph.D.[1,2], Panisadee Avirutnan, M.D., Ph.D.[1,2,3,4,*]

[1]Division of Dengue Hemorrhagic Fever Research, Department of Research and Development, Faculty of Medicine Siriraj Hospital, Mahidol University, Bangkok, Thailand, [2]Siriraj Center of Research Excellence in Dengue and Emerging Pathogens, Faculty of Medicine Siriraj Hospital, Mahidol University, Bangkok, Thailand, [3]Molecular Biology of Dengue and Flaviviruses Research Team, National Center for Genetic Engineering and Biotechnology, National Science and Technology Development Agency, Bangkok, Thailand, [4]Department of Immunology, Faculty of Medicine Siriraj Hospital, Mahidol University, Bangkok, Thailand, [5]Graduate Program, Department of Immunology, Faculty of Medicine Siriraj Hospital, Mahidol University, Bangkok, Thailand.

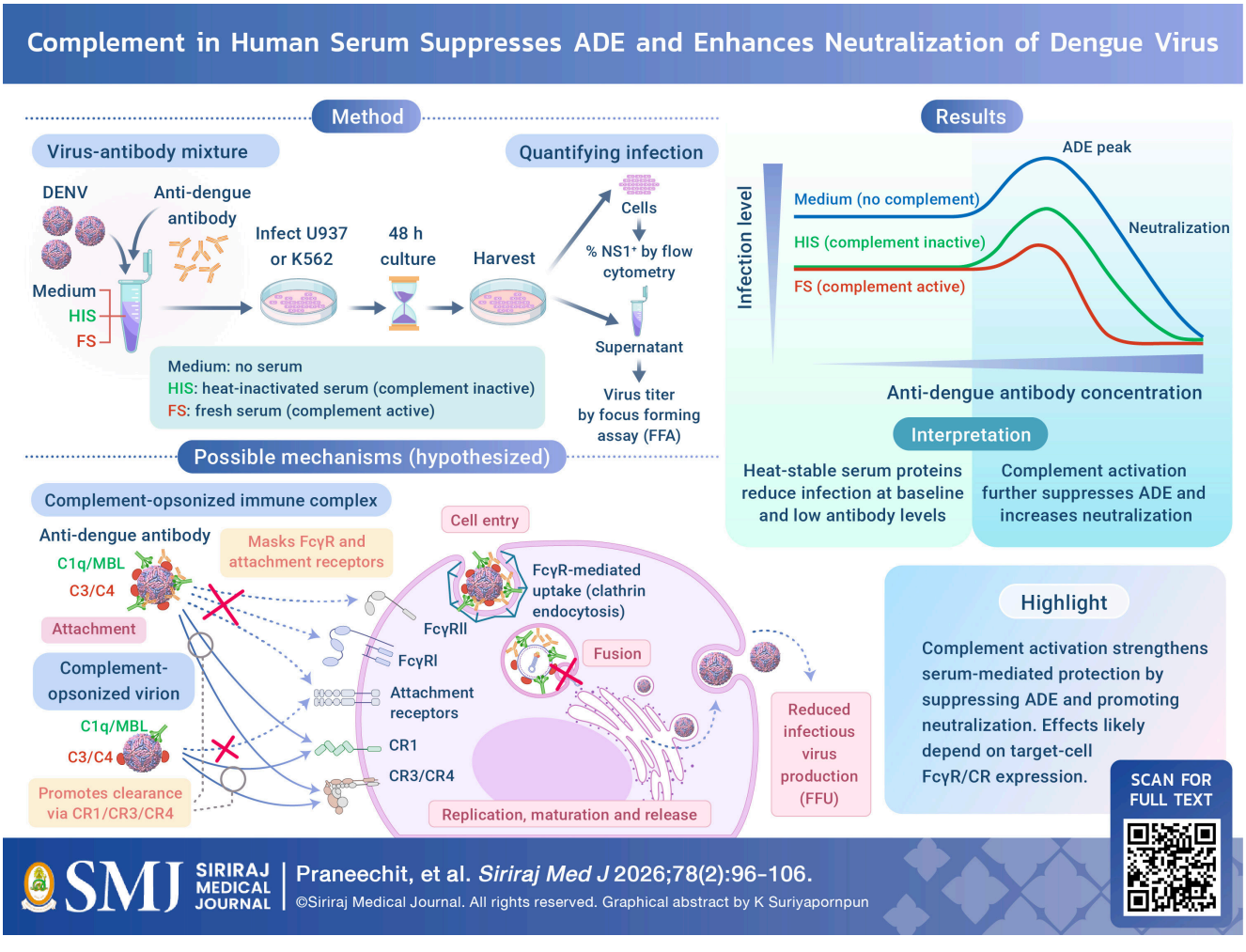

*Corresponding author: Panisadee Avirutnan
E-mail: panisadee.avi@mahidol.edu
Received 30 September 2025 Revised 3 November 2025 Accepted 4 November 2025
ORCID ID:http://orcid.org/0000-0003-0053-3045
https://doi.org/10.33192/smj.v78i2.278008

ABSTRACT

Objective: Antibody-dependent enhancement (ADE), in which pre-existing antibodies increase viral infection, is a major concern in dengue virus (DENV) pathogenesis and vaccine development. While conventional ADE models are well-established, the role of the complement system in modulating this process remains underexplored. This study investigated how complements in human serum influence DENV infection in the presence of enhancing and neutralizing antibodies.

Materials and Methods: U937 and K562 cells were infected with DENV serotype 2 (DENV-2). The virus was pre-incubated with various concentrations of dengue antibodies, purified from pooled convalescence serum, under three conditions: culture medium, heat-inactivated human serum, or fresh human serum (as a source of active complement). After 48 hours, infectious virus production was quantified by a focus-forming assay, and infection rates were measured by flow cytometry.

Results: Both fresh and heat-inactivated human serum significantly reduced DENV infection. In the presence of antibodies, complement activation in fresh serum was significantly more effective at decreasing infection than conditions with inactive complement, particularly at antibody concentrations that mediate ADE and partial neutralization.

Conclusion: Human serum limits DENV infection, and active complement amplifies this neutralizing effect under conditions that typically promote ADE. These findings support incorporating complement into *in vitro* assessments and motivate validation in primary FcγR/complement receptor-expressing target cells.

Keywords: Human serum; complement; antibody-dependent enhancement; neutralization; U937 cells; K562 cells
(Siriraj Med J 2026;78(2):96-106)

INTRODUCTION

Dengue remains a major global public health challenge, with >100 endemic countries and approximately half of the world's population at risk.[1-3] Dengue virus (DENV), a member of the *Flaviviridae* family, comprises four antigenically distinct serotypes (DENV-1 to DENV-4). Infection with any serotype can cause illness ranging from mild dengue fever to severe dengue hemorrhagic fever and dengue shock syndrome (DHF/DSS).[4] Because clinical manifestations are often nonspecific, laboratory confirmation is essential for accurate diagnosis. Current approaches include nucleic acid amplification tests (NAAT/RT-PCR) for viral genome detection, NS1 antigen assays, and serological tests for IgM and IgG antibodies, performed either individually or in combination. Numerous commercial rapid diagnostic tests (RDTs) combining NS1 antigen and antibody detection have been evaluated in multiple settings, showing high specificity but variable sensitivity influenced by the assay type, timing of sample collection, infecting serotype, and host immune status.[5-10] Despite sustained research efforts, no specific antiviral therapy exists, and current vaccines provide context-dependent rather than universal protection.

Secondary infection with a heterologous serotype is the strongest epidemiologic risk factor for severe disease and is explained in part by antibody-dependent enhancement (ADE).[11,12] At sub-neutralizing antibody concentrations, cross-reactive antibodies from prior infection form immune complexes that facilitate virus uptake through Fc-gamma receptors (FcγR) on myeloid cells, increasing viral burden and risk of severe illness.[13,14] The magnitude of ADE depends on antibody concentration, affinity, epitope specificity, and immunoglobulin subclass (primarily IgG1).[15-20]

The complement system is a major effector arm of innate immunity that opsonizes pathogens, generates anaphylatoxins (C3a, C5a), and can lyse susceptible targets.[21] During ADE, immune complexes can trigger classical pathway activation, suggesting that complement could enhance neutralization or, conversely, amplify infection and inflammation. Clinical studies report correlations between complement activation and severe dengue with vascular leakage,[22-24] whereas in the related West Nile virus, complement is protective *in vivo* —underscoring context-dependent effects.[25-28] How complement influences ADE of DENV infection therefore remains unresolved.

Prior *in vitro* findings are mixed. Complement-competent serum—or purified components such as C1q or C3—can attenuate ADE and reduce DENV infection in FcγR-expressing cell lines (U937, K562), particularly near the ADE peak[29,30] yet dengue-immune sera enriched for strongly enhancing antibodies do not always confer protection.[31] Discrepancies likely reflect differences in antibody source (monoclonal vs polyclonal), concentration, epitope specificity, subclass distribution, and complement source.

In natural DENV infection, polyclonal antibodies of diverse specificities and subclasses act in the presence of circulating complement proteins. A systematic analysis is therefore needed to define how physiologic serum factors shift antibody function across the spectrum from enhancement to neutralization. We hypothesized that complement in human serum suppresses ADE and enhances neutralization. To test this, we used U937 and K562 cells—standard ADE/neutralization models—and purified IgG from pooled convalescent sera (PCS) to approximate the human polyclonal response. We then compared fresh (complement-competent) and heat-inactivated human serum, quantifying viral output and infected-cell frequency to clarify complement's contribution to the enhancement-neutralization balance.

MATERIALS AND METHODS

Cell lines and dengue virus

Human monocytic U937 and erythroleukemia K562 cell lines were cultured in RPMI-1640 supplemented with 10% heat-inactivated fetal bovine serum (HI-FBS; Gibco) and 100 U/mL Penicillin-Streptomycin (Pen-Strep; Gibco) at 37 °C in a 5% CO_2 incubator and passaged every 3 days. Routine PCR-based mycoplasma testing confirmed the absence of contamination. Cell-surface complement receptor (CR) expression was assessed by flow cytometry using phycoerythrin (PE)-conjugated anti-human CR1 (CD35, clone E11; BD Biosciences), fluorescein isothiocyanate (FITC)-conjugated anti-human CR3 (CD11b/MAC-1, clone ICRF44; BD Biosciences), and Brilliant Violet 650 (BV650)-conjugated anti-human CR4 (CD11c, clone B-ly6; BD Biosciences). *Aedes albopictus* C6/36 cells were maintained at 28 °C in Leibovitz's L-15 medium (Gibco) with 10% HI-FBS, 10% tryptose phosphate broth (TPB; Sigma), 100 U/mL Pen-Strep, and 2 mM L-glutamine (Gibco). African green monkey kidney (Vero) cells were grown in Minimum Essential Medium (MEM; Gibco) with 10% HI-FBS and 100 U/mL Pen-Strep at 37 °C in 5% CO2.

DENV serotype 2 (strain 16681) was propagated in C6/36 cells (ATCC® CRL-1660™) at a multiplicity of infection (MOI) of 0.01. Infected cells were cultured in L-15 medium containing 1.5% HI-FBS for 5 days; clarified supernatants were harvested and titrated by focus-forming assay (FFA) on Vero cells.

Anti-DENV antibodies

Pooled convalescent dengue sera (PCS) containing polyclonal antibodies against all four DENV serotypes (titers > 1:10,240) were obtained from AFRIM. IgG was purified by Protein G affinity chromatography (Pharmacia); aggregates were reduced by centrifugation (14,000 rpm, 10 min, 4 °C). By Western blot, purified PCS IgG bound multiple DENV proteins, (envelope, capsid, pre-membrane, and NS1) (data not shown). Dengue-specific monoclonal antibodies (mAbs) included anti-NS1 (clones 2G6, DENV-2 specific) and pan-flavivirus anti-E (clone 4G2), kindly provided by Dr. Chunya Puttikhunt, (BIOTEC, NSTDA). Alexa Fluor 647-conjugated goat anti-mouse IgG (Invitrogen) was used as secondary antibody.

Normal human serum (complement source)

Normal human serum (NHS) was collected from an anonymous healthy adult with ethically institutional approval (Faculty of Medicine Siriraj Hospital, Mahidol University, Thailand; Protocol 632/2559). The donor was seronegative for all DENV serotypes by dengue IgG/IgM-capture ELISA and PRNT (data not shown).[32,33] NHS was used either as fresh serum (FS; complement-competent) or heat-inactivated serum (HIS), prepared by incubating at 56 °C for 30 min to inactivate heat-labile complement. Loss of complement activity was confirmed by absence of C3d deposition on yeast (flow cytometry; data not shown).

DENV infection assay

U937 and K562 cells were resuspended in RPMI with 10% HI-FBS. DENV-2 (MOI = 1) was pre-incubated at 37 °C for 30 min with serial dilutions of PCS-derived IgG under three conditions: (i) Medium (RPMI + 10% HI-FBS), (ii) 10% HIS, or (iii) 10% FS. Virus-antibody mixtures were added to cells for 2 hours (h) at 37 °C, followed by two washes with plain RPMI and one wash with RPMI + 10% HI-FBS. Cells were cultured 48 h in 96-well plates. Supernatants were collected (500 x *g*, 5 min, 4 °C) for FFA, and cells were processed for intracellular NS1 staining and flow cytometry.

Detection of DENV-infected cells by flow cytometry

At 48 h post-infection, cells were fixed with 2% formaldehyde (FA) in PBS for 30 min at room temperature (RT), washed with PBS + 2% HI-FBS, and permeabilized with 0.1% Triton X-100 (Fluka) in PBS for 10 min at RT. After washing, intracellular NS1 was labeled with anti-DENV NS1 mAb 2G6 (hybridoma supernatant; 50 µL/well, 1 h, RT), followed by Alexa Fluor 647–conjugated goat anti-mouse IgG (1:500, 30 min, RT, dark). Mock-infected cells (Medium only) were processed in parallel to set $NS1^+$ gates (isotype controls where indicated). Samples were acquired by flow cytometry and analyzed using standard gating (cells by FSC/SSC, singlets by FSC-H vs

FSC-A). The primary readout was % NS1-positive cells (% $NS1^+$).

Background subtraction and limit of detection (LOD) handling. For each experiment, $\%NS1^+$ in mock-infected controls was subtracted from all conditions. Negative values were floored to LOD/2, LOD was the mean $\%NS1^+$ in mock wells for that experiment.

Fold-change calculation (baseline normalization). To evaluate changes relative to baseline infection, fold change was calculated per experiment as the ratio of each condition (Medium, HIS, or FS) at a given antibody dose to the Medium condition at 0 μg/mL PCS. Background-corrected $\%NS1^+$ values were used:

$$\text{Fold change } (\%NS1^+) = \frac{\text{(Percentage of NS1 positive cells in Medium,HIS,or FS at each PCS)}}{\text{(Percentage of NS1 positive cells in Medium at PCS 0 μg/mL)}}$$

If subtraction yielded a value ≤ 0, it was set to LOD/2 before computing the ratio. Fold-change data are summarized as mean ± SEM across independent experiments.

Measurement of infectious virus production by focus-forming assay (FFA)

Viral titers in culture supernatants were quantified by FFA on Vero monolayers. Supernatants were 10-fold serially diluted and added in duplicate to 96-well plates seeded with Vero cells (~90% confluence). After 2 h adsorption at 37 °C (5% CO_2), inocula were replaced with an overlay of 1.2% gum tragacanth (Sigma) in MEM supplemented with 2% HI-FBS, 100 U/mL penicillin–streptomycin, and 2 mM L-glutamine. Plates were incubated for 72 h at 37 °C.

Cells were fixed with 3.7% formaldehyde (FA) in PBS (15 min, RT), permeabilized with 2% Triton X-100 in PBS (10 min, RT), and stained with anti-E mAb 4G2 (1 h, 37 °C), followed by HRP-conjugated goat anti-mouse IgG (Dako; 1:1,000; 1 h, 37 °C, protected from light). After washing, foci were visualized with 3,3'-diaminobenzidine (DAB; Sigma) (typically 0.8 mg/mL containing 0.16% [w/v] $NiCl_2$ and 0.014% [v/v] H_2O_2) for 10-15 min at RT. Foci were counted and titers calculated as focus-forming units per mL (FFU/mL) from dilutions yielding countable foci when multiple dilutions were available, estimates were averaged.

LOD transformations. Samples with no detectable foci (across duplicates) were assigned LOD/2 before analysis; for this assay LOD = 10 FFU/mL, thus LOD/2 = 5 FFU/mL. FFU/mL values were $\log_{10}$-transformed for visualization where indicated.

Fold-change calculation (baseline normalization). Similarly, virus output for each condition was expressed relative to the Medium condition at 0 μg/mL PCS:

$$\text{Fold change (FFU)} = \frac{\text{(Log10 in Medium,HIS,or FS at each PCS)}}{\text{(Log10 in Medium at PCS 0 μg/mL)}}$$

For samples below detection limit, LOD/2 (5 FFU/mL) was substituted before computation. Fold-change data are summarized as mean ± SEM across independent experiments.

Statistical analysis

All analyses were performed in GraphPad Prism (GraphPad Software). Data are presented as mean ± SEM. Normality of distributions was assessed using the Kolmogorov–Smirnov test. For normally distributed data, comparisons between two groups were made using unpaired two-tailed Student's t-test. Comparisons among three conditions (Medium, HIS, FS) were performed by one-way analysis of variance (ANOVA) followed by Bonferroni's multiple-comparison test for pairwise differences. A p-value < 0.05 was considered statistically significant.

Because data in Fig 2 were expressed as fold change relative to the Medium baseline (0 μg/mL PCS), a value of 1 represents no change from baseline. Each data point in the figures represents an independent biological replicate, and all analyses were based on results from at least three independent experiments to ensure reproducibility.

RESULTS

Within-condition antibody titrations establish ADE and neutralization (Fig 1)

To validate ADE, U937 and K562 cells were infected with DENV-2 in the presence of titrated pooled dengue convalescent serum IgG (PCS). In Medium, infection peaked at 1 μg/mL PCS in both cell types: $NS1^+$ cells increased to 5.4% in U937 (from 1.5%; NS, $p = 0.1324$) and to 53.2% in K562 (from 1.5%; $p = 0.0011$). Virus production rose from 4×10^3 to 2×10^5 FFU/mL in U937 ($p = 0.0053$) and from 2×10^5 to 2×10^6 FFU/mL in K562 ($p = 0.0085$). At higher antibody doses, infection declined: complete neutralization occurred at 100 μg/mL in U937 ($p < 0.0001$) and partial neutralization at 50 μg/mL in K562 ($p = 0.0237$), defining the canonical bell-shaped ADE curve followed by neutralization.

We then repeated the within-condition titrations with serum present. With heat-inactivated serum (HIS), U937 showed suppression of the ADE peak (1 μg/mL: 1.6% $NS1^+$; 4×10^2 FFU/mL) relative to its own 0 μg/mL

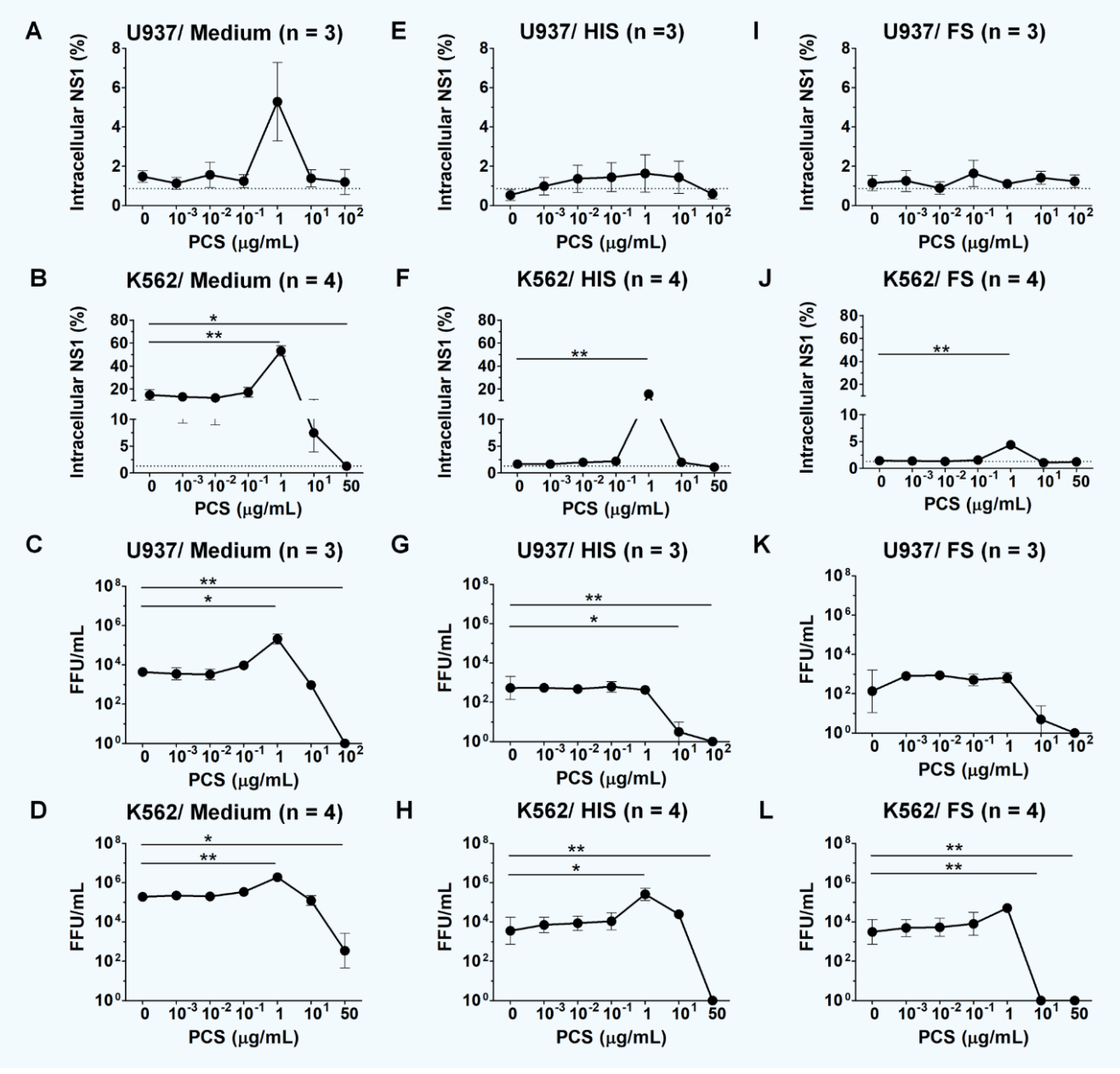

Fig 1. Antibody titrations within each condition reveal ADE and subsequent neutralization in Medium, HIS, and FS.
U937 and K562 were infected with DENV-2 (MOI = 1) in the presence of PCS at 0, 10^{-3}, 10^{-2}, 10^{-1}, 1, and 10 µg/mL (plus 50 µg/mL for K562; 100 µg/mL for U937). Conditions were Medium (A–D), 10% HIS (E–H), or 10% FS (I–L). At 48 hpi, intracellular NS1 was quantified by flow cytometry (A, B, E, F, I, J), and infectious virus production in supernatants by focus-forming assay (FFA) (C, D, G, H, K, L). Data represent mean ± SEM from independent experiments (n as indicated in panels). Statistical comparisons were made using unpaired two-tailed t-tests vs the 0 µg/mL PCS baseline within each condition; significance: * $p < 0.05$, ** $p < 0.01$; NS, not significant.

PCS baseline (0.5%, 5×10^2 FFU/mL), whereas K562 still exhibited ADE (15.7%, 3×10^5 FFU/mL vs 1.6%, 4×10^3 FFU/mL; $p = 0.0487$). At 10 µg/mL PCS, U937 virus production fell markedly (3 FFU/mL; $p = 0.0440$), while K562 showed no significant change. Infectious virus was eliminated by HIS at 100 µg/mL in U937 and at 50 µg/mL in K562 ($p = 0.0097$ and 0.0021, respectively). With fresh serum (FS; complement-competent), infection was broadly reduced across titrations in both cell types; K562 still showed an ADE peak in $NS1^+$ at 1 µg/mL ($p = 0.0013$), but FS yielded complete neutralization of infectious virus by 10 µg/mL PCS. Fig 1 therefore defines the ADE to neutralization curves in Medium, HIS, and FS for each cell line.

Serum effects at matched antibody doses reveal complement-dependent restriction (Fig 2)

For Fig 2, fold-change values at each antibody dose were calculated relative to the Medium baseline (0 µg/mL PCS) within each experiment. Thus, 1 denotes no

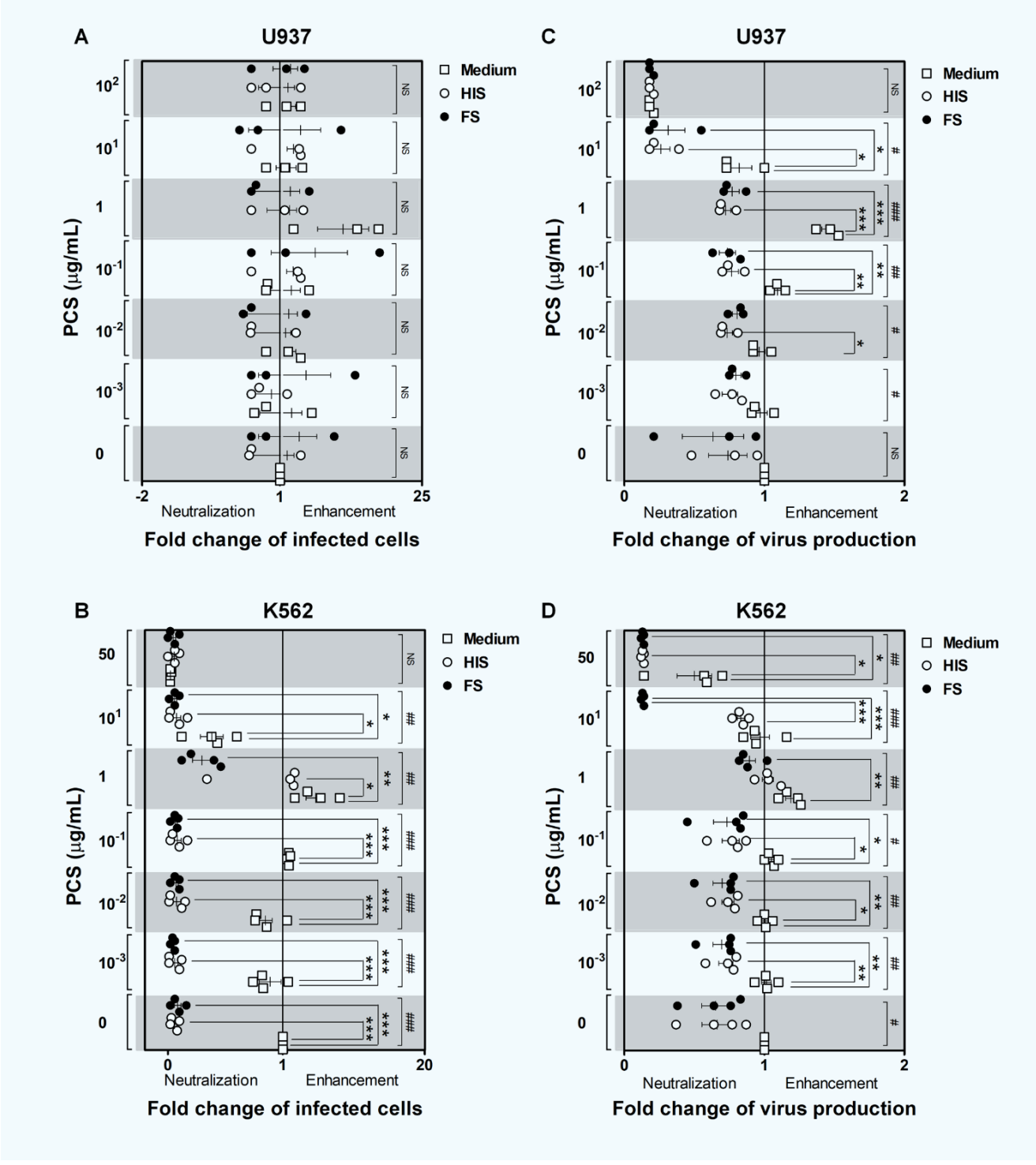

Fig 2. Serum effects at matched antibody doses shown as fold change relative to medium.

For each PCS dose and experiment, the effect of HIS (open circles) and FS (filled circles) vs Medium was computed as fold change (condition/Medium) for % NS1$^+$ cells (A, B) and FFU/mL (C, D) in U937 (A, C) and K562 (B, D). Points show individual experiments; bars show mean ± SEM. The reference line at 1 indicates no difference from Medium. Statistical comparisons show fold change against the reference line and, where indicated, FS vs HIS at the same dose (multiple-comparison adjusted where applicable); exact *p*-values are annotated in the panels. For FFU values at the detection limit, the assay's LOD handling is described in Methods. (Underlying raw titration curves are shown in Fig 1. At each PCS dose, a one-way ANOVA tested differences among Medium, HIS, and FS (sharp symbols: #, ##, ###). Bonferroni-adjusted pairwise comparisons are shown with asterisks (*, **, ***). Symbol thresholds: * or # $p \leq 0.05$; ** or ## $p \leq 0.01$; *** or ### $p \leq 0.001$; NS, not significant. Because data are plotted as fold change, the Medium group equals 1 (reference line).

change from baseline; because ADE/neutralization shifts infection at non-zero doses, Medium can be > 1 (ADE) or < 1 (neutralization).

U937. Across PCS doses, NS1$^+$ fold-changes for HIS and FS clustered near 1 (little consistent difference vs Medium), whereas FFU fold-changes were significantly < 1 at 0.1, 1, and 10 µg/mL PCS for both HIS and FS. Mean FFU fold-changes (n=3 experiments) at 0.1, 1, and 10 µg/mL were 0.77, 0.72, 0.26 (HIS), and 0.74, 0.77, 0.31 (FS); corresponding Medium were 1.09, 1.46, 0.82, reflecting ADE then neutralization. Significant neutralization of the enhancing antibody effects was observed at 0.1 and 1 µg/mL, with near-complete neutralization at 10 µg/mL. Pairwise (Bonferroni-adjusted) mean differences vs Medium were: for HIS, 0.33 (95% CI: 0.1070–0.5464, $p \leq 0.01$), 0.73 (95% CI: 0.5222–0.9445, $p \leq 0.001$), and 0.56 (95% CI: 0.1232–0.9968, $p \leq 0.05$) at 0.1, 1, and 10 µg/mL, respectively; for FS, 0.36 (95% CI: 0.1370–0.5764, $p \leq 0.01$), 0.69 (95% CI: 0.4755–0.8978, $p \leq 0.001$), and 0.51 (95% CI: 0.0699–0.9434, $p \leq 0.05$). Thus, in U937, serum—particularly with intact complement—reduces infectious output (FFU) even when the percentage of infected cells changes little.

K562. NS1$^+$ and FFU fold-changes were < 1 for HIS and FS across 0–1 µg/mL PCS, with significant effects at each dose. At 1 µg/mL, mean NS1$^+$ fold-changes (n=4 experiments) were 0.29 (FS), 1.43 (HIS), and 4.95 (Medium). Bonferroni-adjusted mean differences were FS vs Medium: 4.655 (95% CI 1.347–7.963, $p \leq 0.01$), HIS vs Medium: 3.520 (95% CI 0.2122–6.828, $p \leq 0.05$). At 10 µg/mL, mean NS1$^+$ fold-changes were 0.0575 (FS), 0.0750 (HIS), and 0.3825 (Medium), with FS vs Medium: 0.3250 (95% CI 0.06681–0.5832, $p \leq 0.05$) and HIS vs Medium: 0.3075 (95% CI 0.04931–0.5657, $p \leq 0.05$). For FFU at 10 µg/mL, mean fold-changes were 0.1325 (FS), 0.8325 (HIS), and 0.9700 (Medium); FS vs Medium: 0.8375 (95% CI 0.6668–1.008, $p \leq 0.001$) and FS vs HIS: 0.7000 (95% CI 0.5293–0.8707, $p \leq 0.001$). Under FS at 10 µg/mL, FFU fell below the detection limit (neutralization). These data confirm a complement-dependent amplification of neutralization, most evident in K562 near the ADE peak and at sub-neutralizing antibody levels.

DISCUSSION

Antibody-dependent enhancement (ADE) is a recognized risk factor for severe dengue.[15] *In vitro* models remain essential for dissecting mechanisms and guiding evaluation of vaccine and therapeutics. U937 and K562 are widely used because ADE depends on Fcγ-receptor (FcγR)–mediated uptake.[34,35] Given that severe dengue is frequently linked to DENV-2[36,37] and that DENV-2 has posed a substantial burden in Thailand in the past decade[38], we used DENV-2 infection of U937 and K562 as a relevant model. Consistent with prior studies, both lines supported ADE when DENV-2 was incubated with titrated dengue-immune IgG (PCS). Despite this shared susceptibility, their behaviors diverged, reflecting differences in intrinsic permissivity and FcγR profiles (U937: FcγRI and FcγRII; K562: FcγRII only).[39-43] To separate antibody-driven enhancement from direct infection, we referenced each line's no-PCS baseline. On this "effective enhancement" scale, the ADE peak at 1 µg/mL PCS was larger in U937 than in K562 (Fig 1), indicating that U937 is more sensitive for detecting enhancing activity.

We then examined how human serum shapes this enhancement–neutralization balance. Two points emerged. First, heat-inactivated serum (HIS) reduced infection across a wide antibody range—including in the absence of dengue antibody—implicating heat-stable recognition molecules such as C1q and MBL that can bind virions or immune complexes and interfere with attachment/uptake.[29,30,44-46] Yet, the ADE peak persisted in K562 under HIS (Fig 1), indicating that recognition alone did not fully counter enhancement in this line. Second, fresh serum (FS)—which retains complement activity—produced greater restriction than HIS, most clearly in K562 near the ADE peak and at sub-neutralizing PCS doses. In Fig 2, where fold change values are normalized to the Medium baseline (0 µg/mL PCS), this appears as values < 1 for HIS and FS, with FS < HIS at 1 µg/mL and 10 µg/mL, and complete neutralization (below LOD) in FS at 10 µg/mL.

These patterns fit a model in which immune-complex size and opsonization control complement potency. Complement activation is favored at higher epitope density and at equivalence or antibody excess.[47] At ADE/sub-neutralizing doses, immune complexes are abundant and can recruit C1q/MBL, trigger C4/C3 deposition, and restrict infection by (i) masking FcγR and other entry receptors and/or (ii) reducing the fraction of infectious virions. Notably, in U937 we often observed large decreases in FFU with little change in %NS1$^+$, suggesting that serum—especially with complement—diminishes infectious yield more than initial entry in this line.

DENV can engage all three complement pathways, which have dual roles in protection and pathogenesis. The classical pathway can inhibit infection during ADE (e.g., C1q binding to immune complexes or E protein[30], while the lectin pathway can neutralize via MBL.[45,46] Activation of these pathways promotes viral clearance through

C4/C3 deposition and opsonophagocytosis.[48,49] By contrast, excessive alternative pathway activity correlates with disease severity and inflammatory injury.[50] Our functional data—suppressed ADE and enhanced neutralization in FS versus HIS—are consistent with a predominant contribution of classical/lectin mechanisms under our conditions, though we did not map pathways directly.

Complement can also, under certain conditions, enhance infection through complement-receptor (CR) pathways. Yamanaka *et al.* reported complement-mediated enhancement in U937 at high serum fractions (50–75%), whereas such effects were absent in K562 conditions under their conditions.[29] Complement-facilitated dissemination has also been described for HIV, HSV, and West Nile virus.[51-53] In our study, using 10% serum, restriction predominated in both lines. We detected CR1 on U937 but little/no CR3/CR4, and no CR1/CR3/CR4 on K562 (Supplementary Fig S1). Because primary monocytes express higher CR1 than U937[54,55] and are important DENV targets[56,57], the *in vivo* balance between complement-mediated neutralization and enhancement likely depends on serum fraction/opsonin density, antibody dose, immune-complex size, and the FcγR/CR context of the target cell.

While our experiments in U937 and K562 demonstrate that serum proteins and complement activation suppress ADE—and can lower DENV-2 infection even in the absence of anti-DENV antibody—validation in primary human target cells (monocytes, macrophages, and monocyte-derived dendritic cells) is warranted to confirm physiological relevance. Because complement–antibody interactions can vary by DENV serotype, parallel evaluation across DENV-1–4 should be prioritized.[58-60] Our results provide functional evidence that complement from seronegative human serum inhibits ADE mediated by pooled convalescent IgG. However, the specific complement pathways and IgG subclasses responsible remain to be defined; complement engagement depends on subclass and epitope specificity.[58,59] Accordingly, pathway-resolved studies—e.g., C1q- or C3-depleted sera with add-back, MgEGTA/MBL blockade to parse classical vs lectin/alternative pathways, and virion-associated C4/C3 deposition assays using subclass-defined anti-DENV monoclonal antibodies—will be essential to delineate the antibody–complement mechanisms that modulate ADE.

Beyond neutralization, the protective efficacy of anti-DENV antibodies in people is strongly linked to complement engagement. Complement-fixing antibodies are associated with protection from symptomatic disease and reduced progression to severe disease (DHF/DSS)[61], with murine studies showing that C1q binding antibodies accelerate viremia clearance.[62] In humans, C1q-fixing antibody levels induced by the TAK-003 correlated with neutralizing antibody titers across all four DENV serotypes.[63] Mechanistically, efficient classical pathway activation occurs when C1q binds IgG1/IgG3 arranged in hexamers on antigen surfaces.[64,65] These data argue that evaluating both neutralization potency and complement-activating capacity should improve how we assess vaccine and therapeutic antibody candidates.

Finally, our study has boundaries: we used one DENV-2 strain (16681), two cell lines, and 10% human serum from defined donors; we did not quantify CH50/AH50, C3a/C5a, or virion-associated C4b/C3b/iC3b, nor did we profile IgG subclasses or block FcγR/CR directly. Pathway-specific depletion/reconstitution, opsonin-deposition assays, and studies in primary FcγR/CR-expressing cells will be important next steps.

CONCLUSIONS

Human serum reduces DENV infection during direct infection as well as across low, enhancing, and sub-neutralizing antibody concentrations. Heat-stable recognition (e.g., C1q/MBL) is sufficient to lower infection, but complement activation in fresh serum provides greater restriction, most evident near the ADE peak and at sub-neutralizing antibody levels—particularly in K562. In U937, serum (with or without complement) markedly lowers infectious output (FFU) even when %NS1$^+$ changes little. The magnitude of protection depends on antibody dose and target cell type, consistent with effects of immune-complex size, opsonization, and receptor context. These findings refine how serum and complement shape the ADE–neutralization balance and motivate mechanistic studies in primary FcγR/CR-expressing cells to define pathway-specific roles in dengue infection and immunity.

Data availability

Data and material requests should be addressed to the corresponding author (panisadee.avi@mahidol.ac.th).

ACKNOWLEDGEMENTS

We extend our gratitude to Adisak Songjaeng, staff member of the Division of Dengue Hemorrhagic Fever Research, for his assistance with mycobacterium detections.

DECLARATIONS

Grants and Funding Information

70/2560 and 99/2561/ Mahidol University, Thailand

R016234004/ Faculty of Medicine Siriraj Hospital, Mahidol University, Thailand

R016634008/ Faculty of Medicine Siriraj Hospital, Mahidol University, Thailand

R016637004/ Faculty of Medicine Siriraj Hospital, Mahidol University, Thailand

The Research Excellence Development (RED) Program/ Faculty of Medicine Siriraj Hospital, Mahidol University, Thailand

PHD/0026/2557/ the Royal Golden Jubilee Ph.D. (RGJ-PHD) Program, Thailand

Conflict of Interest

All authors declare no conflicts of interest.

Registration Number of Clinical Trial

None.

Author Contributions

Conceptualization and methodology, H.P. and P.A. ; Investigation, H.P., N.P. ; Formal analysis, H.P. and S.T. ; Visualization and writing – original draft, H.P., S.T. ; Writing – review and editing, H.P., S.T., N.P. and P.A. ; Funding acquisition, P.A. ; Supervision, P.A. All authors have read and agreed to the final version of the manuscript.

Use of Artificial Intelligence

ChatGPT (OpenAI) was used for language editing of the Introduction, Results, selected Methods subsections, Discussion, Conclusions, and Data Availability section. The authors verified and edited all AI-assisted text. No AI was used for data analysis, figure generation, or image editing; no identifiable data were shared with AI tools.

REFERENCES

1. Yang X, Quam MBM, Zhang T, Sang S. Global burden for dengue and the evolving pattern in the past 30 years. J Travel Med. 2021;28(8).
2. Stanaway JD, Shepard DS, Undurraga EA, Halasa YA, Coffeng LE, Brady OJ, et al. The global burden of dengue: an analysis from the Global Burden of Disease Study 2013. Lancet Infect Dis. 2016;16(6):712-23.
3. Bhatt S, Gething PW, Brady OJ, Messina JP, Farlow AW, Moyes CL, et al. The global distribution and burden of dengue. Nature. 2013;496(7446):504-7.
4. Dengue haemorrhagic fever: diagnosis, treatment, prevention and control. 2nd edition. Geneva : World Health Organization. 1997;2:12-23.
5. Suputtamongkol Y, Avirutnan P, Wongsawat E, Kim Y-W. Performance of Two Commercial Dengue NS1 Rapid Tests for the Diagnosis of Adult Patients with Dengue Infection. Siriraj Medical Journal. 2020;72(1):74-8.
6. Wongsawat E, Avirutnan P, Kim Y-W, Suputtamongkol Y. Performance of Two Commercial Dengue NS1 Rapid Tests for the Diagnosis of Adult Patients with Dengue Infection. Siriraj Medical Journal. 2019;72(1):74-8.
7. Hunsperger EA, Yoksan S, Buchy P, Nguyen VC, Sekaran SD, Enria DA, et al. Evaluation of commercially available diagnostic tests for the detection of dengue virus NS1 antigen and anti-dengue virus IgM antibody. PLoS Negl Trop Dis. 2014;8(10):e3171.
8. Blacksell Stuart D, Jarman Richard G, Bailey Mark S, Tanganuchitcharnchai A, Jenjaroen K, Gibbons Robert V, et al. Evaluation of Six Commercial Point-of-Care Tests for Diagnosis of Acute Dengue Infections: the Need for Combining NS1 Antigen and IgM/IgG Antibody Detection To Achieve Acceptable Levels of Accuracy. Clinical and Vaccine Immunology. 2011;18(12):2095-101.
9. Shan X, Wang X, Yuan Q, Zheng Y, Zhang H, Wu Y, et al. Evaluation of the diagnostic accuracy of nonstructural protein 1 Ag-based tests for dengue virus in Asian population: a meta-analysis. BMC Infect Dis. 2015;15:360.
10. Luvira V, Thawornkuno C, Lawpoolsri S, Thippornchai N, Duangdee C, Ngamprasertchai T, et al. Diagnostic Performance of Dengue NS1 and Antibodies by Serum Concentration Technique. Trop Med Infect Dis. 2023;8(2).
11. Halstead SB. Immune enhancement of viral infection. Prog Allergy. 1982;31:301-64.
12. Burke DS, Nisalak A, Johnson DE, Scott RM. A prospective study of dengue infections in Bangkok. Am J Trop Med Hyg. 1988;38(1):172-80.
13. Halstead SB, Nimmannitya S, Cohen SN. Observations related to pathogenesis of dengue hemorrhagic fever. IV. Relation of disease severity to antibody response and virus recovered. Yale J Biol Med. 1970;42(5):311-28.
14. Guzman MG, Alvarez M, Halstead SB. Secondary infection as a risk factor for dengue hemorrhagic fever/dengue shock syndrome: an historical perspective and role of antibody-dependent enhancement of infection. Arch Virol. 2013;158(7):1445-59.
15. Katzelnick LC, Gresh L, Halloran ME, Mercado JC, Kuan G, Gordon A, et al. Antibody-dependent enhancement of severe dengue disease in humans. Science. 2017;358(6365):929-32.
16. O'Driscoll M, Buddhari D, Huang AT, Waickman A, Kaewhirun S, Iamsirithaworn S, et al. Maternally derived antibody titer dynamics and risk of hospitalized infant dengue disease. Proc Natl Acad Sci U S A. 2023;120(41):e2308221120.
17. Rodenhuis-Zybert IA, Moesker B, da Silva Voorham JM, van der Ende-Metselaar H, Diamond MS, Wilschut J, et al. A fusion-loop antibody enhances the infectious properties of immature flavivirus particles. J Virol. 2011;85(22):11800-8.
18. Rodpothong P, Boonarkart C, Ruangrung K, Onsirisakul N, Kanistanon D, Auewarakul P. Relative contribution of dengue prM- and E-specific polyclonal antibodies to neutralization and enhancement. Acta Virol. 2016;60(3):249-59.
19. Ramadhany R, Hirai I, Sasaki T, Ono K, Ramasoota P, Ikuta K, et al. Antibody with an engineered Fc region as a therapeutic agent against dengue virus infection. Antiviral Res. 2015;124:61-8.
20. Littaua R, Kurane I, Ennis FA. Human IgG Fc receptor II mediates antibody-dependent enhancement of dengue virus

infection. J Immunol. 1990;144(8):3183-6.
21. Merle NS, Noe R, Halbwachs-Mecarelli L, Fremeaux-Bacchi V, Roumenina LT. Complement System Part II: Role in Immunity. Front Immunol. 2015;6:257.
22. Bokisch VA, Top FH, Jr., Russell PK, Dixon FJ, Muller-Eberhard HJ. The potential pathogenic role of complement in dengue hemorrhagic shock syndrome. N Engl J Med. 1973;289(19):996-1000.
23. Malasit P. Complement and dengue haemorrhagic fever/shock syndrome. Southeast Asian J Trop Med Public Health. 1987; 18(3):316-20.
24. Avirutnan P, Punyadee N, Noisakran S, Komoltri C, Thiemmeca S, Auethavornanan K, et al. Vascular leakage in severe dengue virus infections: a potential role for the nonstructural viral protein NS1 and complement. J Infect Dis. 2006;193(8):1078-88.
25. Mehlhop E, Diamond MS. Protective immune responses against West Nile virus are primed by distinct complement activation pathways. J Exp Med. 2006;203(5):1371-81.
26. Mehlhop E, Whitby K, Oliphant T, Marri A, Engle M, Diamond MS. Complement activation is required for induction of a protective antibody response against West Nile virus infection. J Virol. 2005;79(12):7466-77.
27. Mehlhop E, Nelson S, Jost CA, Gorlatov S, Johnson S, Fremont DH, et al. Complement protein C1q reduces the stoichiometric threshold for antibody-mediated neutralization of West Nile virus. Cell Host Microbe. 2009;6(4):381-91.
28. Fuchs A, Pinto AK, Schwaeble WJ, Diamond MS. The lectin pathway of complement activation contributes to protection from West Nile virus infection. Virology. 2011;412(1):101-9.
29. Yamanaka A, Kosugi S, Konishi E. Infection-enhancing and -neutralizing activities of mouse monoclonal antibodies against dengue type 2 and 4 viruses are controlled by complement levels. J Virol. 2008;82(2):927-37.
30. Mehlhop E, Ansarah-Sobrinho C, Johnson S, Engle M, Fremont DH, Pierson TC, et al. Complement protein C1q inhibits antibody-dependent enhancement of flavivirus infection in an IgG subclass-specific manner. Cell Host Microbe. 2007;2(6): 417-26.
31. Yamanaka A, Tabuchi Y, Mulyatno KC, Susilowati H, Hendrianto E, Soegijanto S, et al. Dengue virus infection-enhancing and neutralizing antibody balance in children of the Philippines and Indonesia. Microbes Infect. 2012;14(13):1152-9.
32. Innis BL, Nisalak A, Nimmannitya S, Kusalerdchariya S, Chongswasdi V, Suntayakorn S, et al. An enzyme-linked immunosorbent assay to characterize dengue infections where dengue and Japanese encephalitis co-circulate. Am J Trop Med Hyg. 1989;40(4):418-27.
33. Durbin AP, Karron RA, Sun W, Vaughn DW, Reynolds MJ, Perreault JR, et al. Attenuation and immunogenicity in humans of a live dengue virus type-4 vaccine candidate with a 30 nucleotide deletion in its 3'-untranslated region. Am J Trop Med Hyg. 2001;65(5):405-13.
34. Chelluboina S, Kshirsagar D, Panzade G, Mishra AC, Arankalle V, Shrivastava S. Evaluation of methods for the measurement of antibody-dependent enhancement of dengue virus infection using different FcgammaRIIa expressing cell lines. PLoS One. 2025;20(8):e0331320.
35. Shukla R, Ramasamy V, Shanmugam RK, Ahuja R, Khanna N. Antibody-Dependent Enhancement: A Challenge for Developing a Safe Dengue Vaccine. Frontiers in Cellular and Infection Microbiology. 2020;10.
36. Narvaez F, Montenegro C, Juarez JG, Zambrana JV, Gonzalez K, Videa E, et al. Dengue severity by serotype and immune status in 19 years of pediatric clinical studies in Nicaragua. PLoS Negl Trop Dis. 2025;19(1):e0012811.
37. Vicente CR, Herbinger K-H, Fröschl G, Malta Romano C, de Souza Areias Cabidelle A, Cerutti Junior C. Serotype influences on dengue severity: a cross-sectional study on 485 confirmed dengue cases in Vitória, Brazil. BMC Infectious Diseases. 2016;16(1):320.
38. Ungchusak K, Thiparat K, Anantapreecha S, Ketkeaw J. Dengue Disease in Thailand: DonÃ»t Let the Outbreak Keep Going On and On! Siriraj Medical Journal. 2007;59(4):195-6.
39. Looney RJ, Abraham GN, Anderson CL. Human monocytes and U937 cells bear two distinct Fc receptors for IgG. J Immunol. 1986;136(5):1641-7.
40. Dai X, Jayapal M, Tay HK, Reghunathan R, Lin G, Too CT, et al. Differential signal transduction, membrane trafficking, and immune effector functions mediated by FcgammaRI versus FcgammaRIIa. Blood. 2009;114(2):318-27.
41. Christensen J, Leslie RG. Quantitative measurement of Fc receptor activity on human peripheral blood monocytes and the monocyte-like cell line, U937, by laser flow cytometry. J Immunol Methods. 1990;132(2):211-9.
42. Chawla T, Chan KR, Zhang SL, Tan HC, Lim APC, Hanson BJ, et al. Dengue Virus Neutralization in Cells Expressing Fc Gamma Receptors. PLoS ONE. 2013;8(5):e65231.
43. Lubow J, Levoir LM, Ralph DK, Belmont L, Contreras M, Cartwright-Acar CH, et al. Single B cell transcriptomics identifies multiple isotypes of broadly neutralizing antibodies against flaviviruses. PLOS Pathogens. 2023;19(10):e1011722.
44. Douradinha B, McBurney SP, Soares de Melo KM, Smith AP, Krishna NK, Barratt-Boyes SM, et al. C1q binding to dengue virus decreases levels of infection and inflammatory molecules transcription in THP-1 cells. Virus Res. 2014;179:231-4.
45. Fuchs A, Lin TY, Beasley DW, Stover CM, Schwaeble WJ, Pierson TC, et al. Direct complement restriction of flavivirus infection requires glycan recognition by mannose-binding lectin. Cell Host Microbe. 2010;8(2):186-95.
46. Avirutnan P, Hauhart RE, Marovich MA, Garred P, Atkinson JP, Diamond MS. Complement-mediated neutralization of dengue virus requires mannose-binding lectin. mBio. 2011; 2(6):e00276-11-e.
47. Lucisano Valim YM, Lachmann PJ. The effect of antibody isotype and antigenic epitope density on the complement-fixing activity of immune complexes: a systematic study using chimaeric anti-NIP antibodies with human Fc regions. Clin Exp Immunol. 1991;84(1):1-8.
48. Sun J, Chen C, Pan P, Zhang K, Xu J, Chen C. The potential of bacterial anti-phagocytic proteins in suppressing the clearance of extracellular vesicles mediated by host phagocytosis. Front Immunol. 2024;15:1418061.
49. Avirutnan P, Mehlhop E, Diamond MS. Complement and its role in protection and pathogenesis of flavivirus infections. Vaccine. 2008;26 Suppl 8:I100-7.
50. Nascimento EJ, Silva AM, Cordeiro MT, Brito CA, Gil LH, Braga-Neto U, et al. Alternative complement pathway deregulation is correlated with dengue severity. PLoS One. 2009;4(8):e6782.
51. Delibrias CC, Fischer EM, Kazatchkine MD. The enhancing

role of complement in human immunodeficiency virus infection: soluble recombinant CR1 (CD35) inhibits complement-mediated enhancement of infection of a CD4-positive T-cell line with human immunodeficiency virus-1. Scand J Immunol. 2000;51(5): 526-9.
52. Carpentier JL, Lew DP, Paccaud JP, Gil R, Iacopetta B, Kazatchkine M, et al. Internalization pathway of C3b receptors in human neutrophils and its transmodulation by chemoattractant receptors stimulation. Cell Regul. 1991;2(1):41-55.
53. Stoiber H, Frank I, Spruth M, Schwendinger M, Mullauer B, Windisch JM, et al. Inhibition of HIV-1 infection in vitro by monoclonal antibodies to the complement receptor type 3 (CR3): an accessory role for CR3 during virus entry? Mol Immunol. 1997;34(12-13):855-63.
54. Thieblemont N, Haeffner-Cavaillon N, Ledur A, L'Age-Stehr J, Ziegler-Heitbrock HW, Kazatchkine MD. CR1 (CD35) and CR3 (CD11b/CD18) mediate infection of human monocytes and monocytic cell lines with complement-opsonized HIV independently of CD4. Clin Exp Immunol. 1993;92(1):106-13.
55. Schiller C, Spittler A, Willheim M, Szepfalusi Z, Agis H, Koller M, et al. Influence of suramin on the expression of Fc receptors and other markers on human monocytes and U937 cells, and on their phagocytic properties. Immunology. 1994;81(4):598-604.
56. Begum F, Das S, Mukherjee D, Mal S, Ray U. Insight into the Tropism of Dengue Virus in Humans. Viruses. 2019;11(12).
57. Kou Z, Quinn M, Chen H, Rodrigo WW, Rose RC, Schlesinger JJ, et al. Monocytes, but not T or B cells, are the principal target cells for dengue virus (DV) infection among human peripheral blood mononuclear cells. J Med Virol. 2008;80(1):134-46.
58. Byrne AB, Talarico LB. Role of the complement system in antibody-dependent enhancement of flavivirus infections. International Journal of Infectious Diseases. 2021;103:404-11.
59. Vidarsson G, Dekkers G, Rispens T. IgG Subclasses and Allotypes: From Structure to Effector Functions. Frontiers in Immunology. 2014;Volume 5 - 2014.
60. De Alwis R, Williams KL, Schmid MA, Lai C-Y, Patel B, Smith SA, et al. Dengue Viruses Are Enhanced by Distinct Populations of Serotype Cross-Reactive Antibodies in Human Immune Sera. PLoS Pathogens. 2014;10(10):e1004386.
61. Dias AG, Jr., Duarte EM, Zambrana JV, Cardona-Ospina JA, Bos S, Roy V, et al. Anti-dengue virus antibodies that elicit complement-mediated lysis of Zika virion correlate with protection from severe dengue disease. Cell Rep. 2025;44(5):115613.
62. Sampei Z, Koo CXE, Teo FJ, Toh YX, Fukuzawa T, Gan SW, et al. Complement Activation by an Anti-Dengue/Zika Antibody with Impaired Fcγ Receptor Binding Provides Strong Efficacy and Abrogates Risk of Antibody-Dependent Enhancement. Antibodies. 2023;12(2):36.
63. Nascimento EJM, Norwood B, Kpamegan E, Parker A, Fernandes J, Perez-Guzman E, et al. Antibodies Produced in Response to a Live-Attenuated Dengue Vaccine Are Functional in Activating the Complement System. J Infect Dis. 2023;227(11):1282-92.
64. Vidarsson G, Dekkers G, Rispens T. IgG subclasses and allotypes: from structure to effector functions. Front Immunol. 2014;5:520.
65. Byrne AB, Talarico LB. Role of the complement system in antibody-dependent enhancement of flavivirus infections. Int J Infect Dis. 2021;103:404-11.

Emergent Hemodialysis Initiation: A Marker of Suboptimal Pre-Dialysis Care Rather Than an Independent Predictor of Mortality

Kemmawat Cheamsaree, M.D.[1], Luddawan Upekkhawong, M.Sc.[2], Kornchanok Vareesangthip, M.D.[2,*]

[1]Department of Medicine, Faculty of Medicine Siriraj Hospital, Mahidol University, Bangkok, Thailand, [2]Renal Division, Department of Medicine, Faculty of Medicine Siriraj Hospital, Mahidol University, Bangkok, Thailand.

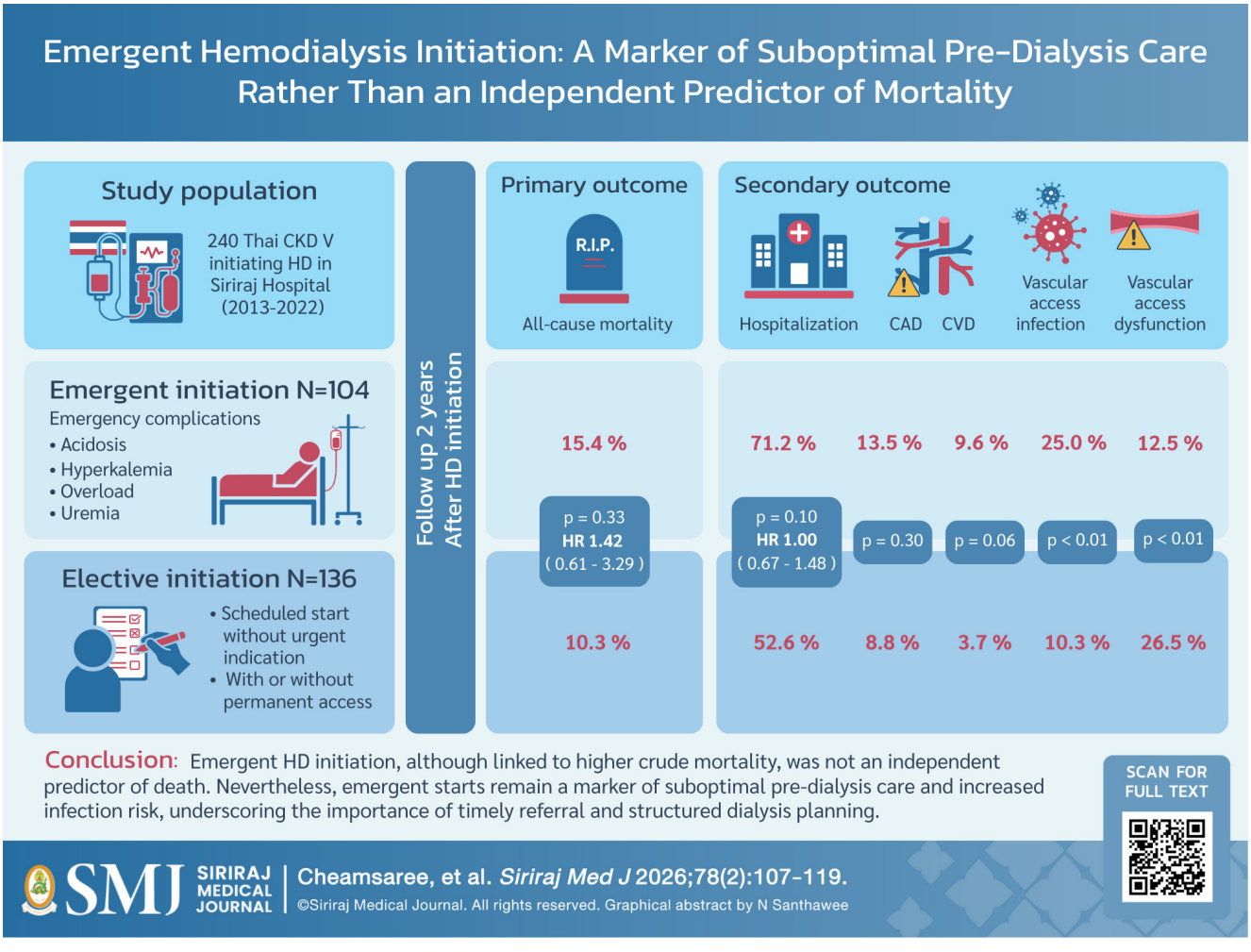

**Corresponding author: Kornchanok Vareesangthip*
E-mail: Kornchanok.var@mahidol.ac.th
Received 14 October 2025 Revised 26 November 2025 Accepted 29 November 2025
ORCID ID:http://orcid.org/0000-0003-2071-1996
https://doi.org/10.33192/smj.v78i2.278277

ABSTRACT

Objective: Emergent hemodialysis (HD) initiation has been consistently linked to higher mortality in prior studies, but evidence from Thailand is limited. This study evaluated the impact of elective versus emergent HD initiation in a tertiary-care setting.

Materials and Methods: This retrospective cohort study included adults with stage 5 chronic kidney disease who initiated HD at Siriraj Hospital between 2013 and 2022. Emergent initiation was defined as HD started for urgent indications without permanent vascular access; elective initiation was nephrologist-scheduled HD without acute complications. The primary outcomes were two-year all-cause mortality, cardiovascular events, hospitalizations, and vascular-access complications.

Results: Among 240 patients, 104 (43.3%) initiated HD emergently. These patients had higher rates of diabetes, poorer nutritional and metabolic profiles, less pre-dialysis care, and greater catheter use. Crude mortality was higher in the emergent group (15.4% vs. 10.3%), but after adjustment for comorbidities, functional status, and laboratory parameters, emergent initiation was not independently associated with mortality (adjusted HR 1.42, 95% CI 0.61–3.29). Infection-related deaths and vascular access infections were more frequent with emergent initiation, while vascular access dysfunction occurred more often in the elective group. Median hospitalization-free survival was shorter in the emergent group.

Conclusion: Emergent HD initiation was not an independent predictor of mortality, suggesting that excess risk observed in prior cohorts may reflect comorbidity and nutritional status rather than initiation type itself. Nevertheless, emergent initiation remained a marker of suboptimal pre-dialysis care and higher infection risk. Strengthening early nephrology referral, structured pre-dialysis planning, and infection prevention remains essential for optimizing ESRD outcomes.

Keywords: Hemodialysis initiation; unplanned start; emergent start; mortality; Thailand; ESRD (Siriraj Med J 2026;78(2):107-119)

INTRODUCTION

Chronic kidney disease (CKD) affects approximately 17%–18% of Thai adults and imposes a substantial burden in terms of morbidity, mortality, and healthcare expenditure.[1-3] As CKD progresses to end-stage renal disease (ESRD), chronic hemodialysis (HD) remains the predominant renal replacement modality in Thailand.[4] Achieving optimal outcomes with HD requires advance preparation, including timely nephrology referral, structured patient education, modality counseling, and permanent vascular access creation, processes that often require 6–12 months of coordinated care. Emerging evidence suggests that artificial intelligence–assisted prediction and care coordination may help facilitate timely preparation for hemodialysis initiation and vascular access planning.[5]

In practice, many patients initiate HD in an emergent manner, often due to life-threatening complications and in the absence of permanent access. Outcomes for patients on HD are influenced by a range of factors, particularly comorbidities such as diabetes mellitus (DM) and hypertension (HT).[6,7] Nonetheless, several prior studies, including those from Asian cohorts, have consistently reported that unplanned or emergent dialysis initiation is associated with higher short-term mortality, increased infection risk, and greater hospitalization compared with planned dialysis initiation.[8-10] In contrast, elective dialysis initiation is typically accompanied by pre-dialysis care, which has been linked to lower mortality, fewer cardiovascular events, and reduced vascular access complications.[11-14] Emergent initiation, frequently undertaken to address urgent CKD complications such as hyperkalemia, metabolic acidosis, or volume overload, typically requires temporary catheter placement, a factor strongly linked to worse clinical outcomes.

Despite this growing body of evidence, real-world data from Thailand on the impact of elective versus emergent HD initiation remain limited. Such context-specific evidence is essential, as healthcare delivery models, dialysis access pathways, and referral practices vary across regions. To address this knowledge gap, we conducted a retrospective cohort study at Siriraj Hospital to compare clinical characteristics and 2-year outcomes between patients initiating HD in an elective versus emergent manner.

MATERIALS AND METHODS

Study design and setting

We conducted a retrospective cohort study of patients

with CKD stage 5 who initiated chronic HD at Siriraj Hospital, a tertiary referral center in Bangkok, Thailand, between December 2013 and December 2022.

Study population

Eligible participants were Thai adults (≥18 years) of Thai nationality who underwent their first session of chronic HD during the study period. Patients were excluded if they initiated HD following kidney graft failure, received HD solely for acute kidney injury during hospitalization, had insufficient clinical data to determine the date of HD initiation, or lacked at least 24 months of follow-up (unless censored earlier due to death or transplantation).

Case identification and data collection

Potential cases were identified through the hospital's electronic database using ICD-9/10 codes related to CKD, ESRD, dialysis dependence, and vascular access procedures (codes N18, N180, N184, N185, N188, N19, Z992, 3995, 389, 3893, 3895, 39, 3927, 3949, 3953, 394, 3942, 3943; details shown in Supplementary Table 1). Medical records of all identified patients were manually reviewed to confirm eligibility and extract data.

Definition of exposure groups

Emergent HD initiation was defined as an urgent, unscheduled first HD session prompted by refractory complications (metabolic acidosis, hyperkalemia, volume overload, or uremia), typically without permanent vascular access and usually initiated in the emergency department. This group also included patients who had partially planned HD initiation (e.g., an AVF/AVG already created) but declined or postponed starting dialysis and subsequently required emergency HD due to emergent complications.

Elective HD initiation was defined as a nephrologist-scheduled first HD session without urgent clinical indication, with or without permanent access at initiation. Patients who had no acute complications and remained non-uremic could be electively initiated when their eGFR declined to below 6 mL/min/1.73 m^2, primarily to allow sufficient time for AVF/AVG maturation.

Variables collected

For each eligible patient, we recorded demographics (age, sex, weight, height, body mass index), comorbidities (including diabetes mellitus, hypertension, coronary artery disease, cerebrovascular disease, peripheral arterial disease, arrhythmia, chronic respiratory disease, cirrhosis, autoimmune disease, and malignancy) and primary kidney disease (diabetic nephropathy, hypertensive nephropathy, glomerular disease, polycystic kidney disease, obstructive nephropathy, cancer-related, other or unknown). We captured elements of pre-dialysis care, namely timing of the first nephrology visits and CKD stage at that visit, number of nephrology clinic visits, receipt and date of renal replacement therapy counseling and the first modality chosen, as well as vascular surgery involvement (whether seen, timing of first visit, and number of visits). Laboratory values were recorded both at CKD stage 5 diagnosis and at HD initiation, including blood urea nitrogen, serum creatinine, estimated glomerular filtration rate, hemoglobin, hematocrit, albumin, bicarbonate, sodium, potassium, chloride, calcium, phosphorus, intact parathyroid hormone, and ferritin. Vascular access type at the first chronic HD session was classified as non-cuffed, non-tunneled catheter, tunneled cuffed catheter, arteriovenous fistula or arteriovenous graft (AVF/AVG).

Outcomes

The primary outcome was all-cause mortality within 24 months of chronic HD initiation. Secondary outcomes included major adverse cardiovascular events (coronary artery disease or cerebrovascular disease), time to first hospitalization for any cause (excluding admissions for elective surgical procedures such as AVF/AVG creation), vascular-access infection and vascular-access dysfunction requiring intervention, all assessed within the same 24-month window. Follow-up time was calculated from the date of HD initiation until the first occurrence of each outcome, with censoring at kidney transplantation, loss to follow-up, or completion of 24 months, whichever came first.

Ethical issues

The study protocol was reviewed and approved by the Human Research Protection Unit, Faculty of Medicine Siriraj Hospital, Mahidol University (SIRB Protocol no. 960/2565 (IRB4), COA no. Si 279/2023). The study was conducted in accordance with the Declaration of Helsinki. Informed consent was waived due to the retrospective nature of the study.

Statistical analysis

All analyses were performed using IBM SPSS Statistics version 29.0.2.0 (IBM Corp., Armonk, NY, USA). Baseline characteristics were summarized as mean ± standard deviation (SD) or median with interquartile range (IQR) for continuous variables, depending on distribution, and as frequencies with percentages for categorical variables. Between-group differences were assessed using Student's t-test for normally distributed

continuous variables, Mann–Whitney U test for skewed distributions, and the chi-square or Fisher's exact test for categorical variables, as appropriate.

Time-to-event analyses were conducted from the date of HD initiation to the event of interest, with censoring at 24 months, kidney transplantation or loss to follow-up. Kaplan–Meier survival curves were generated, and between-group differences were evaluated using the log-rank test. Cox proportional hazards regression models were used to estimate hazard ratios (HRs) with 95% confidence intervals (CIs) for 2-year all-cause mortality and first hospitalization. For model building, variables with a p-value < 0.05 in the univariable analysis were considered eligible for inclusion in the multivariable Cox models. In addition, emergent HD initiation—the primary exposure of interest—was prespecified and included in all multivariable models regardless of its univariable p-value. This approach ensured that the final models incorporated both statistically significant predictors and clinically relevant covariates. The proportional hazards assumption was assessed using log–log survival plots and time-dependent covariate tests and was satisfied for all Cox models. All statistical tests were two-tailed, with $p < 0.05$ considered statistically significant.

RESULTS

A total of 756 patients were initially screened from the hospital database using ICD-9/10 codes. After exclusion of ineligible cases, including those with prior kidney transplant failure, dialysis for acute kidney injury, insufficient documentation, or inadequate follow-up, 240 patients with confirmed CKD stage 5 who initiated chronic HD between 2013 and 2022 were included in the final analysis (Fig 1). Of these, 104 patients (43.3%) initiated HD in an emergent manner, while 136 patients (56.7%) initiated HD in an elective manner.

Baseline demographic, clinical, and laboratory data are summarized in Table 1. The proportion of male patients was significantly lower in the emergent HD initiation group compared with the elective group (46.2% vs. 61.0%, $p = 0.02$). There were no statistically significant differences between groups in age at CKD stage 5 diagnosis, age at HD initiation, body weight, or body mass index.

Comorbidity profiles differed between groups. Diabetes mellitus was more common in the emergent group (72.1% vs. 56.6%, $p = 0.01$), as was peripheral arterial disease (4.8% vs. 1.5%, $p = 0.045$). Diabetic nephropathy was the most common underlying cause of CKD overall, but its prevalence was higher among emergent initiators (63.5% vs. 50.0%, $p = 0.04$). In contrast, glomerular disease was significantly more frequent in the elective group (20.6% vs. 6.7%, $p = 0.003$).

Pre-dialysis care also showed important differences. Four patients (3.8%) in the emergent group had never met a nephrologist before HD initiation. Moreover, a significantly greater proportion of emergently initiated patients had their first nephrology visit only after reaching CKD stage 5. In addition, the percentage of patients receiving vascular surgery care and the number of visits to a vascular surgeon before HD initiation were both markedly lower in the emergent group.

Marked contrasts were observed in vascular access type at initiation. Most emergently initiated patients

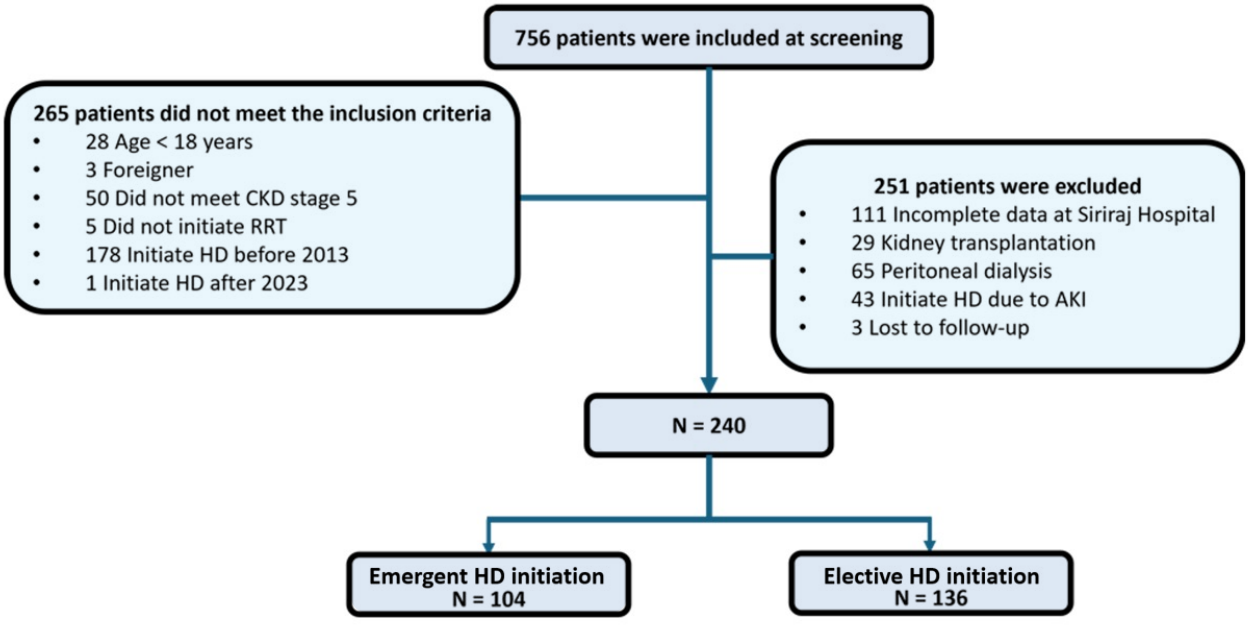

Fig 1. Flow diagram of study inclusion and exclusion criteria.

TABLE 1. Baseline characteristics.

Baseline Factors	Emergent HD initiation (N = 104)	Elective HD initiation (N = 136)	*p*-value
Male, N (%)	48 (46.2)	83 (61.0)	0.02
Age of CKD stage 5, y†	64±13	61±15	0.12
Age at HD initiation, y†	65±13	62±15	0.12
Body weight, kg†	63.1±15.7	63.8±13.8	0.73
Height, cm†	160.0±9.1	161.6±10.2	0.20
BMI, kg/m^{2}†	24.6±5.4	24.5±5.7	0.98
Co-morbidities, N (%)			
Diabetes mellitus	75 (72.1)	77 (56.6)	0.01
Hypertension	98 (94.2)	124 (91.2)	0.37
Dyslipidemia	58 (55.8)	81 (59.6)	0.56
Chronic respiratory disorder	5 (3.8)	3 (2.2)	0.27
Cirrhosis	4 (3.8)	5 (3.7)	0.95
Cerebrovascular disease	15 (14.4)	12 (8.8)	0.17
Coronary artery disease	22 (21.2)	25 (18.4)	0.59
Valvular heart disease	2 (1.9)	2 (1.5)	0.79
Arrhythmia	11 (10.6)	7 (5.1)	0.11
Peripheral arterial disease	5 (4.8)	2 (1.5)	0.04
Autoimmune disease	5 (4.8)	2 (1.5)	0.13
Cancer	10 (9.6)	8 (5.9)	0.28
Mobility status, N (%)			
Total dependent status	6 (5.8)	6 (4.4)	0.63
Need assistance	18 (17.3)	19 (14.0)	0.48
Independent status	80 (76.9)	111 (81.6)	0.37
Cause of CKD, N (%)			
Diabetic nephropathy	66 (63.5)	68 (50.0)	0.04
Hypertensive nephropathy	14 (13.5)	16 (11.8)	0.69
Glomerular disease	7 (6.7)	28 (20.6)	<0.01
Polycystic kidney disease	2 (1.9)	4 (2.9)	0.62
Obstructive nephropathy	5 (4.8)	2 (1.5)	0.13
Genitourinary cancer	0 (0)	1 (0.7)	0.38
Others	5 (4.8)	12 (8.8)	0.23
Unknown	5 (4.8)	5 (3.7)	0.75
Pre-dialysis care by nephrologist, N (%)	100 (96.2)	136 (100)	0.02
Stage of CKD at first visit nephrologist, N (%)			
Stage 2	2 (1.9)	3 (2.2)	0.88
Stage 3	14 (13.5)	32 (23.5)	0.05
Stage 4	43 (41.3)	68 (50.0)	0.18
Stage 5	41 (39.4)	33 (24.3)	0.01
No. of nephrologist visits†	4.5±1.3	4.9±0.5	<0.01

TABLE 1. Baseline characteristics. (Continue)

Baseline Factors	Emergent HD initiation (N = 104)	Elective HD initiation (N = 136)	*p*-value
eGFR at first nephrologist visit (mL/min/1.73 m²)‡	17.7 [12.0, 25.8]	22.2 [15.0, 30.5]	<0.01
Pre-dialysis care by vascular surgeon, N (%)	32 (30.8)	98 (72.1)	<0.01
No. of vascular surgeon visits‡	0 [0, 2]	3 [0, 5]	<0.01
RRT counseling, N (%)	96 (96.0)	136 (100)	0.02
First RRT mode chosen, N (%)			
Hemodialysis	75 (78.1)	119 (87.5)	0.06
Peritoneal dialysis	20 (20.8)	10 (7.4)	<0.01
Kidney transplant	1 (1.0)	7 (5.1)	0.09
Indication for dialysis initiation, N (%)			
GFR < 6 mL/min/1.73 m²	0 (0)	95 (69.9)	<0.01
Volume overload	67 (64.4)	15 (11.0)	<0.01
Hyperkalemia	5 (4.8)	1 (0.7)	0.04
Uremia	31 (29.8)	25 (18.4)	0.04
Acidosis	1 (1.0)	0 (0)	0.25
Vascular access at date of HD initiation, N (%)			
Non-cuffed, non-tunneled catheter	79 (76.0)	22 (16.3)	<0.01
Tunneled cuffed catheter	16 (15.4)	46 (34.1)	<0.01
AVF/AVG	9 (8.7)	67 (49.6)	<0.01
Laboratory data at HD initiation			
BUN (mg/dL)†	92.7±32.5	90.4±31.1	0.58
Creatinine (mg/dL)†	9.9±4.5	10.3±4.1	0.49
eGFR (mL/min/1.73 m²)‡	5.1 [3.6, 6.8]	4.9 [3.7, 6.6]	0.94
Sodium (mmol/L)†	135.4±5.7	135.7±5.3	0.65
Potassium (mmol/L)†	4.5±1.1	4.1±0.8	<0.01
Chloride (mmol/L)†	96.9±7.4	95.8±7.3	0.31
Bicarbonate (mmol/L)†	18.5±5.3	20.6±4.1	<0.01
Albumin (mg/dL)†	3.3±0.6	3.7±0.7	<0.01
Calcium (mg/dL)†	8.3±1.2	8.6±1.1	0.03
Phosphorus (mg/dL)†	6.1±2.6	5.8±1.7	0.47
iPTH (pg/mL)†	281.6±171.7	332.7±240.5	0.32
Hemoglobin (g/dL)†	8.7±1.9	9.5±1.6	<0.01
Hematocrit (%)†	26.9±5.8	28.9±5.0	<0.01
Ferritin (ng/mL)†	976.0±1189.5	612.5±449.3	0.07

†Presented as mean ± standard deviation

‡Presented as median (interquartile range)

Abbreviations: CKD; chronic kidney disease, HD; hemodialysis, BMI; body mass index, eGFR; estimated glomerular filtration rate, RRT; renal replacement therapy, AVF; arteriovenous fistula, AVG; arteriovenous graft, BUN; blood urea nitrogen, iPTH; intact parathyroid hormone

began HD with a non-cuffed, non-tunneled catheter (76.0% vs. 16.3%, $p < 0.001$). Conversely, use of AVF/AVG was significantly higher among elective initiators (49.6% vs. 8.7%, $p < 0.001$). Notably, the small proportion of elective patients who still initiated with a non-cuffed catheter did so mainly due to delayed AVF maturation (often > 6 months) or reimbursement-related delays.

Although eGFR at HD initiation did not differ significantly between groups, emergent initiation was associated with significantly worse biochemical markers, including lower serum albumin, hemoglobin, hematocrit, and bicarbonate levels. Detailed laboratory data at the time of renal replacement therapy counseling, CKD stage 5 diagnosis, and HD initiation are provided in the Supplementary Table 2.

Outcomes

Two-year outcomes by initiation type are summarized in Table 2. Overall mortality did not differ significantly between emergent and elective groups (15.4% vs. 10.3%, $p = 0.33$). Among those who died, infection was the leading cause in both groups, accounting for 81.3% of deaths in the emergent group and 71.4% in the elective group. Cancer and cardiovascular disease were less frequent causes of death and did not differ significantly between groups.

Hospitalization was common in both cohorts, with a numerically higher rate in the emergent group (71.2% vs. 52.6%, $p = 0.10$). Importantly, the median time to first hospitalization was significantly shorter in the emergent group (7.2 months [IQR 3.6 - 10.8]) compared with the elective group (16.4 months [IQR 10.6 - 22.2], $p = 0.03$). Rates of major adverse cardiovascular events were low in both groups and showed no significant differences.

Clear differences were observed in vascular access–related outcomes. Vascular access infection was significantly more common in the emergent group (25.0% vs. 10.3%, $p = 0.003$), consistent with greater reliance on temporary catheters. In contrast, vascular access dysfunction was more frequent in the elective group (26.5% vs. 12.5%, $p = 0.008$), likely reflecting the longer duration of AVF/AVG use.

In summary, while overall mortality did not differ by initiation type, unplanned initiation was associated with a shorter hospitalization-free interval and higher risk of vascular access infection, whereas planned initiation was linked to greater vascular access dysfunction over time.

TABLE 2. Comparative outcomes between emergent and elective HD initiation group.

Outcomes	Emergent HD initiation (N = 104)	Elective HD initiation (N = 136)	*p*-value
Overall death, N (%)	16 (15.4)	14 (10.3)	0.33
Cause of death, N (%)			
Infection	13 (81.3)	10 (71.4)	0.53
Cancer	3 (18.2)	2 (14.4)	0.74
Coronary artery disease	0 (0)	1 (7.1)	0.28
Hospitalization, N (%)	74 (71.2)	82 (52.6)	0.10
Median time to first hospitalization, months‡	7.2 [3.6, 10.8]	16.4 [10.6, 22.2]	0.03
Coronary artery disease, N (%)	14 (13.5)	12 (8.8)	0.30
Cerebrovascular disease, N (%)	10 (9.6)	5 (3.7)	0.06
Vascular access infection, N (%)	26 (25.0)	14 (10.3)	<0.01
Vascular access dysfunction, N (%)	13 (12.5)	36 (26.5)	<0.01

‡Presented as median (interquartile range)
Abbreviation: HD; hemodialysis

Survival analysis and predictors of two-year mortality

Overall cumulative survival for the cohort was 95% at 12 months and 87% at 24 months following HD initiation. Survival was numerically lower among patients with emergent initiations at both time points (12 months: 92% vs. 98%; 24 months: 85% vs. 89%), although differences between groups appeared modest on visual inspection of Kaplan–Meier curves (Fig 2a).

In univariate Cox analysis, emergent initiation was associated with a nonsignificant trend toward higher mortality (HR 1.58, 95% CI 0.77 -3.23; $p = 0.21$). After multivariable adjustment for demographic, clinical, and laboratory covariates, emergent initiation was not independently associated with mortality (adjusted HR 1.42, 95% CI 0.61 - 3.29; $p = 0.42$). Independent predictors of mortality included older age at HD initiation, non-dependent functional status (protective effect of independence) and lower serum albumin levels at initiation. Other comorbidities (e.g., diabetes, coronary artery disease, prior cerebrovascular disease) and initiation with AVF/AVG were not significant in the adjusted model (Table 3).

Hospitalization

Hospitalization was frequent in both groups, with a clearly shorter hospitalization-free interval among emergent HD initiators. The Kaplan–Meier curves (Fig 2b) show earlier divergence in the emergent group, consistent with a higher hospitalization burden.

In Cox models (Table 4), emergent initiation was associated with a higher risk of first hospitalization in univariate analysis (HR 1.60, 95% CI 1.17 -2.19; $p = 0.004$) but this association was no longer significant after multivariable adjustment (adjusted HR 1.00, 95% CI 0.67 - 1.48; $p = 0.98$). Several factors were linked to hospitalization in univariate analyses: diabetes mellitus, coronary artery disease, and lower serum albumin were associated with higher risk, while initiation with AVF/AVG and pre-dialysis nephrology care appeared protective. In the multivariable model, higher eGFR at HD initiation remained independently associated with an increased risk of hospitalization (adjusted HR 1.09 per mL/min/1.73 m^2, 95% CI 1.03 -1.15; $p < 0.01$), whereas initiation with AVF/AVG and higher albumin showed borderline protective trends. These findings indicate that the excess hospitalization observed with emergent starts is largely explained by case-mix and baseline clinical status rather than the initiation pathway per se.

Subgroup analysis by vascular access

This sensitivity analysis was performed to address potential misclassification of patients who initiated with a non-cuffed, non-tunneled catheter but were categorized as elective. To disentangle the initiation pathway from the access type, we stratified outcomes by vascular access used at first HD and then compared elective vs. emergent initiation within each access subgroup. Among patients starting with a non-cuffed, non-tunneled catheter, emergent initiation was not associated with higher two-year mortality or shorter hospitalization-free survival. Results were likewise nonsignificant within the tunneled cuffed catheter and AVF/AVG groups (data provided in the Supplementary Table 3). Overall, these findings indicate that inclusion of some non-cuffed, non-tunneled catheter cases within the elective initiation group does not explain the absence of an independent mortality effect of unplanned initiation. Rather, the null association appears consistent across access types, though interpretation is limited by wide confidence intervals in smaller subgroups.

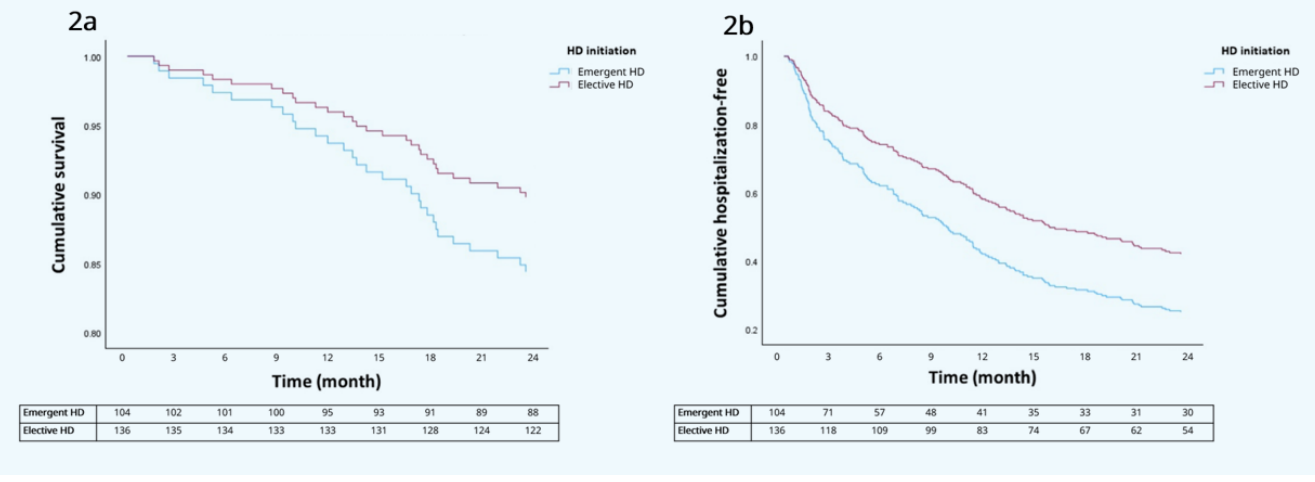

Fig 2. **(A)** Patient survival in emergent and elective HD initiation groups. **(B)** Hospitalization-free survival in emergent and elective HD initiation groups.

TABLE 3. Cox regression analysis of factors associated with patient survival.

Factors	Univariate analysis		Multivariate analysis	
	HR (95% CI)	*p*-value	HR (95% CI)	*p*-value
Female	1.58 (0.77-3.25)	0.22		
Age at HD initiation	1.07 (1.03-1.11)	<0.01	1.06 (1.02-1.11)	<0.01
BMI	0.99 (0.92-1.06)	0.72		
Co-morbidities				
Diabetes mellitus	1.40 (0.64-3.05)	0.40		
Hypertension	1.17 (0.28-4.91)	0.83		
Dyslipidemia	0.95 (0.46-1.95)	0.88		
Chronic respiratory disorder	1.07 (0.15-7.85)	0.95		
Cirrhosis	5.30 (1.85-15.20)	<0.01	3.19 (0.78-12.96)	0.11
Cerebrovascular disease	1.28 (0.44-3.63)	0.66		
Coronary artery disease	1.82 (0.83-3.98)	0.13		
Valvular heart disease	2.24 (0.31-16.44)	0.43		
Arrhythmia	3.46 (1.41-8.47)	<0.01	2.19 (0.76-6.34)	0.15
Peripheral arterial disease	0.05 (0.00-957.55)	0.55		
Autoimmune disease	1.08 (0.15-7.93)	0.94		
Cancer	3.65 (1.49-8.95)	<0.01	0.63 (0.17-2.34)	0.49
Totally independent status	0.20 (0.10-0.40)	<0.01	0.31 (0.13-0.76)	0.01
Pre-dialysis nephrologist care	20.64 (0.00-3703933.93)	0.62		
eGFR at first nephrologist visit	0.99 (0.96-1.02)	0.51		
Pre-dialysis nephrologist visit no.	1.16 (0.71-1.90)	0.56		
Pre-dialysis RRT counseling	0.40 (0.06-2.96)	0.37		
Pre-dialysis vascular surgeon visit	0.35 (0.16-0.76)	<0.01	1.21 (0.15-9.99)	0.86
Pre-dialysis vascular surgeon visit no.	0.76 (0.62-0.94)	<0.01	0.80 (0.42-1.53)	0.49
Emergent HD initiation	1.58 (0.77-3.23)	0.21	1.42 (0.61-3.29)	0.42
HD initiation with AVF/AVG	0.14 (0.03-0.60)	<0.01	0.31 (0.03-3.05)	0.31
Laboratory at HD initiation				
Albumin	0.39 (0.22-0.70)	<0.01	0.44 (0.20-0.96)	0.04
Hematocrit	0.97 (0.90-1.03)	0.28		
eGFR	1.10 (1.02-1.19)	0.02	1.03 (0.91-1.17)	0.67

Abbreviations: HD; hemodialysis, BMI; body mass index, eGFR; estimated glomerular filtration rate, RRT; renal replacement therapy, AVF; arteriovenous fistula, AVG; arteriovenous graft

TABLE 4. Cox regression analysis of factors associated with time to first hospitalization.

Factors	Univariate analysis		Multivariate analysis	
	HR (95% CI)	*p*-value	HR (95% CI)	*p*-value
Female	1.14 (0.83-1.56)	0.42		
Age at HD initiation	1.01 (1.00-1.02)	0.04	1.01 (0.99-1.02)	0.28
BMI	1.01 (0.99-1.04)	0.38		
Co-morbidities				
• Diabetes mellitus	1.56 (1.11-2.18)	0.01	1.08 (0.72-1.62)	0.73
• Hypertension	1.26 (0.67-2.40)	0.47		
• Dyslipidemia	1.15 (0.83-1.58)	0.41		
• Chronic respiratory disorder	0.64 (0.24-1.73)	0.38		
• Cirrhosis	1.65 (0.77-3.52)	0.20		
• Cerebrovascular disease	1.29 (0.80-2.09)	0.30		
• Coronary artery disease	1.57 (1.09-2.27)	0.02	1.44 (0.92-2.23)	0.11
• Valvular heart disease	2.23 (0.85-6.33)	0.10		
• Arrhythmia	1.66 (0.99-2.78)	0.06		
• Peripheral arterial disease	1.83 (0.75-4.46)	0.19		
• Autoimmune disease	1.55 (0.64-3.78)	0.34		
• Cancer	1.52 (0.88-2.64)	0.13		
Totally independent status	0.79 (0.54-1.15)	0.22		
Pre-dialysis nephrologist care	0.36 (0.13-0.98)	0.04	0.54 (0.13-2.25)	0.40
eGFR at first nephrologist visit	1.00 (0.99-1.01)	0.90		
Pre-dialysis nephrologist visit no.	0.89 (0.76-1.04)	0.14		
Pre-dialysis RRT counseling	1.56 (0.39-6.29)	0.53		
Pre-dialysis vascular surgeon visit	0.88 (0.64-1.21)	0.43		
Pre-dialysis vascular surgeon visit no.	0.96 (0.89-1.03)	0.26		
Emergent HD initiation	1.60 (1.17-2.19)	<0.01	1.00 (0.67-1.48)	0.98
HD initiation with AVF/AVG	0.55 (0.38-0.80)	<0.01	0.63 (0.39-1.03)	0.07
Lab at HD initiation				
• Albumin	0.64 (0.49-0.83)	<0.01	0.76 (0.55-1.05)	0.09
• Hematocrit	0.99 (0.96-1.02)	0.39		
• eGFR	1.10 (1.05-1.15)	<0.01	1.09 (1.03-1.15)	<0.01

Abbreviations: HD; hemodialysis, BMI; body mass index, eGFR; estimated glomerular filtration rate, RRT; renal replacement therapy, AVF; arteriovenous fistula, AVG; arteriovenous graft

DISCUSSION

In this single-center Thai cohort, emergent HD initiation was associated with poorer baseline nutritional and metabolic status, greater catheter use, a shorter hospitalization-free interval, and higher rates of vascular access infection. However, it was not an independent predictor of two-year all-cause mortality after adjustment. Instead, survival was influenced by age, functional dependence, and hypoalbuminemia at initiation. These results suggest that emergent initiation serves more as a marker of case-mix and clinical frailty than as a direct causal factor for mortality in this setting.

Although 96% of patients who initiated HD emergently had received pre-dialysis nephrology care, their CKD stage at first nephrology visit was substantially more advanced, and they had significantly fewer nephrology visits compared with the elective group. These factors likely limited opportunities for timely education, access planning, and preparation. Additional contributors may include patient refusal or postponement of planned dialysis and rapid acute deterioration. Together, these findings highlight that mere nephrology contact does not ensure planned initiation, underscoring the need for earlier referral and more structured, frequent pre-dialysis follow-up.

Earlier work links late referral or unplanned/emergency starts to worse outcomes, including higher mortality, longer hospital stays, and less optimal access preparation.[11,15-18] A recent systematic review and meta-analysis also confirmed a lower risk of mortality, shorter lengths of initial hospitalization and better preparations for renal replacement therapy among patients referred early to nephrologists.[19] Previous Thai data also suggested better survival among patients who accepted renal replacement therapy after counseling.[20]

Conversely, studies focused specifically on emergency or urgent dialysis starts, such as the French REIN registry analysis,[9] a Taiwanese cohort stratifying planned elective vs planned/unplanned urgent starts,[10] and a Japanese retrospective cohort,[21] generally reported higher mortality with emergency/unplanned pathways. Another study in a Thai population also showed an increased mortality in patients initiating HD with a catheter compared to AVF/AVG.[22]

Our adjusted null association contrasts with those reports, but the direction of crude effects in our data (higher unadjusted mortality and infection with emergent starts) is consistent with the prior signal. Several contextual and methodological factors likely explain the discrepancy. Firstly, the definitions of initial pathways used were different. We used manual chart review to classify initiation, whereas many prior studies relied on administrative definitions (e.g., very short referral intervals, first dialysis within 24 h of a nephrology visit, or access type as a proxy). Administrative approaches may pool heterogeneous patients and overestimate the risk of emergent status. Manual review likely reduced misclassification and better captured clinical context.

Secondly, pre-dialysis exposure in emergently initiated patients may be of significance. A notable proportion of patients labeled emergent in our cohort had some prior nephrology contact, medication optimization, and elements of education, all of which are features that could attenuate risk relative to emergency-start cohorts in other settings.

Thirdly, the timing of dialysis initiation in our cohort was at a lower eGFR than some Western datasets, potentially narrowing differences in early hazard between groups. If both elective and emergent initiation occur late (biochemically), residual between-group mortality differences may be muted.

Fourthly, the health-system capacity at Siriraj Hospital, a tertiary care center, may provide rapid stabilization and infection control that blunts early excess risk associated with emergent starts, especially when temporary catheters are promptly converted or rigorously managed. In addition, post-initiation factors may further influence outcomes. Differences in dialysis adequacy and prescription adjustments can have an effect, these include electrolytes and clearance.[23,24] Although evidence shows that modern dialyzers achieve adequate delivered dose even at lower dialysate flow rates and with reuse, suggesting that adequacy depends more on appropriate prescription than intensity alone.[25] Fluid management is another key determinant, as subclinical volume overload—better detected by lung ultrasound than routine examination—has been associated with higher hospitalization and mortality.[26] Patient-level factors such as biological aging and metabolic burden may also increase morbidity.[27-29] Together, these considerations highlight that outcomes after HD initiation are shaped not only by the mode of start but also by ongoing adequacy, volume control, and individualized treatment adjustments.

Lastly, access-based misclassification was addressed. Since some elective patients began HD with a non-cuffed, non-tunneled catheter (e.g., delayed AVF maturation, reimbursement delays), we performed access-stratified analyses. Within each access subgroup, emergent initiation was not associated with mortality or hospitalization, suggesting that the null association was not due to misclassification.

The excess vascular-access infection observed in

emergent starts aligns with the biological risk conferred by catheter dependence and is consistent with literature linking catheters to infectious complications and adverse outcomes.[30,31] Conversely, the higher access dysfunction in elective starters likely reflects their greater and longer exposure to AVF/AVG, with complications occurring over time rather than early catastrophic events. Recurrent stenosis is a major driver of access failure, hospitalization, and subsequent catheter use, underscoring the importance of durable access function. Prior studies further suggest that drug-coated balloon angioplasty offers superior primary patency compared with plain balloon angioplasty, highlighting the potential to mitigate long-term restenosis.[32] Together, these findings support a model in which catheter-related infection and patient frailty drive near-term events, while long-term access maintenance dominates later morbidity.

The strengths of our study include detailed manual classification of initiation type, accurate characterization of pre-dialysis care, and adjustment for functional and biochemical status. Limitations include the retrospective, single-center design, potential residual confounding, and limited statistical power for subgroup analyses (as evidenced by wide CIs, especially in the AVF/AVG subgroup). We also did not assess patient-reported outcomes of quality of life, which may differ between initiation pathways despite similar mortality.

CONCLUSION

Our study challenges the assumption that emergent HD initiation inevitably leads to worse survival, showing instead that mortality risk is more strongly influenced by patient comorbidity and nutritional status. However, emergent initiation remains a marker of suboptimal pre-dialysis care and higher infection risk. Improving early referral, structured education, and multidisciplinary planning remain essential for ESRD care.

Data Availability Statement

The data that support the findings of this study are not publicly available due to their containing information that could compromise the privacy of research participants but are available from the corresponding author (K.V.) upon reasonable request.

ACKNOWLEDGEMENT

None.

DECLARATIONS

Grants and Funding Information

This research did not receive any specific funding.

Conflict of Interest

The authors declare that they have no competing interests.

Registration Number of Clinical Trial

Not applicable.

Authors' Contributions

Conceptualization and methodology, K.V. and K.C.; Investigation, K.V., K.C. and L.U.; Formal analysis, K.V. and K.C.; Visualization and writing – original draft, K.V., K.C. and L.U.; Writing – review and editing, K.V. and L.U., Supervision, K.V. All authors have read and agreed to the final version of the manuscript.

Use of Artificial Intelligence

This research did not use any artificial intelligence in any of the processes.

IRB Approval

The study protocol was reviewed and approved by the Human Research Protection Unit, Faculty of Medicine Siriraj Hospital, Mahidol University (SIRB Protocol no. 960/2565 (IRB4), COA no. Si 279/2023) and was conducted according to the principles of the Declaration of Helsinki. Informed consent was waived due to the retrospective nature of the study.

REFERENCES

1. Ingsathit A, Thakkinstian A, Chaiprasert A, Sangthawan P, Gojaseni P, Kiattisunthorn K, et al. Prevalence and risk factors of chronic kidney disease in the Thai adult population: Thai SEEK study. Nephrol Dial Transplant. 2010;25(5):1567-75.
2. Ong-Ajyooth L, Vareesangthip K, Khonputsa P, Aekplakorn W. Prevalence of chronic kidney disease in Thai adults: a national health survey. BMC Nephrol. 2009;10:35.
3. Perkovic V, Cass A, Patel AA, Suriyawongpaisal P, Barzi F, Chadban S, et al. High prevalence of chronic kidney disease in Thailand. Kidney Int. 2008;73(4):473-9.
4. Thai Renal Replacement Therapy (TRT) Registry 2023 Annual Data Report: The Subcommittee of the Thai Renal Replacement Therapy (TRT) Registry 2024, The Nephrology Society of Thailand; March 2025 [cited 2025 Apr 21]. Available from: https://www.nephrothai.org/wp-content/uploads/2025/03/Ebook-TRT-book-2023-10-Mar-2025Final.pdf.
5. Alnaser RI, Abed MN, Alassaf FA, Alsaaty MH. Integrating Artificial Intelligence into Chronic Kidney Disease Care: Enhancing Hemodialysis Scheduling, Comorbidity Management, and Diagnostic Capabilities. Siriraj Med J. 2025;77(7):543-52.
6. Mori K, Nishide K, Okuno S, Shoji T, Emoto M, Tsuda A, et al. Impact of diabetes on sarcopenia and mortality in patients undergoing hemodialysis. BMC Nephrol. 2019;20(1):105.
7. Couchoud C, Moranne O, Frimat L, Labeeuw M, Allot V, Stengel B. Associations between comorbidities, treatment choice and outcome in the elderly with end-stage renal disease.

Nephrol Dial Transplant. 2007;22(11):3246-54.
8. Anutrakulchai S, Mairiang P, Pongskul C, Thepsuthammarat K, Chan-On C, Thinkhamrop B. Mortality and treatment costs of hospitalized chronic kidney disease patients between the three major health insurance schemes in Thailand. BMC Health Serv Res. 2016;16(1):528.
9. Michel A, Pladys A, Bayat S, Couchoud C, Hannedouche T, Vigneau C. Deleterious effects of dialysis emergency start, insights from the French REIN registry. BMC Nephrol. 2018; 19(1):233.
10. Chen YM, Wang YC, Hwang SJ, Lin SH, Wu KD. Patterns of Dialysis Initiation Affect Outcomes of Incident Hemodialysis Patients. Nephron. 2016;132(1):33-42.
11. Stack AG. Impact of timing of nephrology referral and pre-ESRD care on mortality risk among new ESRD patients in the United States. Am J Kidney Dis. 2003;41(2):310-8.
12. Hwang SJ, Yang WC, Lin MY, Mau LW, Chen HC, Taiwan Society of N. Impact of the clinical conditions at dialysis initiation on mortality in incident haemodialysis patients: a national cohort study in Taiwan. Nephrol Dial Transplant. 2010;25(8): 2616-24.
13. Wu LC, Lin MY, Hsieh CC, Chiu HC, Mau LW, Chiu YW, et al. Planned creation of vascular access saves medical expenses for incident dialysis patients. Kaohsiung J Med Sci. 2009;25(10): 521-9.
14. Ethier J, Mendelssohn DC, Elder SJ, Hasegawa T, Akizawa T, Akiba T, et al. Vascular access use and outcomes: an international perspective from the Dialysis Outcomes and Practice Patterns Study. Nephrol Dial Transplant. 2008;23(10):3219-26.
15. Kazmi WH, Obrador GT, Khan SS, Pereira BJ, Kausz AT. Late nephrology referral and mortality among patients with end-stage renal disease: a propensity score analysis. Nephrol Dial Transplant. 2004;19(7):1808-14.
16. Pena JM, Logrono JM, Pernaute R, Laviades C, Virto R, Vicente de Vera C. Late nephrology referral influences on morbidity and mortality of hemodialysis patients. A provincial study. Nefrologia. 2006;26(1):84-97.
17. Gallego E, Lopez A, Lorenzo I, Lopez E, Llamas F, Illescas ML, et al. Influence of early or late referral to nephrologist over morbidity and mortality in hemodialysis. Nefrologia. 2003;23(3): 234-42.
18. Diegoli H, Silva MC, Machado DS, Cruz CE. Late nephrologist referral and mortality association in dialytic patients. J Bras Nefrol. 2015;37(1):32-7.
19. Cheng L, Hu N, Song D, Liu L, Chen Y. Early versus late nephrology referral and patient outcomes in chronic kidney disease: an updated systematic review and meta-analysis. BMC Nephrol. 2025;26(1):25.
20. Watcharotone N, Moolvong P, Matula K, Kosukhvivadhana D. Survival outcome after decision making for renal replacement therapy in chronic renal failure. Journal of the Nephrology Society of Thailand. 2022;28(1):68-76.
21. Shimizu Y, Nakata J, Yanagisawa N, Shirotani Y, Fukuzaki H, Nohara N, et al. Emergent initiation of dialysis is related to an increase in both mortality and medical costs. Sci Rep. 2020;10(1): 19638.
22. Wara-aswapati S, Chuasuwan A. Survival rate and associated factors of unplanned hemodialysis initiation among end stage kidney disease patients. Royal Thai Air Force Medical Gazette. 2022;68(1):10-20.
23. Vareesangthip K, Davenport A. Reducing the risk of intradialytic hypotension by altering the composition of the dialysate. Hemodial Int. 2020;24(3):276-81.
24. Vareesangthip K, Yincharoen P, Winijkul A, Chanchairujira T. Cardiac arrhythmia during early-week and mid-week dialysis in hemodialysis patients. Ther Apher Dial. 2021;25(6):890-8.
25. Srisuwan W, Charoensri S, Jantarakana K, Chanchairujira T. Increasing Dialysate Flow Rate over 500 ml/min for Reused High-Flux Dialyzers do not Increase Delivered Dialysis Dose: A Prospective Randomized Cross Over Study. Siriraj Med J. 2022; 74(3):152-60.
26. Vareesangthip K, Thanapattaraborisuth B, Chanchairujira K, Wonglaksanapimon S, Chanchairujira T. Assessment of Volume Status in Chronic Hemodialysis: Comparison of Lung Ultrasound to Clinical Practice and Bioimpedance. Siriraj Med J. 2023;75(3): 224-33.
27. Taesilapasathit C, Spanuchart I, Suppadungsuk S, Sutharattanapong N, Vipattawat K, Sethakarun S, et al. Accumulation of Advanced Glycation End Products Independently Increases the Risk of Hospitalization Among Hemodialysis Patients. Siriraj Med J. 2022;74(5):305-13.
28. Thaweethamcharoen T, Vasuvattakul S, Noparatayaporn P. Comparison of Utility Scores and Quality of Life Scores in Thai Patients between Twice and Thrice-Weekly Hemodialysis. Siriraj Med J. 2020;64(3):94-7.
29. Tangwonglert T, Vareesangthip K, Vongsanim S, Davenport A. Comparison of skin autofluorescence, a marker of tissue advanced glycation end-products in the fistula and non-fistula arms of patients treated by hemodialysis. Artif Organs. 2020; 44(11):1224-7.
30. Mohamed H, Ali A, Browne LD, O'Connell NH, Casserly L, Stack AG, et al. Determinants and outcomes of access-related blood-stream infections among Irish haemodialysis patients; a cohort study. BMC Nephrol. 2019;20(1):68.
31. Campos E, Cuevas-Budhart MA, Cedillo-Flores R, Candelario-Lopez J, Jimenez R, Flores-Almonte A, et al. Is central venous catheter in haemodialysis still the main factor of mortality after hospitalization? BMC Nephrol. 2024;25(1):90.
32. Chaivanit T, Chaivanit P, Bumrungrachapukdee P, Unprasert P, Wattanavaekin K, Benyakorn T. Comparison of Primary Patency Rate between Drug- Coated Balloon and Plain Balloon Angioplasty in Hemodialysis Access. Siriraj Med J. 2022;74(6): 388-94.

Integrative Transcriptomic Analysis Reveals Synaptic Pathway-Enriched Prognostic Gene Signature in Glioblastoma

Vivin Andriani, S.Si., M.Sc.[1], Fenny Fitriani, S.Si., M.Si.[2], Sari Setyo Ningrum[2], Gangga Anuraga, Ph.D.[2,*]

[1]Department of Biology, Faculty of Engineering and Science, Universitas PGRI Adi Buana Surabaya, Indonesia, [2]Department of Statistics, Faculty of Engineering and Science, Universitas PGRI Adi Buana Surabaya, Indonesia.

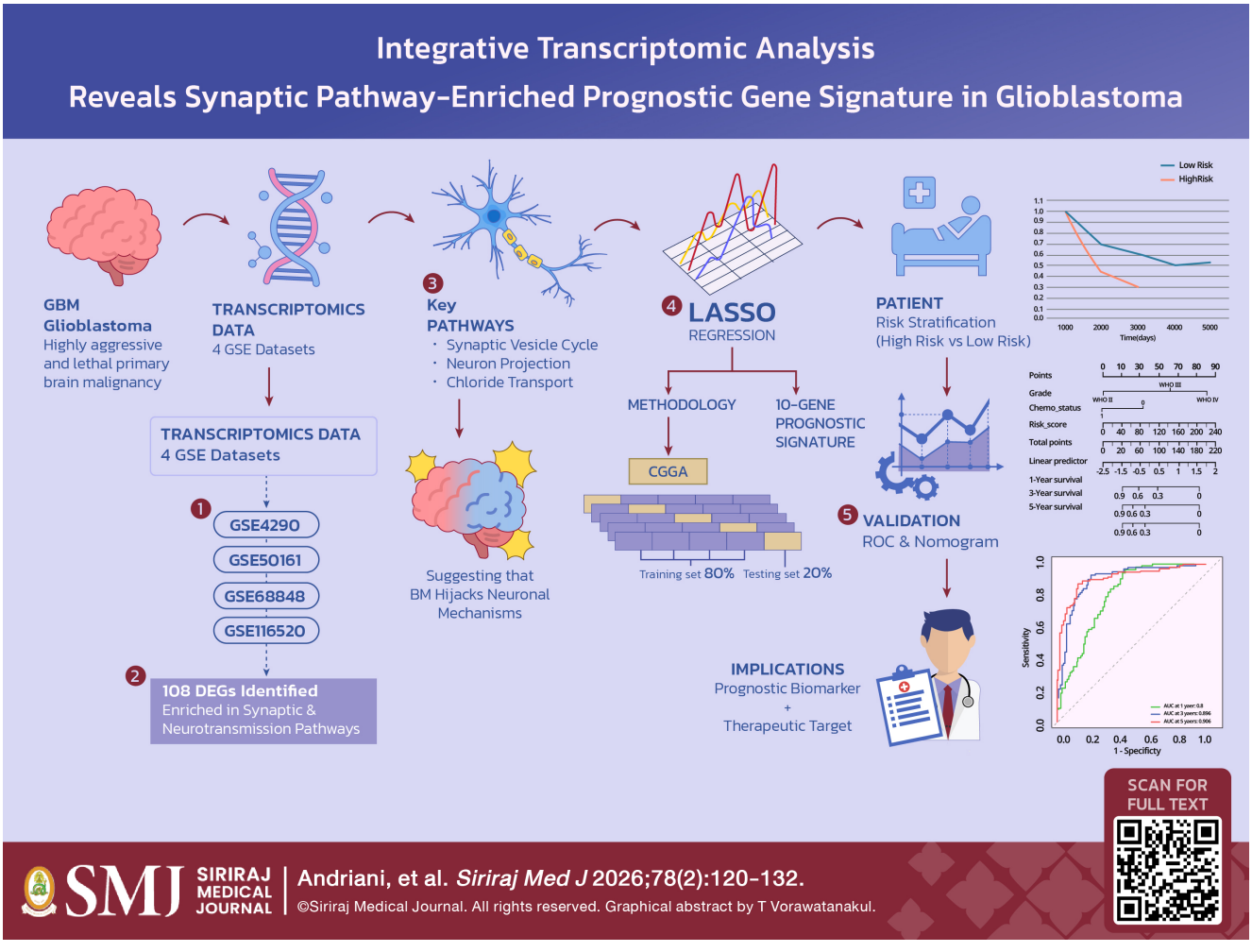

*Corresponding author: Gangga Anuraga
E-mail: g.anuraga@unipasby.ac.id
Received 29 September 2025 Revised 29 November 2025 Accepted 22 December 2025
ORCID ID:http://orcid.org/0000-0002-0902-3968
https://doi.org/10.33192/smj.v78i2.277969

ABSTRACT

Objective: This study aimed to elucidate the transcriptomic landscape of glioblastoma (GBM) by integrating multiple datasets to identify prognostically significant gene signatures and investigate the involvement of synaptic pathways.

Materials and Methods: Four transcriptomic datasets were analyzed using the limma pipeline for differential gene expression analysis with empirical Bayes moderation to identify differentially expressed genes (DEGs). Functional enrichment analyses were conducted via Gene Ontology and KEGG. A prognostic model was constructed using LASSO-Cox regression on the CGGA mRNAseq_693 cohort (n=693) and validated on the CGGA_325 cohort (n=325). Multivariate Cox proportional hazards regression assessed the model's independent prognostic value. External validation of gene expression was performed using TCGA (n=163) and GTEx (n=207) datasets.

Results: A total of 108 consistently dysregulated DEGs were identified, enriched in synaptic vesicle cycling, neuronal projection, and chloride transport pathways. A robust ten-gene prognostic signature (SPRY1, CD58, RCC1, E2F7, BUB1, FAM46A, TYMS, NEDD9, CHST14, REPS2) effectively stratified patients, with time-dependent ROC AUCs of 0.718, 0.755, and 0.757 at 1-, 3-, and 5-year survival points. Multivariate Cox analysis confirmed the model's independent prognostic value, further refined by a nomogram with AUCs of 0.8, 0.898, and 0.906. Differential expression of all ten genes was validated externally.

Conclusion: This study reveals a previously underexplored synaptic pathway-related gene signature with strong prognostic relevance for GBM. The ten-gene model offers a clinically applicable tool for risk stratification and highlights neuron-tumor synaptic interactions as critical drivers of tumor progression, providing a foundation for future therapeutic strategies.

Keywords: Glioblastoma; transcriptomics; prognostic model; synaptic pathways; differentially expressed genes (Siriraj Med J 2026;78(2):120-132)

INTRODUCTION

Glioblastoma (GBM) is the most aggressive and lethal primary brain tumor, characterized by rapid progression and poor patient survival despite advances in surgical, radiotherapeutic, and chemotherapeutic interventions.[1] The median survival time remains approximately 15 months, underscoring the urgent need for improved prognostic biomarkers and therapeutic strategies for this disease.[1,2] Recent research has increasingly recognized the critical role of synaptic signaling in the pathophysiology of GBM.[3-5] Neuron-glioma synaptic interactions have been shown to facilitate tumor growth, invasion, and resistance to treatment by creating a tumor-supportive microenvironment.[6-8] These findings position synaptic pathways as promising targets for both prognostic biomarker discovery and novel therapeutic interventions.

Transcriptomic profiling serves as a systematic approach to explore biological processes by linking synaptic-associated gene expression with clinical outcomes,[9-12] thereby offering a precise strategy for developing prognostic models with biological relevance. This methodology facilitates the identification of differentially expressed genes (DEGs) that can act as prognostic markers or therapeutic targets. However, despite numerous transcriptomic studies, the integration of multiple datasets to construct robust, biologically informed prognostic models remains a challenge. Focusing specifically on synaptic pathway-related genes offers a targeted strategy to uncover the functional impact of neuron-tumor synaptic interactions on GBM progression.

This study employed integrative bioinformatics analyses of multiple publicly available GBM transcriptomic datasets to identify DEGs enriched in synaptic processes and correlated with patient prognosis. Through rigorous statistical modeling, including LASSO-Cox regression and multivariate Cox proportional hazards analyses, a synaptic pathway-enriched gene signature with strong prognostic value was constructed and validated in the TCGA cohort. This signature not only effectively stratifies patients but also highlights the molecular mechanisms underlying tumor progression mediated by synaptic signaling.

By bridging transcriptomic insights with the biological mechanisms of neuron-glioma interplay, this study advances the understanding of the GBM's molecular drivers of GBM. The identified gene signature enhances risk stratification beyond current prognostic markers, offering a clinically applicable tool for personalized management of patients. Furthermore, it provides a foundation for the development of targeted therapies aimed at disrupting tumor-promoting synaptic communication, which could improve treatment outcomes.

In summary, this synaptic-centric transcriptomic investigation addresses a critical gap in GBM research by integrating pathway-specific molecular data with clinical prognostic data. These findings provide novel insights into the role of synaptic signaling in GBM progression and present a validated prognostic model with potential clinical utility. This study supports the ongoing pursuit of precision medicine approaches that incorporate tumor microenvironmental interactions to improve prognosis and therapeutic efficacy in this devastating disease.

MATERIALS AND METHODS

Gene expression data acquisition and preprocessing

The gene expression data utilized in this study were derived from multiple publicly available microarray datasets. Four datasets—GSE4290,[13] GSE50161,[14] GSE68848,[15] and GSE11652016—were retrieved from the Gene Expression Omnibus (GEO) database (http://www.ncbi.nlm.nih.gov/geo/). These four GEO datasets were selected based on predefined criteria, including availability of both GBM and normal tissues, sufficient sample size, comparable profiling platforms, and high-quality normalized expression data enabling integrative analysis. Specifically, GSE4290, GSE50161, and GSE68848 were based on the Affymetrix Human Genome U133 Plus 2.0 Array (GPL570 platform), encompassing a total of 339 glioblastoma (GBM) tumor samples and 64 normal brain tissue samples. The GSE116520 dataset, generated using the Illumina HumanHT-12 V4.0 platform (GPL10558), comprises 17 GBM tumor samples and 8 normal controls, offering a comprehensive transcriptomic landscape for identifying robust DEGs.

Prognostic modeling employed gene expression and survival data from the mRNAseq_693 cohort of the CGGA (https://www.cgga.org.cn/index.jsp), constructing a LASSO-Cox risk model,[17,18] with clinical validation and nomogram development conducted using the CGGA_325 cohort. Expression validation of prognostic candidates was further corroborated using TCGA and GTEx datasets, enabling comparative analysis between GBM and normal brain tissues.

Identification of DEGs

DEGs were conducted using the "limma" package in R (v4.3.0), identifying DEGs based on $|\log2FC| > 1$ and $p < 0.05$, with Benjamini-Hochberg correction for false discovery rate. Venn diagram analysis (https://bioinfogp.cnb.csic.es/tools/venny/index.html) was employed to identify overlapping DEGs across datasets, with subsequent functional enrichment analysis to elucidate their biological relevance in GBM pathophysiology.

Functional enrichment analysis to elucidate biological relevance

Functional enrichment analysis was performed using the Enrichr platform (https://maayanlab.cloud/Enrichr/),[19-21] encompassing gene ontology (GO) analysis to elucidate overrepresented biological processes (BP), cellular components (CC), and molecular functions (MF),[22] alongside KEGG pathway analysis to delineate the involvement of DEGs in key signaling and metabolic pathways.[23] Input gene lists comprising DEGs with FDR-adjusted p-values below 0.05 were analyzed via Enrichr, prioritizing top-enriched GO terms and KEGG pathways based on a combined score that integrates p-value and z-score, thereby revealing key molecular mechanisms underlying GBM pathophysiology.

Construction of prognostic risk model via LASSO-Cox regression

The CGGA mRNAseq_693 dataset was randomly partitioned into training (80%) and testing (20%) subsets using stratified sampling based on survival status, with reproducibility ensured by applying a fixed random seed (set.seed = 123). LASSO regression was employed for simultaneous feature selection and model regularization,[17,24,25] with five-fold cross-validation to determine the optimal λ, minimizing prediction error and enhancing model generalizability.

The LASSO model was validated using the independent testing set, with risk scores calculated as a linear combination of gene expression values weighted by the LASSO-derived coefficients. Correlation analysis was conducted to assess gene-risk score associations, with the top ten genes visualized in a bar plot to delineate risk-promoting versus protective genes based on the direction and magnitude of their impact.

To evaluate the clinical utility of the risk score, patients in the test cohort were stratified into high- and low-risk groups based on the median risk score, followed by Kaplan–Meier survival analysis to compare overall survival.[18,26,27] Time-dependent ROC curves at 1, 3, and 5 years were generated to assess model discriminative power, with AUC values calculated to quantify predictive accuracy.

Clinicopathologic correlation analysis

Patients were stratified into high- and low-risk groups based on the median risk score. Differences in clinical characteristics were assessed using the Wilcoxon rank-sum test for Age (continuous variable) and Chi-square tests for categorical variables, including Gender, WHO Grade, Radiotherapy status, Chemotherapy status,

MGMT methylation status, and IDH mutation status. Statistical significance was defined as $p < 0.05$.

Independent prognostic factor analysis and nomogram construction

Cases with missing values in essential clinical variables, such as survival data, MGMT methylation, or IDH mutation status, were excluded from the multivariate Cox analysis, and no imputation was performed. The multivariate Cox regression analysis was conducted within the CGGA_325 cohort to assess the independent prognostic significance of the gene expression-derived risk score in conjunction with clinical and molecular variables, including age, gender, tumor grade, treatment status, MGMT methylation, and IDH mutation status, with hazard ratios (HRs) calculated at $p < 0.05$.

A prognostic nomogram was constructed using statistically significant variables,[28] assigning scores based on regression coefficients to predict 1-, 3-, and 5-year survival probabilities, with predictive accuracy assessed via time-dependent ROC curves and AUC values.[26,27] The CGGA_325 cohort showed comparable demographic characteristics to the CGGA mRNAseq_693 training cohort, particularly in terms of age distribution and sex proportion, supporting its suitability for external validation.

Expression validation of LASSO-selected genes utilizing GEPIA

Boxplot analyses performed via GEPIA, utilizing log2 (TPM + 1) normalization, $|\log2 \text{ fold change}| \geq 1$, and $p < 0.01$,[29] demonstrated significant differential expression of all selected genes between tumor and normal tissues, with most exhibiting marked overexpression in GBM samples, reinforcing their oncogenic potential and validation for inclusion in the LASSO-based prognostic model.

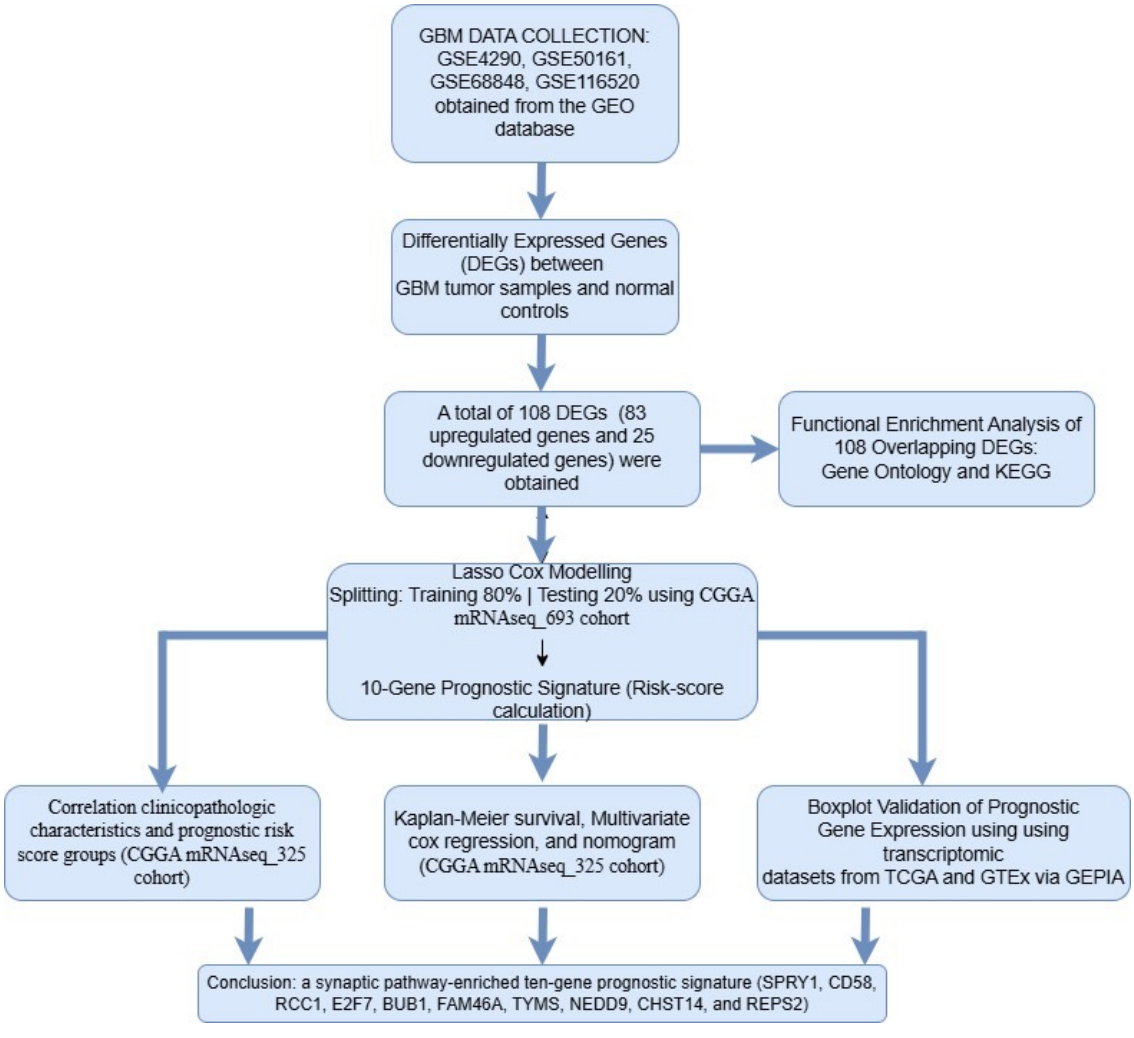

Fig 1. Overview of the study workflow. Transcriptomic datasets (GSE4290, GSE50161, GSE68848, GSE116520) were integrated for the screening of differentially expressed genes (DEGs), followed by synaptic-pathway enrichment and LASSO Cox modeling to develop a 10-gene prognostic signature. Validation was conducted using survival curves, receiver operating characteristic (ROC) analysis, and nomogram assessment. Clinical correlation analysis associated risk scores with grade, IDH status, and age, underscoring its potential clinical applicability.

RESULTS

Identification of DEGs and enrichment analysis in GBM

A comprehensive analysis was conducted involving 356 GBM tissue samples and 72 normal tissue samples. Each dataset was individually processed and analyzed using R software to generate lists of DEGs. Specifically, the GSE4290, GSE50161, GSE68848, and GSE116520 datasets were systematically examined, yielding 4,631 DEGs (2,284 upregulated, 2,349 downregulated), 5,385 DEGs (2,523 upregulated, 2,862 downregulated), 6,493 DEGs (3,412 upregulated, 3,081 downregulated), and 3,370 DEGs (1,862 upregulated, 1,508 downregulated), respectively (Fig 2A–D). Integration of datasets using a Venn diagram analysis identified 83 consistently upregulated DEGs (log2FC > 1) and 25 consistently downregulated DEGs (log2FC < -1) across all four datasets (Fig 2E, F).

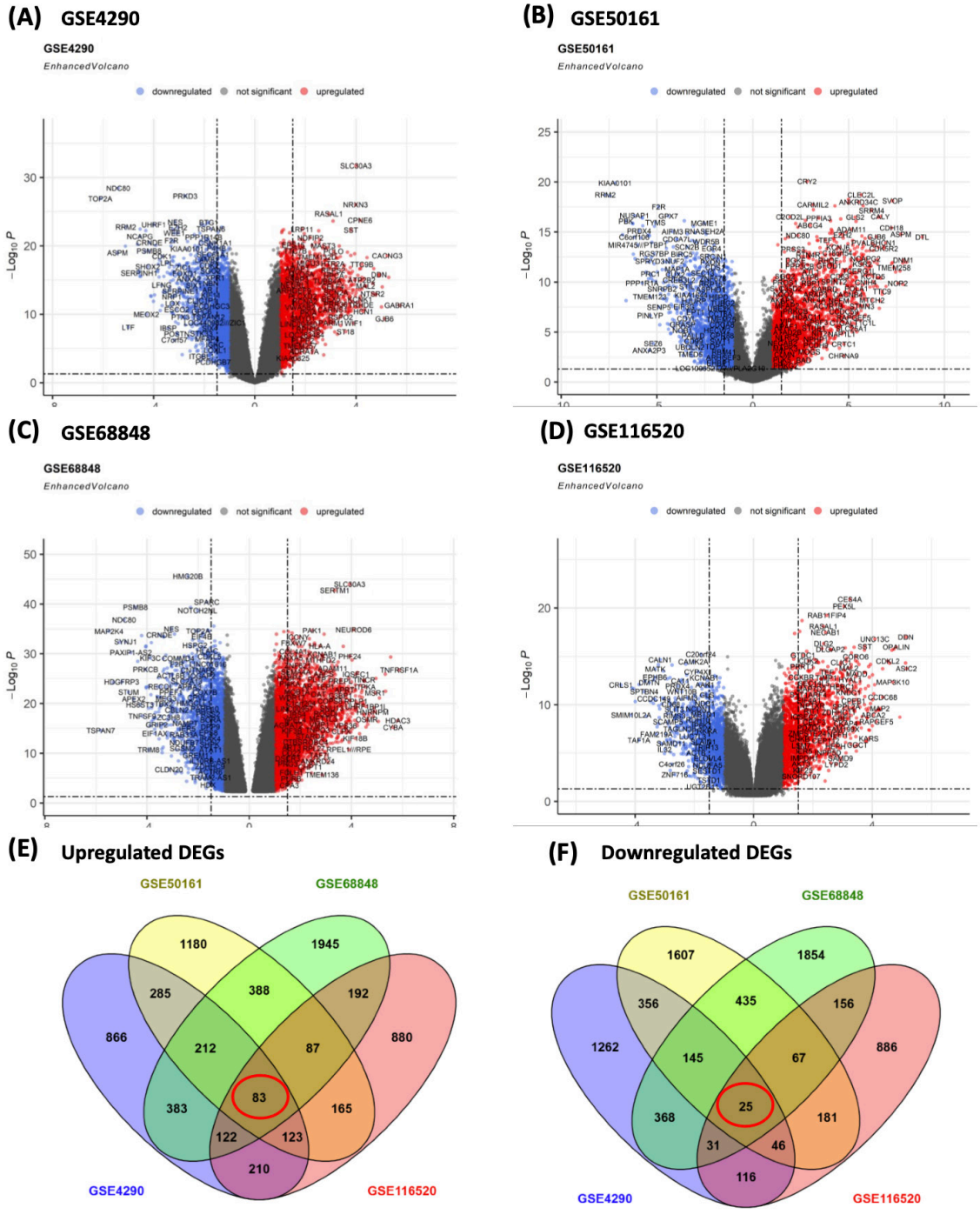

Fig 2. Identification of Differentially Expressed Genes (DEGs) in GBM Across Multiple Datasets. (A–D) Volcano plots illustrating DEGs across four GBM datasets, highlighting upregulated genes (log2FC ≥ 1, p < 0.05) in red, downregulated genes (log2FC ≤ -1, p < 0.05) in blue, and non-significant genes in gray, with log2 fold change on the x-axis and -log10(p) values on the y-axis. **(E, F)** Venn diagrams depicting the intersection of DEGs across GSE50161, GSE68848, GSE4290, and GSE116520, identifying 83 consistently upregulated **(E)** and 25 consistently downregulated DEGs **(F)**, potentially representing pivotal molecular drivers and candidate biomarkers in GBM pathogenesis.

GO and KEGG pathway enrichment analyses of the 108 overlapping DEGs in GBM revealed significant associations with neuronal projection, synaptic function, and chloride transmembrane transporter activity (Fig 3A–D). As shown in Fig 3A, the most significantly enriched BPs included chemical synaptic transmission (GO:0050804), positive regulation of catecholamine secretion (GO:0033605), and the synaptic vesicle cycle (GO:0099504). The synaptic vesicle cycle, a neuronal mechanism traditionally implicated in neurotransmitter release and recycling[30] has been increasingly recognized for its role in the synaptic integration of high-grade gliomas within neural networks, a process that significantly contributes to glioma progression in both preclinical models[4,31] and clinical patient samples.[32]

Cellular component (CC) analysis further identified significant enrichment in neuron projection (GO:0043005), exocytic vesicle membrane (GO:0099501), and synaptic vesicle membrane (GO:0030672) (Fig 3B). Meanwhile, molecular function (MF) analysis highlighted the enrichment of guanyl-nucleotide exchange factor activity (GO:0005085), protein heterodimerization (GO:0046982), and chloride transmembrane transporter activity (GO:0015108) (Fig 3C).

KEGG pathway analysis revealed significant enrichment in pathways associated with the synaptic vesicle cycle, neuroactive ligand-receptor interaction, insulin secretion, and GABAergic synapse (Fig 3D), highlighting the potential involvement of synaptic and neurotransmission-related genes in GBM pathogenesis and identifying promising therapeutic targets to disrupt tumor-neuron crosstalk.

LASSO analysis for prognostic gene identification in GBM

LASSO-Cox regression was applied to the 108 GBM-associated genes to construct a prognostic model, with the coefficients of selected genes plotted against the lambda parameter, illustrating the reduction of non-zero coefficients and refinement of a parsimonious model (Fig 4A). The optimal lambda value, balancing model complexity and predictive accuracy, was determined by plotting partial likelihood deviation against log(λ) (Fig 4B).

The analysis identified ten pivotal prognostic markers—SPRY1, CD58, RCC1, E2F7, BUB1, FAM46A, TYMS, NEDD9, CHST14, and REPS2—as the most robust predictors (Fig 4C), with correlation heatmap

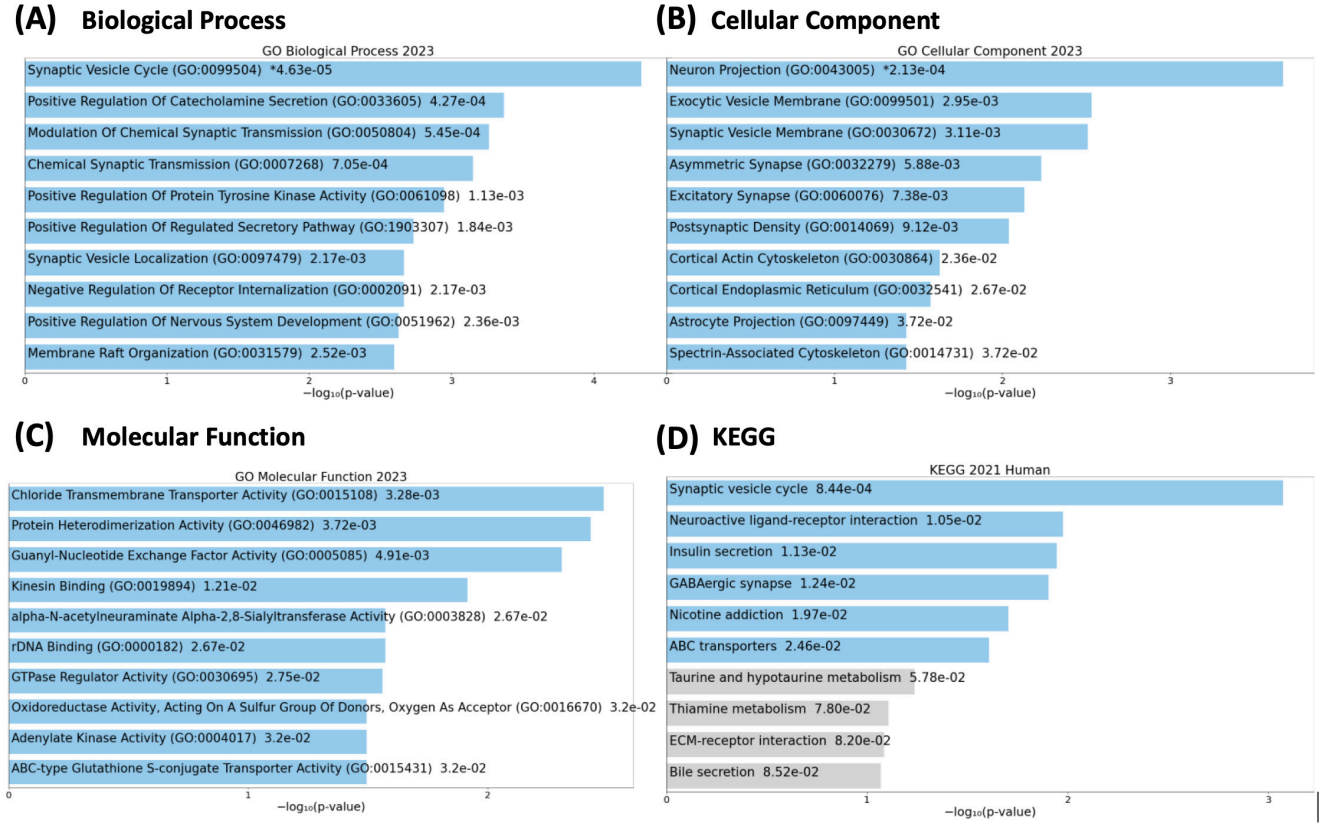

Fig 3. Functional Enrichment Analysis of 108 Overlapping DEGs in Glioblastoma (GBM). Bar plots illustrate significantly enriched GO terms across **(A)** Biological Processes, **(B)** Cellular Components, and **(C)** Molecular Functions, with **(D)** KEGG Pathway Analysis emphasizing pathways implicated in synaptic function, neurotransmission, and tumor-neuron interactions.

analysis revealing significant co-expression patterns (Fig 4D). The ten-gene signature effectively stratified patients into high- and low-risk groups, with Kaplan-Meier analysis indicating markedly worse survival in the high-risk group (Fig 4E). Time-dependent ROC analysis demonstrated progressive enhancement in predictive accuracy, with AUC values of 0.718, 0.755, and 0.757 for 1-, 3-, and 5-year overall survival, respectively (Fig 4F), underscoring the prognostic relevance of the gene signature in GBM.

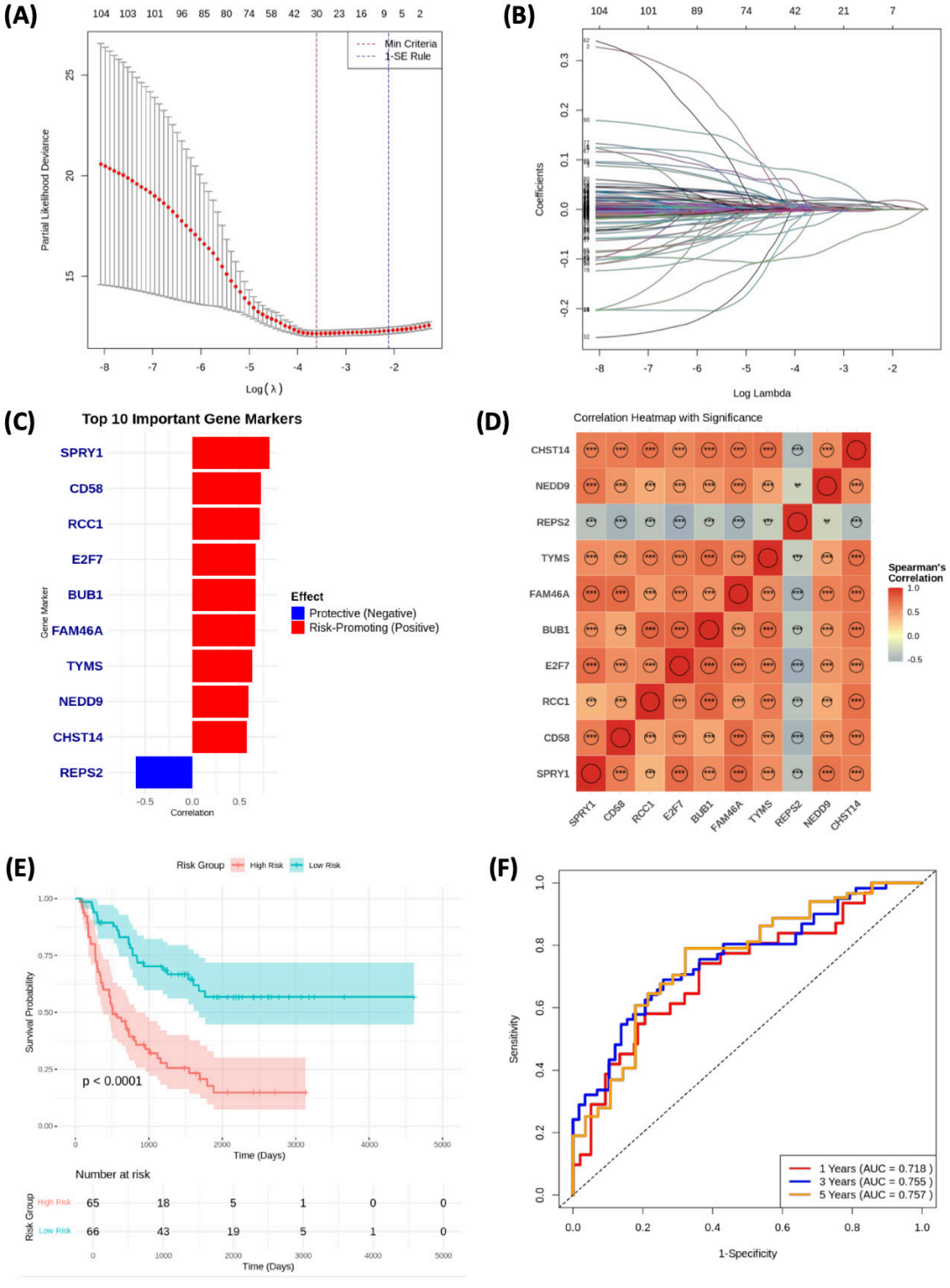

Fig 4. LASSO Analysis of Prognostic Genes Derived from DEGs in GBM. (A) Gene coefficients plotted against the lambda (λ) parameter, illustrating the reduction in non-zero coefficients as λ increases. **(B)** Partial likelihood deviation vs. log(λ), with the optimal λ value marked, balancing model complexity and predictive accuracy. **(C)** Ten most prognostic marker genes identified by LASSO as key predictors in GBM. **(D)** Correlation heatmap depicting the co-expression patterns of the top ten genes, with color intensity reflecting correlation strength (red: positive, blue: negative). **(E)** Kaplan-Meier survival analysis stratifying patients into high- and low-risk groups, revealing significantly worse survival in the high-risk cohort (log-rank $p < 0.05$). **(F)** Time-dependent ROC curves demonstrating the prognostic model's predictive accuracy over 1-, 3-, and 5-year intervals, with AUC values of 0.718, 0.755, and 0.757, respectively.

Correlation analysis of clinical variables and risk score stratification

To explore the clinical relevance of the prognostic model, we examined associations between the risk score and patient clinicopathologic variables. As summarized in Table 1, patients in the High-risk group exhibited a significantly greater proportion of WHO grade IV tumors and a higher frequency of IDH–wild-type status (both $p < 0.05$), indicating increased malignancy in this group. Chemotherapy-treated cases were more common in the High-risk group, whereas no significant differences were observed for gender or MGMT methylation status (all $p > 0.05$). Age was significantly higher in the High-risk group based on the Wilcoxon comparison, suggesting that older individuals tend to fall into higher-risk molecular subgroups.

Independent prognostic factors for GBM

Multivariate Cox regression analysis evaluated the independent prognostic value of the risk score alongside clinical variables, with tumor grade (WHO III: $p = 2.50 \times 10^{-6}$; WHO IV: $p = 6.54 \times 10^{-13}$), chemotherapy status ($p = 0.0028$), and risk score ($p = 2.54 \times 10^{-5}$) emerging as significant predictors of overall survival in GBM patients (Fig 5A).

A prognostic nomogram was subsequently developed by integrating the risk score with clinical parameters, assigning weighted point values to estimate 1-, 3-, and 5-year survival probabilities (Fig 5B). Time-dependent ROC analysis demonstrated the model's robust predictive performance, with AUC values of 0.8, 0.898, and 0.906 for 1-, 3-, and 5-year survival, respectively, underscoring its prognostic utility in GBM (Fig 5C).

Validation of prognostic gene expression in GBM

The expression profiles of ten prognostic genes identified through LASSO regression—SPRY1, CD58, RCC1, E2F7, BUB1, FAM46A, TYMS, NEDD9, CHST14, and REPS2—were validated using transcriptomic datasets from TCGA and GTEx, comparing GBM tumor tissues (n = 163) and normal brain tissues (n = 207). All ten genes demonstrated statistically significant differential

TABLE 1. Association between clinicopathologic characteristics and prognostic risk score groups.

Variable	Category	Low risk	High risk	P value	Sig
Age (years, median [IQR])		39 [IQR 11]	45 [IQR 17]	< 0.001	***
Gender	Female	70 (42.9%)	52 (32.1%)	0.0569	n.s.
	Male	93 (57.1%)	110 (67.9%)	0.0569	n.s.
Grade	WHO II	94 (57.7%)	9 (5.7%)	0.0000	***
	WHO III	38 (23.3%)	41 (25.9%)	0.0000	***
	WHO IV	31 (19%)	108 (68.4%)	0.0000	***
Radiotherapy status	Untreated	130 (82.3%)	114 (75%)	0.1538	n.s.
	Treated	28 (17.7%)	38 (25%)	0.1538	n.s.
Chemotherapy status	Untreated	85 (55.9%)	108 (71.1%)	0.0088	**
	TMZ Treated	67 (44.1%)	44 (28.9%)	0.0088	**
MGMT methylation status	methylated	82 (54.7%)	75 (48.1%)	0.2990	n.s.
	unmethylated	68 (45.3%)	81 (51.9%)	0.2990	n.s.
IDH mutation status	Mutant	128 (79%)	47 (29%)	0.0000	***
	Wildtype	34 (21%)	115 (71%)	0.0000	***

Significance indicators: *p < 0.05, **p < 0.01, ***p < 0.001
Abbreviation: n.s. = not significant

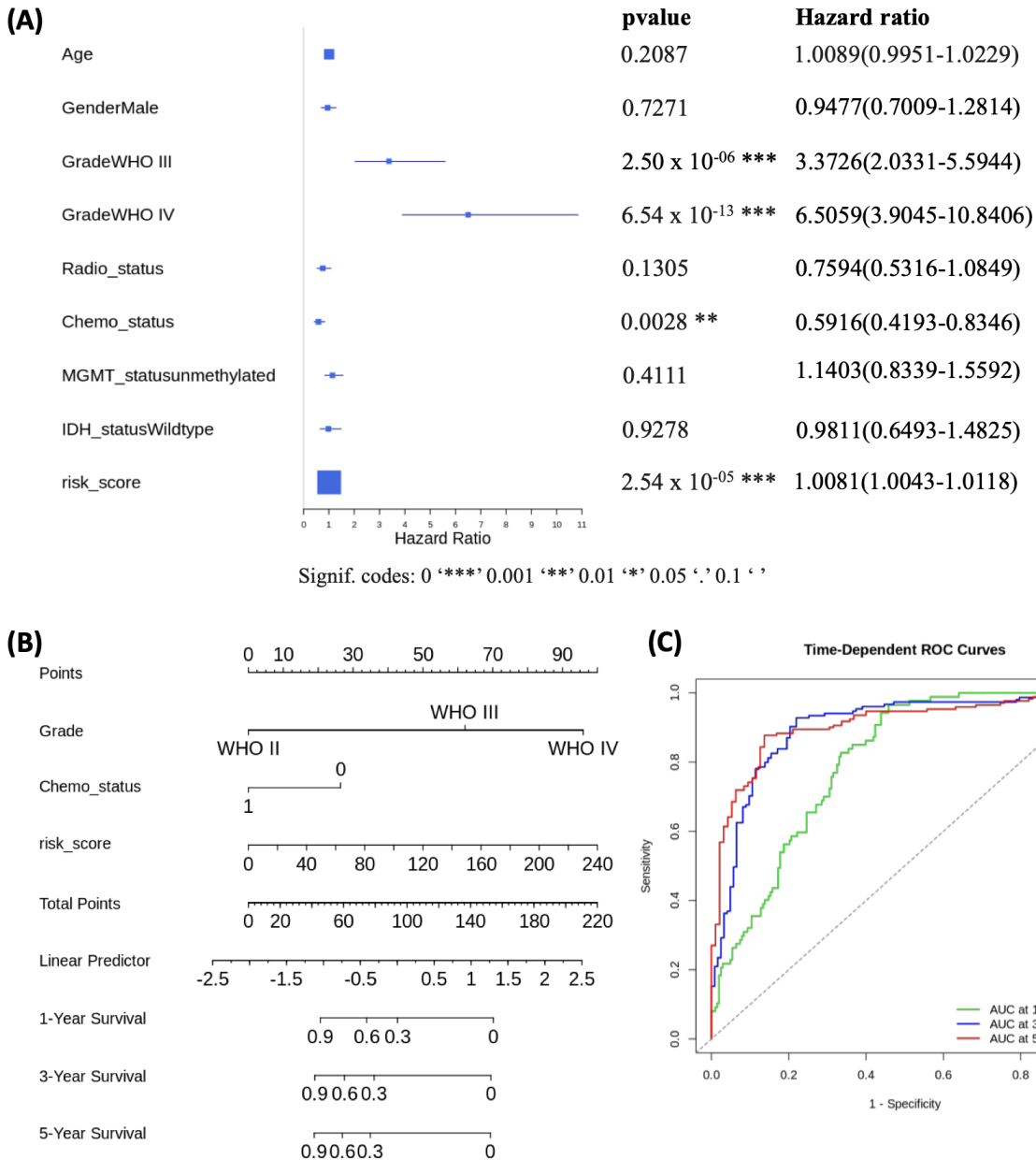

Fig 5. Independent Prognostic Factors in GBM. (A) Forest plot from multivariate Cox regression analysis assessing the prognostic independence of the risk score relative to clinical parameters, including age, gender, WHO grade, radiotherapy, chemotherapy, MGMT methylation, and IDH mutation, with HRs and 95% CIs indicated (**p < 0.01, ***p < 0.001). **(B)** Prognostic nomogram integrating the risk score and key clinical variables to estimate 1-, 3-, and 5-year survival probabilities in GBM, with points assigned to each parameter and summed to derive the total risk score. **(C)** Time-dependent ROC curves illustrating the predictive accuracy of the nomogram for 1-year (green), 3-year (blue), and 5-year (red) survival, with AUC values of 0.8, 0.898, and 0.906, respectively, underscoring robust temporal predictive performance.

expression ($p < 0.05$), with SPRY1, CD58, RCC1, E2F7, BUB1, FAM46A, TYMS, NEDD9, and CHST14 exhibiting marked upregulation, indicating potential oncogenic roles, while REPS2 showed significant downregulation, suggesting a tumor suppressor function (Fig 6). These findings reinforce the prognostic relevance of the selected genes, underscoring their potential as biomarkers for GBM pathogenesis and clinical stratification.

DISCUSSION

This study utilized a comprehensive bioinformatics framework to identify key differentially expressed genes (DEGs) and establish a prognostic model in glioblastoma multiforme (GBM), contributing novel insights into tumor biology and revealing potential biomarkers and therapeutic targets. Integration of four GEO datasets (GSE4290, GSE50161, GSE68848, and GSE116520)

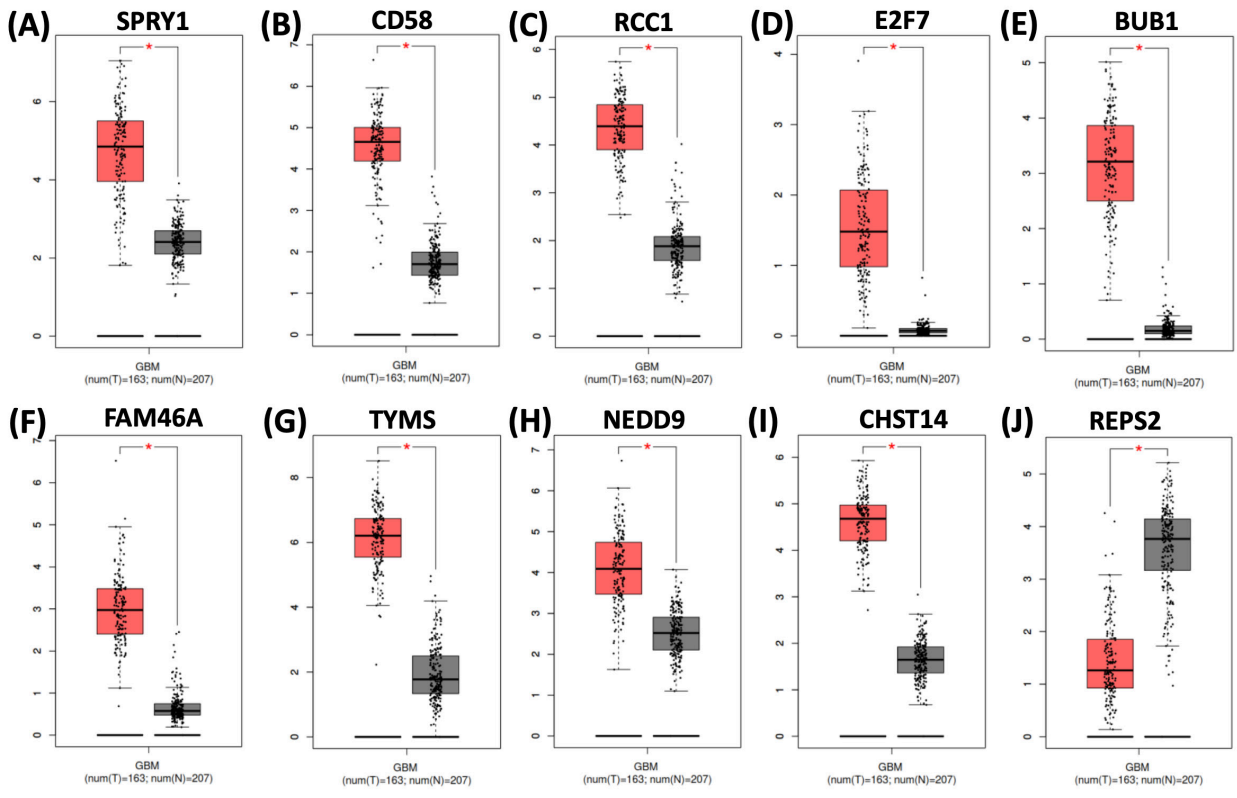

Fig 6. Differential Expression Analysis of LASSO-Identified Prognostic Genes in GBM. (A-J) Box plots illustrate the mRNA expression levels of ten LASSO-selected prognostic genes— SPRY1, CD58, RCC1, E2F7, BUB1, FAM46A, TYMS, NEDD9, CHST14, and REPS2—in GBM tumor tissues (n = 163) versus normal brain tissues (n = 207) using TCGA and GTEx datasets. Red box plots denote GBM samples, while grey box plots represent normal tissues, with asterisks (*) indicating statistically significant differential expression ($p < 0.05$). Group expression differences were evaluated using Student's t-test. Most genes, except REPS2, exhibited marked upregulation in GBM, underscoring their oncogenic potential, whereas REPS2 was significantly downregulated, suggesting a tumor suppressor role. These expression profiles further validate the diagnostic and prognostic relevance of the gene signature in GBM.

identified 108 overlapping DEGs—83 upregulated and 25 downregulated—predominantly enriched in synaptic-associated biological processes and signaling pathways. Notably, the enrichment of neuron projection, synaptic vesicle cycling, and chloride transmembrane transport pathways suggests that GBM cells may functionally integrate into neuronal networks. This observation is consistent with emerging evidence indicating that glioma cells exploit synaptic mechanisms to enhance proliferation, invasion, and therapeutic resistance, underscoring neuron–glioma interactions as pivotal determinants of GBM progression.[33-36] These synaptic-like mechanisms, including GABAergic neurotransmission, represent an underexplored but promising therapeutic axis requiring further mechanistic and pharmacologic investigation.[37-40]

Using LASSO regression, we identified a ten-gene prognostic signature (SPRY1, CD58, RCC1, E2F7, BUB1, FAM46A, TYMS, NEDD9, CHST14, REPS2) with diverse regulatory roles across cancer types. Several components of this signature—such as SPRY1 in MAPK signaling,[41] CD58-mediated immune modulation,[42] RCC1 in mitotic regulation,[43-45] and E2F7 in cell-cycle control[46-48] —have been implicated in oncogenic progression. Likewise, BUB1 family kinases contribute to chromosomal instability,[49-51] and upregulation of FAM46A,[52] TYMS,[53-55] NEDD9,[56-58] and CHST14[59] has been associated with aggressive tumor phenotypes, while REPS2 exhibits tumor-suppressive properties in several malignancies.[60] Collectively, these genes encompass biological pathways central to cell-cycle progression, apoptosis, immune evasion, and metastasis.

The ten-gene model demonstrated strong prognostic capacity, with AUC values of 0.718, 0.755, and 0.757 for 1-, 3-, and 5-year overall survival, respectively, comparable to or surpassing previously published signatures.[61,62] Importantly, multivariate Cox analysis confirmed the risk score as an independent prognostic factor alongside clinical variables such as tumor grade and chemotherapy status, and integration into a nomogram further improved predictive performance, achieving an AUC of 0.906 at 5 years.[63,64] Expression validation in TCGA and GTEx datasets corroborated the differential expression patterns of all ten genes, including downregulation of REPS2, consistent with its tumor-suppressive role.[65]

Our clinicopathologic correlation analysis further

supported the biological and clinical relevance of the risk model. High-risk patients were more frequently diagnosed with WHO grade IV tumors and IDH wild-type status, consistent with established indicators of aggressive GBM behavior. The positive correlation between age and risk score reinforces age as a contributing prognostic factor. Although MGMT methylation did not differ significantly between risk groups in this cohort, the ability of the gene signature to stratify survival independently of MGMT suggests that it captures molecular features beyond traditional markers. This implies that the synaptic-related signature may serve as a complementary tool rather than a replacement for MGMT, offering additional discrimination power in cases where conventional markers are insufficient. Clinically, this signature has the potential to complement established biomarkers—including MGMT methylation and IDH mutation status—by providing additional molecular stratification to guide individualized treatment planning.

Through this research, a comprehensive prognostic model for GBM was constructed, grounded in transcriptomic changes, and its reliability was substantiated by independent validation across multiple cohorts. Future studies incorporating functional experimentation and prospective clinical cohorts are warranted to elucidate mechanistic roles and support translation into therapeutic strategies.

CONCLUSIONS

This study identified a synaptic pathway-enriched ten-gene prognostic signature (SPRY1, CD58, RCC1, E2F7, BUB1, FAM46A, TYMS, NEDD9, CHST14, and REPS2) that can robustly stratify patients with glioblastoma based on survival risk. The model demonstrated strong predictive accuracy and independence from conventional clinical indicators, suggesting its potential value as a complementary tool for risk assessment and treatment planning. Our results reinforce the contribution of neuron–glioma interactions to GBM progression and highlight synaptic mechanisms as promising therapeutic entry points. While these findings provide a foundation for translational development, further in vitro and in vivo experimental validation, followed by prospective clinical studies, will be essential to confirm the biological relevance of this signature and support its integration into clinical workflows.

Data Availability Statement

The datasets analyzed in this study are publicly available. Transcriptomic and clinical data were obtained from The Cancer Genome Atlas (TCGA), Chinese Glioma Genome Atlas (CGGA), and the Gene Expression Omnibus (GEO) databases. All accession numbers are provided in the Methods section.

ACKNOWLEDGEMENTS

The authors would like to thank Universitas PGRI Adi Buana Surabaya for providing research facilities and administrative support. We also acknowledge the contributors of The Cancer Genome Atlas (TCGA), Chinese Glioma Genome Atlas (CGGA) and the Gene Expression Omnibus (GEO) databases for making their data publicly available.

DECLARATIONS

Grants and Funding Information

This research was supported by the Directorate of Research and Community Service, Directorate General of Research and Development, Ministry of Higher Education, Science, and Technology of the Republic of Indonesia, under Grant Nos. 128/C3/DT.05.00/PL/2025, 037/LL7/DT.05.00/PL/2025, and 040.16/Kontrak/LPPM/VI/2025.

Conflict of Interest

The authors declare that there is no conflict of interest regarding the publication of this article.

Registration Number of Clinical Trial

Not applicable. This study did not involve a clinical trial.

Author Contributions

Conceptualization and methodology: V.A., G.A.; Investigation: V.A., G.A.; Formal analysis: G.A., F.F., S.S.N.; Visualization and writing—original draft: G.A.; Writing—review and editing: V.A., G.A.; Funding acquisition: V.A.; Supervision: V.A., G.A. All authors have read and agreed to the final version of the manuscript.

Use of Artificial Intelligence

During the preparation of this manuscript, the authors used ChatGPT to assist with language editing and to improve the clarity and fluency of the text. The authors subsequently reviewed and edited the content critically and take full responsibility for the accuracy, integrity, and scholarly quality of the work.

REFERENCES

1. Sipos D, Raposa BL, Freihat O, Simon M, Mekis N, Cornacchione P, et al. Glioblastoma: Clinical Presentation, Multidisciplinary Management, and Long-Term Outcomes. Cancers (Basel). 2025; 17(1):146.
2. Pouyan A, Ghorbanlo M, Eslami M, Jahanshahi M, Ziaei E, Salami A, et al. Glioblastoma multiforme: insights into

pathogenesis, key signaling pathways, and therapeutic strategies. Mol Cancer. 2025;24(1):58.
3. Lim-Fat MJ, Wen PY. Glioma progression through synaptic activity. Nat Rev Neurol. 2020;16(1):6-7.
4. Venkataramani V, Yang Y, Schubert MC, Reyhan E, Tetzlaff SK, Wißmann N, et al. Glioblastoma hijacks neuronal mechanisms for brain invasion. Cell. 2022;185(16):2899-917. e31.
5. Dresselhaus EC, Meffert MK. Cellular specificity of NF-κB function in the nervous system. Front Immunol. 2019;10:1043.
6. Zhang GL, Wang CF, Qian C, Ji YX, Wang YZ. Role and mechanism of neural stem cells of the subventricular zone in glioblastoma. World J Stem Cells. 2021;13(7):877-93.
7. Feng J, Yang J. Glioma-neuron interactions: insights from neural plasticity. Front Oncol. 2025;15:1661897.
8. Hua T, Shi H, Zhu M, Chen C, Su Y, Wen S, et al. Glioma-neuronal interactions in tumor progression: Mechanism, therapeutic strategies and perspectives (Review). Int J Oncol. 2022;61(3).
9. Williams JB, Cao Q, Yan Z. Transcriptomic analysis of human brains with Alzheimer's disease reveals the altered expression of synaptic genes linked to cognitive deficits. Brain Commun. 2021;3(3):fcab123.
10. Nguyen DPQ, Pham S, Jallow AW, Ho N-T, Le B, Quang HT, et al. Multiple Transcriptomic Analyses Explore Potential Synaptic Biomarker Rabphilin-3A for Alzheimer's Disease. Sci Rep. 2024;14(1):18717.
11. Bhattacharya A, Stutvoet TS, Perla M, Loipfinger S, Jalving M, Reyners AKL, et al. Transcriptional pattern enriched for synaptic signaling is associated with shorter survival of patients with high-grade serous ovarian cancer. eLife. 2025;13:RP101369.
12. Yoshino Y, Roy B, Kumar N, Shahid Mukhtar M, Dwivedi Y. Molecular pathology associated with altered synaptic transcriptome in the dorsolateral prefrontal cortex of depressed subjects. Transl Psychiatry. 2021;11(1):73.
13. Sun L, Hui AM, Su Q, Vortmeyer A, Kotliarov Y, Pastorino S, et al. Neuronal and glioma-derived stem cell factor induces angiogenesis within the brain. Cancer Cell. 2006;9(4):287-300.
14. Griesinger AM, Birks DK, Donson AM, Amani V, Hoffman LM, Waziri A, et al. Characterization of distinct immunophenotypes across pediatric brain tumor types. J Immunol. 2013;191(9):4880-8.
15. Madhavan S, Zenklusen JC, Kotliarov Y, Sahni H, Fine HA, Buetow K. Rembrandt: helping personalized medicine become a reality through integrative translational research. Mol Cancer Res. 2009;7(2):157-67.
16. Kruthika BS, Jain R, Arivazhagan A, Bharath RD, Yasha TC, Kondaiah P, et al. Transcriptome profiling reveals PDZ binding kinase as a novel biomarker in peritumoral brain zone of glioblastoma. J Neurooncol. 2019;141(2):315-25.
17. Alnaser RI, Abed MN, Alassaf FA, Alsaaty MH. Integrating Artificial Intelligence into Chronic Kidney Disease Care: Enhancing Hemodialysis Scheduling, Comorbidity Management, and Diagnostic Capabilities. Siriraj Med J. 2025;77(7):543-52.
18. Saenmanot N, Ruangchainikom M, Ariyawatkul T, Korwutthikulrangsri E, Saenmanot S, Luksanapruksa P, et al. Survival Analysis of and Prognostic Factors for Metastatic Epidural Spinal Cord Compression Compared between Preoperative Known and Unknown Primary Tumors. Siriraj Med J. 2022;74(10):684-92.
19. Chen EY, Tan CM, Kou Y, Duan Q, Wang Z, Meirelles GV, et al. Enrichr: interactive and collaborative HTML5 gene list enrichment analysis tool. BMC Bioinformatics. 2013;14:128.
20. Kuleshov MV, Jones MR, Rouillard AD, Fernandez NF, Duan Q, Wang Z, et al. Enrichr: a comprehensive gene set enrichment analysis web server 2016 update. Nucleic Acids Res. 2016;44(W1):W90-W97.
21. Xie Z, Bailey A, Kuleshov MV, Clarke DJB, Evangelista JE, Jenkins SL, et al. Gene Set Knowledge Discovery with Enrichr. Curr Protoc. 2021;1(3):e90.
22. Ashburner M, Ball CA, Blake JA, Botstein D, Butler H, Cherry JM, et al. Gene ontology: tool for the unification of biology. Nat Genet. 2000;25(1):25-9.
23. Kanehisa M, Goto S. KEGG: kyoto encyclopedia of genes and genomes. Nucleic acids research. 2000;28(1):27-30.
24. Tian Y, Chen Le, Jiang Y. LASSO-based screening for potential prognostic biomarkers associated with glioblastoma. Front Oncol. 2023;12:1057383.
25. Yu SH, Cai JH, Chen DL, Liao SH, Lin YZ, Chung YT, et al. LASSO and Bioinformatics Analysis in the Identification of Key Genes for Prognostic Genes of Gynecologic Cancer. J Pers Med. 2021;11(11).
26. Kamarudin AN, Cox T, Kolamunnage-Dona R. Time-dependent ROC curve analysis in medical research: current methods and applications. BMC Medical Research Methodology. 2017;17(1):53.
27. Geanphun S, Rerkpichaisuth V, Ruangchira-urai R, Thongcharoen P. Survival of Non-Small Cell Lung Cancer Patients with Unexpected N2 after Complete Resection: Role of Aggressive Invasive Mediastinal Staging Should be Considered. Siriraj Med J. 2022;74(3):161-8.
28. Jia Z, Wu H, Xu J, Sun G. Development and validation of a nomogram to predict overall survival in young non-metastatic rectal cancer patients after curative resection: a population-based analysis. Int J Colorectal Dis. 2022;37(11):2365-74.
29. Tang Z, Li C, Kang B, Gao G, Li C, Zhang Z. GEPIA: a web server for cancer and normal gene expression profiling and interactive analyses. Nucleic Acids Res. 2017;45(W1):W98-W102.
30. Sudhof TC. The synaptic vesicle cycle. Annu Rev Neurosci. 2004;27:509-47.
31. Venkataramani V, Tanev DI, Strahle C, Studier-Fischer A, Fankhauser L, Kessler T, et al. Glutamatergic synaptic input to glioma cells drives brain tumour progression. Nature. 2019;573(7775):532-8.
32. Krishna S, Choudhury A, Keough MB, Seo K, Ni L, Kakaizada S, et al. Glioblastoma remodelling of human neural circuits decreases survival. Nature. 2023;617(7961):599-607.
33. Venkataramani V, Tanev DI, Strahle C, Studier-Fischer A, Fankhauser L, Kessler T, et al. Glutamatergic synaptic input to glioma cells drives brain tumour progression. Nature. 2019;573(7775):532-8.
34. Venkatesh HS, Morishita W, Geraghty AC, Silverbush D, Gillespie SM, Arzt M, et al. Electrical and synaptic integration of glioma into neural circuits. Nature. 2019;573(7775):539-45.
35. Venkataramani V, Tanev DI, Kuner T, Wick W, Winkler F. Synaptic input to brain tumors: clinical implications. Neuro Oncol. 2021;23(1):23-33.
36. Tetzlaff SK, Reyhan E, Layer N, Bengtson CP, Heuer A, Schroers J, et al. Characterizing and targeting glioblastoma neuron-tumor networks with retrograde tracing. Cell. 2025;188(2):390-411. e36.
37. Taylor KR, Barron T, Hui A, Spitzer A, Yalçin B, Ivec AE, et al. Glioma synapses recruit mechanisms of adaptive plasticity. Nature. 2023;623(7986):366-74.
38. Hua T, Shi H, Zhu M, Chen C, Su Y, Wen S, et al. Glioma-neuronal

interactions in tumor progression: Mechanism, therapeutic strategies and perspectives (Review). Int J Oncol. 2022;61(3):104.
39. Sisakht AK, Malekan M, Ghobadinezhad F, Firouzabadi SNM, Jafari A, Mirazimi SMA, et al. Cellular Conversations in Glioblastoma Progression, Diagnosis and Treatment. Cell Mol Neurobiol. 2023;43(2):585-603.
40. Barron T, Yalçın B, Su M, Byun YG, Gavish A, Shamardani K, et al. GABAergic neuron-to-glioma synapses in diffuse midline gliomas. Nature. 2025;639(8056):1060-8.
41. Jovčevska I, Zottel A, Šamec N, Mlakar J, Sorokin M, Nikitin D, et al. High FREM2 Gene and Protein Expression Are Associated with Favorable Prognosis of IDH-WT Glioblastomas. Cancers (Basel). 2019;11(8):1060.
42. Ho P, Melms JC, Rogava M, Frangieh CJ, Poźniak J, Shah SB, et al. The CD58-CD2 axis is co-regulated with PD-L1 via CMTM6 and shapes anti-tumor immunity. Cancer Cell. 2023;41(7):1207-21.e12.
43. Bannoura SF, Aboukameel A, Khan HY, Uddin MH, Jang H, Beal E, et al. Regulator of Chromosome Condensation (RCC1) a novel therapeutic target in pancreatic ductal adenocarcinoma drives tumor progression via the c-Myc-RCC1-Ran axis. bioRxiv [Preprint]. 2023.12.18.572102.
44. Xu K, Li W, Li X, Liu C, Yi C, Tang J, et al. RNA binding motif protein 25 is a negative prognostic biomarker and promotes cell proliferation via alternative splicing in hepatocellular carcinoma. Pathol Res Pract. 2025;269:155941.
45. Xu K, Li W, Li X, Liu C, Yi C, Tang J, et al. RNA binding motif protein 25 is a negative prognostic biomarker and promotes cell proliferation via alternative splicing in hepatocellular carcinoma. Pathol Res Pract. 2025;269:155941.
46. Chen K-q, Lei H-b, Liu X, Wang S-z. The roles of E2F7 in cancer: Current knowledge and future prospects. Heliyon. 2024;10(14).
47. Gugnoni M, Lorenzini E, Faria do Valle I, Remondini D, Castellani G, Torricelli F, et al. Adding pieces to the puzzle of differentiated-to-anaplastic thyroid cancer evolution: the oncogene E2F7. Cell Death Dis. 2023;14(2):99.
48. Hao F, Wang N, Zhang Y, Xu W, Chen Y, Fei X, et al. E2F7 enhances hepatocellular carcinoma growth by preserving the SP1/SOX4/Anillin axis via repressing miRNA-383-5p transcription. Mol Carcinog. 2022;61(11):975-88.
49. Kim T, Gartner A. Bub1 kinase in the regulation of mitosis. Anim Cells Syst (Seoul). 2021;25(1):1-10.
50. Huang W, Chen Z, Tang Y, Li J, Fan L. A Pan-Cancer Analysis of the Immunological and Prognostic Role of BUB1 Mitotic Checkpoint Serine/Threonine Kinase B (BUB1B) in Human Tumors. Clin Lab. 2024;70(1).
51. Pokaew N, Prajumwongs P, Vaeteewoottacharn K, Wongkham S, Pairojkul C, Sawanyawisuth K. Overexpression of BubR1 Mitotic Checkpoint Protein Predicts Short Survival and Influences the Progression of Cholangiocarcinoma. Biomedicines. 2024;12(7):1611.
52. Liang S, Yueyang L, Jianhui H, Tian G, Lanying L, and He S. Family with sequence similarity 46 member a confers chemo-resistance to ovarian carcinoma via TGF-β/Smad2 signaling. Bioengineered. 2022;13(4):10629-39.
53. Guijarro MV, Nawab A, Dib P, Burkett S, Luo X, Feely M, et al. TYMS promotes genomic instability and tumor progression in Ink4a/Arf null background. Oncogene. 2023;42(23):1926-39.
54. Geng Y, Xie L, Wang Y, Wang Y. Unveiling the oncogenic significance of thymidylate synthase in human cancers. Am J Transl Res. 2024;16(10):5228-47.
55. Zhang F, Ye J, Guo W, Zhang F, Wang L, Han A. TYMS-TM4SF4 axis promotes the progression of colorectal cancer by EMT and upregulating stem cell marker. Am J Cancer Res. 2022;12(3):1009-26.
56. Yu HG, Bijian K, da Silva SD, Su J, Morand G, Spatz A, et al. NEDD9 links anaplastic thyroid cancer stemness to chromosomal instability through integrated centrosome asymmetry and DNA sensing regulation. Oncogene. 2022;41(21):2984-99.
57. Purazo ML, Ice RJ, Shimpi R, Hoenerhoff M, Pugacheva EN. NEDD9 Overexpression Causes Hyperproliferation of Luminal Cells and Cooperates with HER2 Oncogene in Tumor Initiation: A Novel Prognostic Marker in Breast Cancer. Cancers. 2023;15(4):1119.
58. Han D, Owiredu JN, Healy BM, Li M, Labaf M, Steinfeld JS, et al. Susceptibility-Associated Genetic Variation in NEDD9 Contributes to Prostate Cancer Initiation and Progression. Cancer Res. 2021;81(14):3766-76.
59. Zhan J, Zhou L, Zhang H, Zhou J, He Y, Hu T, et al. A comprehensive analysis of the expression, immune infiltration, prognosis and partial experimental validation of CHST family genes in gastric cancer. Transl Oncol. 2024;40:101843.
60. Zhang H, Duan CJ, Zhang H, Cheng YD, Zhang CF. Expression and clinical significance of REPS2 in human esophageal squamous cell carcinoma. Asian Pac J Cancer Prev. 2013;14(5):2851-7.
61. He Z, Wang C, Xue H, Zhao R, Li G. Identification of a Metabolism-Related Risk Signature Associated With Clinical Prognosis in Glioblastoma Using Integrated Bioinformatic Analysis. Front Oncol. 2020;10:1631.
62. Liu X, Liu X. A novel immune-related gene prognostic signature combining immune cell infiltration and immune checkpoint for glioblastoma patients. Transl Cancer Res. 2024;13(11):6136-53.
63. Su Y, Yang DS, Li Yq, Qin J, Liu L. Early-onset locally advanced rectal cancer characteristics, a practical nomogram and risk stratification system: a population-based study. Front Oncol. 2023;13:1190327.
64. Yang D, Zhu M, Xiong X, Su Y, Zhao F, Hu Y, et al. Clinical features and prognostic factors in patients with microvascular infiltration of hepatocellular carcinoma: Development and validation of a nomogram and risk stratification based on the SEER database. Front Oncol. 2022;12:987603.
65. Doolan P, Clynes M, Kennedy S, Mehta JP, Germano S, Ehrhardt C, et al. TMEM25, REPS2 and Meis 1: Favourable Prognostic and Predictive Biomarkers for Breast Cancer. Tumor Biology. 2009;30(4):200-9.

Binocular Diplopia After Cataract Surgery: Incidence and Associated Factors in a Tertiary Teaching Eye Center

Chayanan Wangpaitoon, M.D., Wasawat Sermsripong, M.D., Thammanoon Surachatkumtonekul, M.D.*

Department of Ophthalmology, Faculty of Medicine Siriraj Hospital, Mahidol University, Bangkok, Thailand.

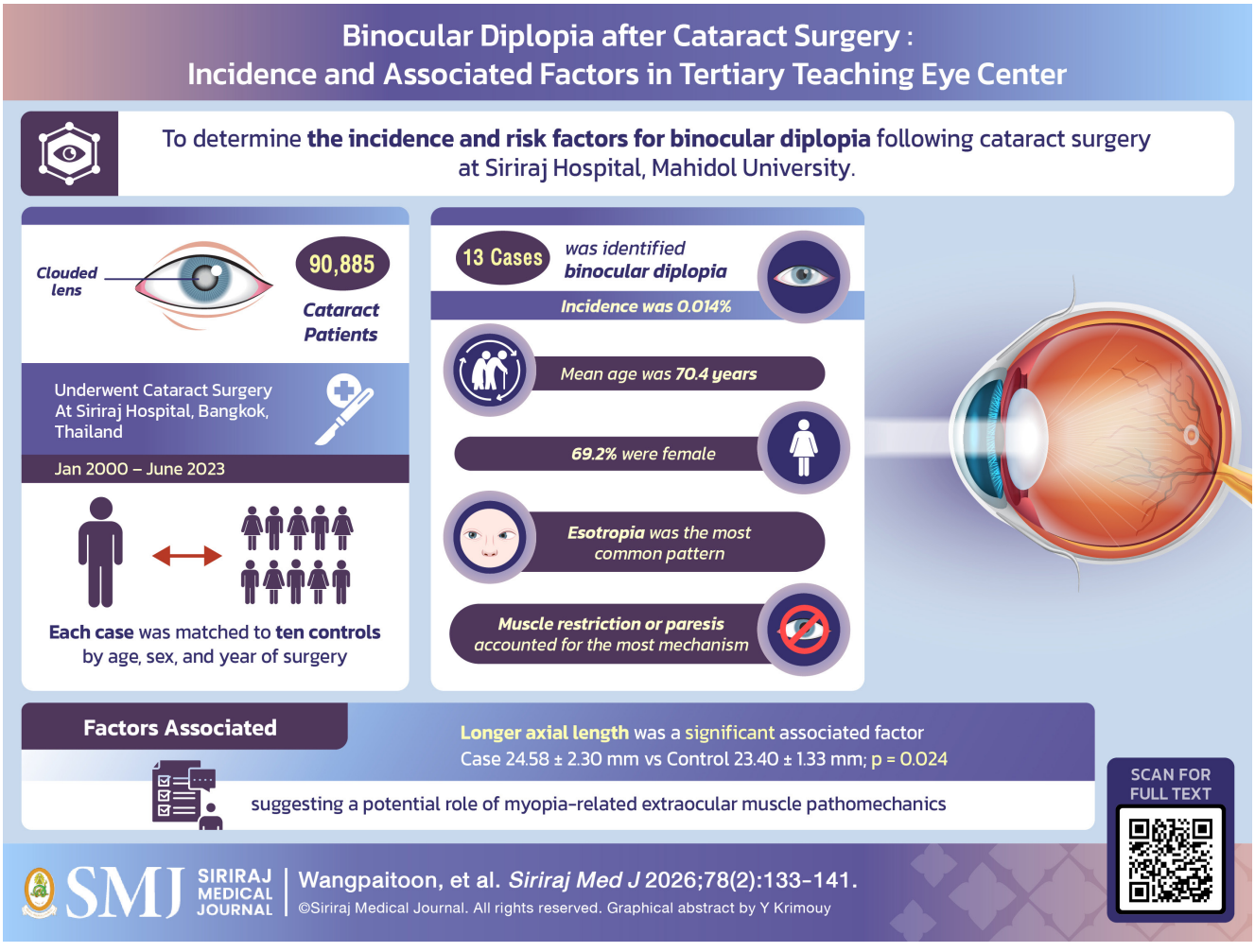

*Corresponding author: Thammanoon Surachatkumtonekul
E-mail: si95thim@gmail.com
Received 19 September 2025 Revised 26 December 2025 Accepted 26 December 2025
ORCID ID:http://orcid.org/0000-0002-0037-6863
https://doi.org/10.33192/smj.v78i2.277766

ABSTRACT

Objective: To determine the incidence and risk factors for binocular diplopia following cataract surgery at Siriraj Hospital, Mahidol University.

Materials and Methods: This retrospective case–control study included patients who underwent cataract surgery between January 2000 and June 2023. Postoperative binocular diplopia was defined as symptomatic diplopia with documented ocular misalignment within 90 days of surgery, identified using ICD-10 codes. Demographic, systemic, biometric, and operative data were extracted. Each case was matched to ten controls by age, sex, and year of surgery. Statistical analyses included Chi-square tests, paired t-tests, and logistic regression.

Results: Among 90,885 cataract surgeries, 13 cases of postoperative binocular diplopia were identified, yielding an incidence of 0.0143%, substantially lower than previously reported rates (0.18–0.85%). The mean age of affected patients was 70.4 years, and 69.2% were female. Esotropia was the most common strabismic pattern (46.2%), while muscle restriction or paresis accounted for the majority of mechanisms (53.9%). Compared with matched controls, cases had significantly longer axial lengths (24.58 ± 2.30 mm vs. 23.40 ± 1.33 mm; p = 0.024), corresponding to an odds ratio of 1.426 (95% CI: 1.047–1.942) per millimeter increase. No significant associations were found with systemic comorbidities (diabetes, hypertension, dyslipidemia) or anesthesia type.

Conclusion: Postoperative binocular diplopia following cataract surgery was rare in this large tertiary-center cohort. Longer axial length was the only significant risk factor identified, suggesting a potential role of myopia-related extraocular muscle pathomechanics. Awareness of this risk factor may aid in preoperative counseling and surgical planning.

Keywords: Binocular diplopia; cataract surgery; complication; risk factors; axial length (Siriraj Med J 2026;78(2):133-141)

INTRODUCTION

Cataract surgery is the most frequently performed ophthalmic operation and typically restores excellent visual function.[1] However, postoperative binocular diplopia — although uncommon — remains a clinically meaningful complication that can adversely affect patient-reported outcomes and functional vision.[2] Reported incidence rates have varied across settings and time periods, partly due to evolving anesthesia practices and surgical techniques. Previous studies have reported the incidence of binocular diplopia after cataract surgery at 0.18% to 0.67% overall[3-5], and 0.093% to 0.85% among patients receiving retrobulbar anesthesia.[6,7] Contemporary large-scale data from Asian populations are limited, and potential risk markers have not been delineated with sufficient precision to guide preoperative counselling or risk stratification.[8]

Multiple pathophysiological pathways may contribute to diplopia following cataract surgery, including transient sensory disruption with loss of fusion, decompensation of pre-existing heterophoria or strabismus, restrictive or paretic extraocular muscle dysfunction, and abnormalities of the pulley or connective-tissue system. Ocular biometry may modulate susceptibility to these mechanisms. In particular, axial length (AL), a marker of myopic ocular anatomy, may influence extraocular muscle vector balance, pulley position, and fusional reserves, thereby plausibly increasing the risk of postoperative misalignment.[2,8,9] However, the association between AL and postoperative binocular diplopia has not been systematically quantified.[10]

To address these gaps, we investigated the incidence of postoperative binocular diplopia and evaluated its risk factors in cataract surgeries performed at a tertiary eye centre over two decades (2000–2023). Using a retrospective matched case–control design nested within this cohort; we tested the prior hypothesis that greater AL is associated with increased odds of postoperative binocular diplopia and explored perioperative factors — including anesthesia type and surgical technique — as secondary exposures. Our objective was to generate precise, contemporary estimates and biologically coherent signals to guide preoperative counselling, inform clinical decision-making, and motivate confirmatory studies.

MATERIALS AND METHODS

Study design

This investigation was a retrospective, individually matched case–control study of cataract surgeries performed at Siriraj Hospital, Bangkok, Thailand, between January 2000 and June 2023. The study protocol was approved by the Siriraj Institutional Review Board (IRB No. Si 760/2023) and was registered with the Thai Clinical Trials Registry (TCTR20231026007). The required sample size to ensure sufficient statistical power was calculated to be 85,901 participants.[5,11]

Data collection

Patient data were collected through a retrospective chart review using a standardized case record form. The source cohort included all lens-extraction procedures documented in institutional administrative and clinical databases during the study period. Procedures were identified using relevant ICD-9 procedure codes. Clinical variables were abstracted from the electronic medical record using a prespecified data dictionary and identified based on ICD-9 procedure codes for lens extraction:

- 131: Intracapsular extraction of the lens
- 132: Extracapsular extraction of the lens by linear extraction technique
- 133: Extracapsular extraction of the lens by simple aspiration and irrigation
- 134: Extracapsular extraction of the lens by fragmentation and aspiration technique
- 135: Other extracapsular extraction of the lens
- 136: Other cataract extraction

This search yielded a total cohort of 90,885 cataract surgery patients.

The outcome of interest was postoperative binocular diplopia occurring within 90 days of cataract surgery.[9,20] Potential cases were identified by ICD-10 diagnostic codes for diplopia, strabismus, or ocular motor nerve palsy and were verified by manual chart review. A confirmed case required: (i) patient-reported binocular diplopia, and (ii) documented ocular misalignment on examination within 90 days after the index surgery. Encounters indicating monocular diplopia were excluded a priori. If multiple qualifying encounters were present, the earliest encounter was designated as the case index date. The diagnostic codes used were:

- H49.0: Third (oculomotor) nerve palsy
- H49.1: Fourth (trochlear) nerve palsy
- H49.2: Sixth (abducent) nerve palsy
- H51: Other disorders of binocular movement
- H53.2: Diplopia
- H53.3: Other disorders of binocular vision

For each confirmed case, ten controls[13] without evidence of postoperative binocular diplopia were randomly sampled from the source cohort. Controls were individually matched to each case by sex, age, and year of surgery to account for demographic differences and secular trends. Each case and its matched controls formed a matched set. Controls were required to meet cohort eligibility and to have no conflicting outcome codes within 90 days of surgery.

Prespecified variables included demographics (age, sex), systemic comorbidities (diabetes mellitus, hypertension, dyslipidaemia), ocular biometry — particularly axial length (AL; millimetres) — and perioperative factors (anesthesia type: topical, sub-Tenon, peribulbar, retrobulbar, or general; surgical technique: phacoemulsification, extracapsular cataract extraction, or other). Where available, ocular alignment patterns (e.g., esotropia, exotropia, vertical deviations) and clinical mechanisms (restriction versus paresis) were also recorded. Ocular biometry reflected routine preoperative measurements obtained as part of standard care.

Matching by age, sex, and surgery year was used to reduce confounding and mitigate secular trend bias. The outcome definition combined patient-reported symptoms with objective documentation to minimize misclassification. A 90-day attribution window was prespecified to support temporal plausibility. Planned sensitivity analyses (described below) assessed the impact of outcome definition stringency and temporal effects.

Statistical analysis

Categorical variables were summarized as frequencies and percentages, and continuous variables as means with standard deviations. The primary outcome, the incidence of postoperative binocular diplopia, was reported as a proportion. Secondary analyses compared cases and controls using Chi-square tests for categorical variables and paired t-tests for continuous variables. Logistic regression analysis was subsequently performed to evaluate the association between axial length and postoperative binocular diplopia. A two-sided p-value of less than 0.05 was considered statistically significant.

RESULTS

During the study period, 90,885 cataract surgeries were recorded at Siriraj Hospital, Bangkok, Thailand. Thirteen patients met the prespecified case definition of postoperative binocular diplopia within 90 days and were each matched to ten controls by age, sex, and year of surgery (Table 1).

The incidence of postoperative binocular diplopia was 0.0143%, indicating an exceedingly rare complication in contemporary practice.

Baseline characteristics

Matched variables (age, sex, year) were comparable by design (Table 1). The mean age of patients in the case group was 70.38 ± 8.92 years, and nine of the 13 patients (69.23%) were female. The prevalence of common systemic comorbidities (diabetes mellitus, hypertension, dyslipidaemia) did not differ meaningfully between groups (Table 1).

TABLE 1. Baseline characteristics.

Characteristic	Case (n=13)	Control (n=130)	P value
Gender			
Male	4 (30.77%)	40 (30.77%)	-
Female	9 (69.23%)	90 (69.23%)	-
Age (years)	70.38 ± 8.92	70.38 ± 8.60	0.966†
Underlying disease			
Diabetes Mellitus	3 (23.08%)	49 (37.69%)	0.375†
Hypertension	9 (69.23%)	80 (61.54%)	0.767†
Dyslipidemia	7 (53.85%)	52 (40.00%)	0.384†

Data are presented as number (percentage) or mean ± standard deviation.
† Chi-square test

	Case (n=13)	Control (n=130)	Odds Ratio (95% CI)	P value
Axial Length	24.58 ± 2.30	23.40 ± 1.33	1.426 (1.047-1.942)	0.024*

Data are presented as mean ± standard deviation.
* Paired-sample t-test

Associated factors

Analysis of associated factors revealed that longer axial length was significantly associated with the development of postoperative binocular diplopia. The mean axial length was 24.58 ± 2.30 mm in the case group compared to 23.40 ± 1.33 mm in the control group (p = 0.024). In regression analyses, each 1 mm increase in axial length was associated with higher odds of postoperative binocular diplopia (odds ratio 1.43, 95% CI 1.05–1.94).

Operative details

Distributions of anesthesia type and surgical technique are summarised in Table 2. Comparisons across anesthesia categories were limited by small cell counts, resulting in imprecise effect estimates and no consistent associations.

Clinical presentation

Among the 13 patients who developed postoperative binocular diplopia, six (46.2%) demonstrated esotropia (ET), three (23.1%) exhibited exotropia (XT), and four (30.8%) presented with combined horizontal and vertical strabismus. The most frequently identified etiology was extraocular muscle restriction or paresis, observed in seven patients (53.8%), followed by decompensation of pre-existing strabismus in four patients (30.8%). Management was predominantly conservative, with 10 patients (76.9%) undergoing observation alone and three patients (23.1%) receiving prism therapy. (Table 3)

DISCUSSION

Our study is centered on an Asian population, in contrast to prior research, which has predominantly focused on Western populations. In this single-center cohort, new-onset binocular diplopia after cataract surgery was uncommon but clinically meaningful. The preponderance of vertical deviations and the observed association with regional (needle) anesthesia are directionally concordant with prior series, in which extraocular-muscle (EOM) dysfunction — most often involving the inferior rectus — dominates the phenotype.[5,9,13–15] Decompensation of latent strabismus and sensory fusion disturbances accounted for a nontrivial subset, consistent with orthoptic clinic–based reviews.[9,16] Our finding linking longer axial length with postoperative diplopia is biologically plausible in the context of high-myopia–related EOM pathomechanics and pulley displacement, which predispose to acquired strabismus patterns.[10,17,23] The low incidence may be attributed to the study population having a small angle of deviation, and the fact that these patients were not examined by a pediatric ophthalmologist, which could have led to the condition being undetected by the examining physician. Other reasons for the low incidence may arise from variations in data collection methods, as well as from

TABLE 2. Operative details.

	Case (n=13)	Control (n=130)	P value
Side of operation			0.244†
Right	4 (30.77%)	67 (51.54%)	
Left	9 (69.23%)	63 (48.46%)	
Type of surgery			0.495†
Phacoemulsification+IOL	12 (92.31%)	124 (95.38%)	
ECCE+IOL	1 (7.69%)	6 (4.62%)	
Type of IOL			0.406†
Monofocal IOL	13 (100%)	114 (87.69%)	
Toric IOL	0 (0.00%)	12 (9.23%)	
Multifocal IOL	0 (0.00%)	4 (3.07%)	
Position of IOL			0.581†
In capsular bag (posterior chamber IOL)	13 (100%)	127 (97.69%)	
In sulcus (IOL in sulcus)	0 (0.00%)	3 (2.31%)	
Complication			0.966†
No complication	13 (100%)	121(93.08%)	
Ruptured posterior capsule	0 (0.00%)	4 (3.08%)	
Torn anterior CCC	0 (0.00%)	2 (1.54%)	
Ruptured posterior capsule + Torn anterior CCC	0 (0.00%)	1 (0.77%)	
Zonule dialysis	0 (0.00%)	1 (0.77%)	
Aqueous misdirection	0 (0.00%)	1 (0.77%)	
Type of anesthesia			0.592†
Topical	9 (69.23%)	96 (73.85%)	
Subconjunctival	0 (0.00%)	8 (6.15%)	
Retrobulbar	3 (23.08%)	18 (13.85%)	
GA	0 (0.00%)	4 (3.08%)	
Topical+Subconjunctival	1 (7.69%)	4 (3.08%)	
Anesthetic agents used			0.604†
0.5%Tetracaine ed	9 (69.23%)	96 (73.85%)	
1%Lidocaine	0 (0.00%)	1 (0.77%)	
2%Lidocaine	0 (0.00%)	8 (6.15%)	
0.5%Bupivacaine	0 (0.00%)	0 (0.00%)	
2%Lidocaine+0.5%Bupivacaine	3 (23.08%)	17 (13.08%)	
0.5%Tetracaine ed+2%Lidocaine	1 (7.69%)	4 (3.08%)	
Anesthetic drug in GA cases	0 (0.00%)	4 (3.08%)	

Note: Data are presented as number (%).

† Chi-square test

Abbreviations: ECCE = extracapsular cataract extraction; IOL = intraocular lens; CCC = continuous curvilinear capsulorhexis; GA = general anesthesia. ed = eye drop

TABLE 3. Baseline characteristics, operative details and diplopia details of cases.

Case	Sex	Age	Underlying Disease	AXL (mm)	Side	Operation	Anesthesia type	Anesthetic Drug	Strabismic pattern	Mechanism of diplopia	Treatment	Outcome
1	F	69	No	22.21	LE	ECCE+IOL	Retrobulbar	2% lidocaine with 0.5% bupivacaine	XT	muscle restriction or paresis	observe	Success
2	M	66	DM, HT	21.69	RE	PE+IOL	Topical with Subconjunctival	0.5% tetracaine ed with 2% lidocaine	ET	muscle restriction or paresis	observe	Success
3	F	79	DM, HT	23.35	RE	PE+IOL	Topical	0.5% tetracaine ed	ET with vertical strabismus	decompensation	observe	Success
4	F	57	HT, DLP	29.1	LE	PE+IOL	Topical	0.5% tetracaine ed	ET	muscle restriction or paresis	observe	Success
5	F	85	HT, DLP	22.2	LE	PE+IOL	Topical	0.5% tetracaine ed	ET	muscle restriction or paresis	observe	Success
6	F	55	HT, DLP	26.97	LE	PE+IOL	Retrobulbar	2% lidocaine with 0.5% bupivacaine	XT	muscle restriction or paresis	observe	Success
7	F	75	DM, HT, DLP	23.23	LE	PE+IOL	Topical	0.5% tetracaine ed	ET with vertical strabismus	decompensation	observe	Failure
8	M	75	HT	25.13	RE	PE+IOL	Topical	0.5% tetracaine ed	XT with vertical strabismus	muscle restriction or paresis	observe	Success
9	F	72	HT, DLP	24.12	LE	PE+IOL	Topical	0.5% tetracaine ed	ET	muscle restriction or paresis	observe	Success
10	M	72	No	25.09	LE	PE+IOL	Topical	0.5% tetracaine ed	ET	decompensation	prism	Success
11	F	61	No	27.47	LE	PE+IOL	Topical	0.5% tetracaine ed	XT	undetermined	prism	Success
12	F	80	HT, DLP	22.91	LE	PE+IOL	Retrobulbar	2% lidocaine with 0.5% bupivacaine	ET	decompensation	observe	Failure
13	M	69	DLP	26.11	RE	PE+IOL	Topical	0.5% tetracaine ed	XT with vertical strabismus	Epiretinal membrane	prism	Failure

Abbreviations: M=Male, F=Female, DM = Diabetes Mellitus, HT = Hypertension, DLP = Dyslipidemia, AXL = Axial Length, LE= Left eye, RE = Right eye, ECCE+IOL = Extracapsular cataract extraction with intraocular lens, PE+IOL = phacoemulsification with intraocular lens, XT = Exotropia, ET = Esotropia, ed = eye drops

differences in the population groups with distinct ethnic backgrounds, which can lead to anatomical variations in the eyes. Additionally, differing inclusion criteria can also have a significant impact on the results.

How do these results compare with existing literature?

Large case reviews suggest that most post-cataract diplopia arises from two main mechanisms: (i) anesthesia-related myotoxicity or direct EOM injury, and (ii) decompensation of pre-existing ocular misalignment once blur/aniseikonia and sensory deprivation are relieved. In the largest orthoptic clinic series (n=150), decompensation of preexisting strabismus accounted for approximately 34% of cases, whereas restriction/paresis comprised about 25%; notably, the introduction of topical anesthesia shifted the case-mix toward decompensation rather than restriction.[9] A Spanish hospital series of 3,542 cases reported significantly higher diplopia rates after regional compared with topical anesthesia (21/2,122 vs 3/1,420; P=0.005), with all motility-related cases confined to the regional group.[5] Furthermore, peribulbar anesthesia without hyaluronidase was associated with a sharp rise in diplopia (0.75%), implicating reduced injectate dispersion and focal myotoxicity; reintroduction of hyaluronidase eliminated observed cases.[18] Dedicated neuroophthalmology referral cohorts after cataract surgery have likewise identified decompensated strabismus as the most common efferent cause of postoperative visual disturbance.[19]

Pathophysiological considerations

Regional anesthesia can damage EOMs through mechanical needle trauma, vascular compromise, or myotoxicity from local anesthetics, resulting in contracture, paresis, or both. Classic patterns include inferior rectus overaction/underaction with subsequent spread of comitance over time.[9,13–15] In contrast, under topical-only anesthesia, diplopia more often reflects the unmasking of latent deviations when fusion demands change postoperatively.[9,16,19] In highly myopic eyes, axial elongation displaces the globe relative to the rectus pulleys, producing characteristic heavy-eye or related sagging-eye syndromes with vertical/horizontal incomitance. Such anatomical changes plausibly lower the threshold for postoperative decompensation when sensory cues shift after lens extraction.[10,17,23]

Clinical implications

Preoperative screening

Our data support the value of short preoperative assessments of refractive error, anisometropia, amblyopia and alignment assessment, including cover-alternate cover testing at distance/near, vertical offset checks, and a history review for childhood strabismus or prism wear, along with targeted counseling for patients with long axial length or orthoptic risk markers.[9,17,19,21,22]

An increased axial length complicates cataract surgery, and at the same time, patients with high myopia due to elongated axial length are at risk of developing strabismus. This may result from abnormal pulley system function, soft tissue irregularities around the eye, or anisometropia and amblyopia, which depend on the degree of anisometropia and amblyopia. These conditions lead to the loss of binocular function, which can cause the transition from phoria to tropia after cataract surgery, especially when one eye is occluded, disrupting binocular function.

Anesthesia choice and technique

For patients at elevated risk (e.g., high axial length, prior strabismus, restrictive motility, or anticipated difficult block), topical anesthesia (with or without intracameral supplementation) should be preferred when surgically feasible.[5] Where regional anesthesia is indicated, standardized low-volume peribulbar techniques with hyaluronidase appear protective and should be protocolized.[18]

Early recognition and management

Early orthoptic assessment can help differentiate transient sensory phenomena from myotoxic patterns. Prism therapy is effective for many comitant deviations.[9] Persistent restrictive or vertical incomitance warrants imaging and, when stable, tailored strabismus surgery; inferior rectus recession and related procedures have shown favorable outcomes in selected cases.[9,13,15]

LIMITATIONS

Diplopia that was transient, rapidly resolved, or managed without a specific ICD-10 code for strabismus/diplopia might have been missed, potentially leading to underreporting of the true incidence.

Other factors, such as underlying diseases, which were found to be non-significant, may in fact be associated factors. However, the extremely small sample size (13 cases) may have limited the ability to detect significant associations. Additionally, although axial length was found to be significant, the results cannot be conclusive due to the small sample size. The research team acknowledges that future studies with a larger sample size will be necessary to further explore and identify the associated factors of binocular diplopia following cataract surgery.

CONCLUSIONS

In this large, single-center cohort, postoperative binocular diplopia following cataract surgery was exceedingly rare, yet matched analyses suggested that longer axial length was associated with increased odds of this complication. The clinical phenotype was dominated by vertical deviations with features of restrictive or paretic extraocular muscle dysfunction, alongside a subset attributable to decompensation of latent strabismus. Given the sparse number of events, effect estimates carry substantial uncertainty and should be interpreted as hypothesis-generating signals rather than definitive causal effects. Pragmatic implications include brief preoperative alignment screening, axial-length-informed counselling, preference for topical anesthesia when feasible in higher-risk profiles, and early orthoptic assessment when symptoms arise. Validation in multicenter cohorts using rare-event-robust, match-aware methods and standardized orthoptic assessments is warranted.

Data Availability Statement

The datasets underlying this article are available from the corresponding author upon reasonable request and subject to institutional approval and data-sharing agreements.

ACKNOWLEDGEMENT

Suchawadee Leelasrisoonton assisted with manuscript preparation.

DECLARATIONS

Grants and Funding Information

This research received no external funding.

Conflicts of Interest

The authors declare no conflicts of interest related to this publication.

Registration Number of Clinical Trial

Not applicable. This was a retrospective study and was not registered as a clinical trial.

Author Contributions

General research process and framework of the study, T.S., W.S. ; Investigation, Data collection and Data analysis, C.W. ; Writing-original draft preparation, review and editing, T.S., C.W. ; supervision, T.S. All authors read and approved the final manuscript.

Use of Artificial Intelligence

During preparation of the manuscript, the authors used Grammarly and ChatGPT 5.2 to refine grammar and enhance readability.

REFERENCES

1. Han X, Zhang J, Liu Z, Tan X, Jin G, He M, Luo L, Liu Y. Real-world visual outcomes of cataract surgery based on population-based studies: a systematic review. Br J Ophthalmol. 2023;107(8):1056-65.
2. Kalantzis G, Papaconstantinou D, Karagiannis D, Koutsandrea C, Stavropoulou D, Georgalas I. Post-cataract surgery diplopia: aetiology, management and prevention. Clin Exp Optom. 2014;97(5):407-10.
3. Johnson DA. Persistent vertical binocular diplopia after cataract surgery. Am J Ophthalmol. 2001;132(6):831-5.
4. Pearce IA, McCready PM, Watson MP, Taylor RH. Vertical diplopia following local anaesthetic cataract surgery: predominantly a left eye problem? Eye (Lond). 2000;14(Pt 2):180–184.
5. Yangüela J, Gómez-Arnau JI, Martín-Rodrigo JC, Andueza A, Gili P, Paredes B, et al. Diplopia after cataract surgery: comparative results after topical or regional injection anesthesia. Ophthalmology. 2004;111(4):686-92.
6. Costa PG, Debert I, Passos LB, Polati M. Persistent diplopia and strabismus after cataract surgery under local anesthesia. Binocul Vis Strabismus Q. 2006;21(3):155-8.
7. Golnik KC, West CE, Kaye E, Corcoran KT, Cionni RJ. Incidence of ocular misalignment and diplopia after uneventful cataract surgery. J Cataract Refract Surg. 2000;26(8):1205-9.
8. Gawęcki M, Grzybowski A. Diplopia as the Complication of Cataract Surgery. J Ophthalmol. 2016;2016:2728712.
9. Nayak H, Kersey JP, Oystreck DT, Cline RA, Lyons CJ. Diplopia following cataract surgery: a review of 150 patients. Eye (Lond). 2008;22(8):1057–64.
10. Demer JL. Muscle paths matter in strabismus associated with axial high myopia. Am J Ophthalmol. 2010;149(2):184-6.e1.
11. Naing L, Nordin RB, Abdul Rahman H, Naing YT. Sample size calculation for prevalence studies using Scalex and ScalaR calculators. BMC Med Res Methodol. 2022;22(1):209.
12. Setia MS. Methodology Series Module 2: Case-control Studies. Indian J Dermatol. 2016;61(2):146-51.
13. Gómez-Arnau JI, Yangüela J, González A, Andrés Y, García del Valle S, Gili P, et al. Anaesthesia-related diplopia after cataract surgery. Br J Anaesth. 2003;90(2):189-93.
14. Han SK, Kim JH, Hwang J-M. Persistent diplopia after retrobulbar anesthesia. J Cataract Refract Surg. 2004;30(6):1248-53.
15. Pearce IA, McCready PM, Watson MP, Taylor RH. Vertical diplopia following local anaesthetic cataract surgery: predominantly a left eye problem? Eye (Lond). 2000;14(Pt 2):180-4.
16. Gunton KB, Armstrong B. Diplopia in adult patients following cataract extraction and refractive surgery. Curr Opin Ophthalmol. 2010;21(5):341-4.
17. Rossel-Zemkouo MJ, Bergholz R, Salchow DJ. Strabismus patterns after cataract surgery in adults. Strabismus. 2021;29(1):19-25.
18. Hamada S, Devys JM, Xuan TH, Ganem S, Sahel JA, Héran F, Plaud B. Role of hyaluronidase in diplopia after peribulbar anesthesia for cataract surgery. Ophthalmology. 2005;112(5):879-82.
19. Lin S-C, Giang A, Liu GT, Avery RA, Shindler KS, Hamedani AG, Ross AG, Tamhankar MA. Frequency and etiologies of visual

disturbance after cataract surgery identified in neuro-ophthalmology clinics. J Neuroophthalmol. 2023;43(3):359-63.
20. Wylie J, Henderson M, Doyle M, Hickey-Dwyer M. Persistent binocular diplopia following cataract surgery: Aetiology and management. Eye (Lond). 1994;8:543-6.
21. Surachatkumtonekul T, Tongsai S, Sathianvichitr K, Sangsre P, Saiman M, Sermsripong W, et al. Corneal Curvature Change After Strabismus Surgery: An Experience from a Single Academic Center. Siriraj Med J. 2024;76(10):713-21.
22. Surachatkumtonekul T, Subhadhirasakul S, Sermsripong W. Visual Prognosis in Craniosynostosis Patients: A 20-year Retrospective Cohort Study at a Tertiary Referral Center in Thailand. Siriraj Med J. 2024;76(10):679-86.
23. ธรรมนูญ สุรชาติกำธรกุล. ภาวะตาเหล่ในผู้ป่วยสายตาสั้นมาก. ใน: ศักดิ์ชัย วงศกิตติรักษ์ ธนาพงษ์ สมกิจรุ่งโรจน์, บรรณาธิการ. จักษุวิชาการ โดยราชวิทยาลัยจักษุแพทย์แห่งประเทศไทย เล่ม 7. กรุงเทพฯ: โรงพิมพ์มหาวิทยาลัยธรรมศาสตร์; 2566. หน้า 153-66. (In Thai)

Development and Psychometric Properties of Short-Video Applications Addiction Questionnaire (S-VAAQ)

Viraya Leelawat, M.D., Chanvit Pornnoppadol, M.D., Sirinda Chanpen, M.Sc., Wanlop Atsariyasing, M.D.*

Department of Psychiatry, Faculty of Medicine Siriraj Hospital, Mahidol University, Thailand.

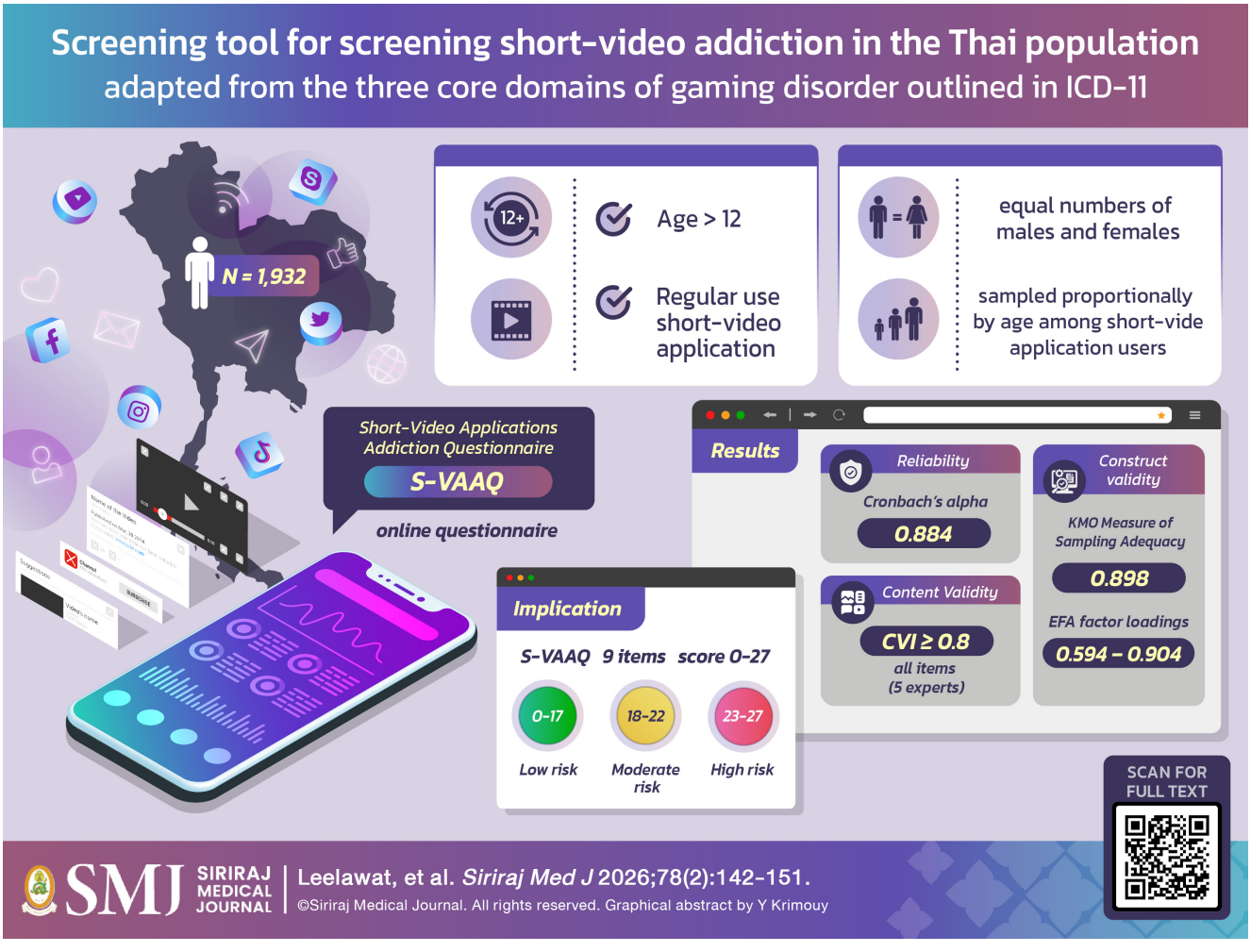

*Corresponding author: Wanlop Atsariyasing
E-mail: wanlop.atr@mahidol.ac.th
Received 28 October 2025 Revised 25 November 2025 Accepted 15 December 2025
ORCID ID:http://orcid.org/0000-0001-8868-8302
https://doi.org/10.33192/smj.v78i2.278550

ABSTRACT

Objective: This cross-sectional study aimed to develop and validate the Short-Video Applications Addiction Questionnaire (S-VAAQ) and evaluate its reliability and validity among Thai individuals aged 13 years and older.

Materials and Methods: The S-VAAQ is a 9-item screening tool adapted from the three core domains of gaming disorder outlined in ICD-11: impaired control over usage, increased priority given to gaming, and continued use despite negative consequences. Items were modified to better reflect short-form video consumption behaviors. Data were collected through an online questionnaire distributed via short-form video platforms and Line, targeting Thai participants aged 13 and above who regularly watched short-form videos and were proficient in Thai. Statistical analyses included content validity index (CVI) assessments by five experts, Cronbach's alpha for internal consistency, and exploratory factor analysis (EFA).

Results: A total of 1,932 participants aged 13 years and older were included. The median daily duration of short-form video viewing was three hours. All items demonstrated CVI scores exceeding 0.78. The scale exhibited good internal consistency, with a Cronbach's alpha of 0.884. KMO Measure of Sampling Adequacy of 0.898 and EFA revealed factor loadings ranging from 0.594 to 0.904 supporting the scale's construct validity.

Conclusions: In conclusion, the S-VAAQ demonstrated good reliability and validity. This instrument can serve as a useful tool for screening short-form video addiction in the Thai population and support further research and intervention strategies.

Keywords: Adolescent; psychometrics; surveys and questionnaires; internet addiction disorder; social networking; short-video addiction (Siriraj Med J 2026;78(2):142-151)

This research was presented as a new research poster at the 2025 annual meeting of the American Academy of Child and Adolescent Psychiatry. Therefore, the abstract is scheduled for publication in the *Journal of the American Academy of Child & Adolescent Psychiatry,* Volume 64, Issue 10, S307.

INTRODUCTION

Short videos have rapidly gained popularity on social media platforms, becoming comparable to other forms of social media content. People consume short videos mainly for entertainment and to access information on topics of interest through audiovisual clips lasting only seconds to minutes. The popularity of short videos has significantly increased over the past two to three years. During the COVID-19 pandemic, in 2022, TikTok emerged as the most downloaded application on the App Store, reaching approximately 700 million downloads.[1] This surpassed YouTube and WhatsApp, which ranked second and third with approximately 400 million downloads each. Moreover, the average time spent on TikTok continues to rise, with users spending approximately 19.6 hours per month on the app[1]— a figure comparable to Facebook's 23.7 hours per month and second only to YouTube. In Thailand, TikTok ranks eighth globally in user numbers, with 38 million users.[2]

As short-video consumption grows, various studies show that excessive use can lead to addiction and negatively impact mental health. For example, excessive TikTok use has been linked to increased depression, anxiety, stress, and memory loss.[3] Addiction to short videos has also been associated with poorer academic performance and reduced quality of life.[4] Despite their popularity as a source of entertainment and information, excessive or compulsive use of short-video platforms can have detrimental effects on individuals, families, and society. Therefore, it is essential to develop preventive measures from the outset.

Existing social media addiction screening tools, such as the Social Media Addiction Scale (S-MASS)[5] and the Bergen Social Media Addiction Scale[6], were developed prior to the rise of short-video platforms and thus do not include items that specifically address short-video addiction. Due to the lack of standardized diagnostic criteria for short video addiction, previous studies[7-9] often adapted existing addiction scales designed for social media, smartphones, or gaming addiction to assess this issue.

In the past two to three years, several additional assessment tools for short-video addiction have been developed, such as the TikTok Addiction Scale (TTAS)[10] and the Problematic TikTok Use Scale (PTTUS).[11] However, both instruments were created to evaluate addiction solely related to TikTok. Moreover, PTTUS includes items from both user perspectives — content creators and viewers — although current surveys[12] indicate that most users are viewers only. Additionally, the sample

sizes in the validation studies for TTAS and PTTUS were relatively small (around 300–400 participants) and limited age ranges, with data collection beginning at ages 18 and 16, respectively. Yet, short-video use is now prevalent among younger adolescents, even below these age thresholds. The Short Video Addiction Scale (SVAS)[13] was developed to assess addiction to various short-video platforms, but it was designed specifically designed for adolescents and includes only six items, evaluating functional impact in a single domain — sleep disturbance.

The present study aims to develop an assessment tool to measure overall short-video addiction across multiple platforms, based on the diagnostic criteria for gaming disorder outlined in the eleventh revision of the International Classification of Diseases (ICD-11).[14] This tool is intended to serve as a foundation for future research and to promote societal awareness, understanding, and preventive measures against excessive and problematic short-video consumption.

MATERIALS AND METHODS

Population and sample

This study employed a cross-sectional survey design using a structured questionnaire. Data collection was conducted between May and August 2025. The inclusion criteria were individuals aged 13 years and older who were able to read Thai and regularly consumed short-form video applications. The exclusion criteria were participants who provided incomplete questionnaire responses. Participants were recruited through online data collection via Google Forms, promoted across multiple social media channels. Participation was voluntary and individuals of all age groups could voluntarily click and complete the questionnaire. For participants aged 13–17, data collection was coordinated through four schools, with three located in Bangkok and one in the Southern region.

The researchers aimed to collect data from 1,932 individuals. A stratified random sampling method, based on age groups, was employed initially, followed by convenience sampling until the calculated target population size for each age stratum was reached. The sample was proportionally distributed according to the TikTok usage data from 2022[16] as follows: 13–17 years: 425 (22%); 18–24 years: 576 (29.8%); 25–34 years: 446 (23.1%); 35–44 years: 242 (12.5%); 45–54 years: 141 (7.3%); and 55 and above: 102 (5.3%). The final sample was balanced for sex, including an equal number of male and female participants.

Sample size calculation

The sample size was calculated using a one-group proportion formula at a 95% confidence level:

$$n = \frac{|p|(1-p)Z^2}{(0.01^2)} = \frac{0.952(1-0.952)(1.96^2)}{(0.01^2)} = 1,756$$

Where p = 95.2%[15] (the estimated population proportion), (Z) = 1.96 (for 95% confidence), and d = 1% (margin of error). To account for potential responses (10%), the total sample size was increased accordingly, resulting in a total sample size of approximately 1,932 participants (1,756 + 176).

Instruments

The questionnaire consisted of three parts:

1) Demographic information: This includes education level, occupation, marital status, chronic physical illnesses, psychiatric conditions, and family structure.

2) Social media and short-form video application usage behavior: This includes purpose of smartphone and social media use, most frequently used short-form video application, usage patterns, and perceived addiction to short-form videos.

3) Short-Video Application Addiction Questionnaire (S-VAAQ): The S-VAAQ was adapted from the Gaming Disorder Scale (GAME-S)[17]: a self-report version with nine items. It assesses three distinct categories of gaming disorder symptoms based on ICD-11 criteria, including difficulty controlling engagement (three items), prioritization of gaming over other activities (three items), and continued gaming despite negative consequences (three items). Items were reworded to reflect behaviors associated with short-video consumption. Responses were rated on a 4-point Likert scale: 0 (not at all) to 3 (definitely).

The questionnaire developed by the research team underwent expert content validation by five experts. After revising the questions until a good content validity score was achieved, the questionnaire was taken to a focus group to assess clarity and comprehension of the questions. This focus group consisted of five individuals aged 13-24 years and five aged 25 years and older. Adjustments were made based on their feedback, resulting in the final questionnaire used for further analysis.

Data analysis

Descriptive statistics, including median, standard deviation, percentiles, were used to summarize demographic characteristics and social media and short-form video application usage behaviors. Internal consistency of the S-VAAQ was evaluated using Cronbach's alpha. Content

validity was evaluated by five experts using the Content Validity Index (CVI). Construct validity was examined through the KMO Measure of Sampling Adequacy and Exploratory Factor Analysis (EFA) to identify the factor analysis of the S-VAAQ. Additionally, Latent Class Analysis (LCA) was employed to classify individuals based on response patterns.

RESULTS

From the total 4,476 online responses, 99.6% reported using short video applications. Among them, 3,416 people (76.3%) were regular users. The researchers selected the first 1,932 participants for data analysis based on age and gender distribution.

Demographic characteristics of participants

Most participants held a Bachelor's degree or higher. Demographics showed that 61% of participants were single. The majority reported overall good health, with 78% indicating no chronic physical illnesses and 85% reporting no psychiatric disease. Nearly half (49%) lived in nuclear family structures as shown in Table 1. The median daily time spent watching short-form videos was three hours per day.

Smartphones were primarily used for social media (69%), with only 5% reporting making phone calls as the main purpose. The most common objective for using social media was chatting/communication (41%), followed by watching/sharing short-form videos (36%), a rate four times higher than the next highest objective. Nearly half of the population favored TikTok as their primary platform. The majority (76%) reported being viewers rather than content creators. Significantly, over half of the population believed they were either potentially addicted or already addicted to short-video applications.

Content validity of the S-VAAQ

Content validity was established by five expert reviewers using the Content Validity Index (CVI). The evaluation covered relevance, clarity, and simplicity. All items achieved CVI scores of 0.79 or higher in all three aspects, confirming the instrument's content validity (Table 3).

Construct validity of the S-VAAQ

The scale exhibited internal consistency, with a Cronbach's alpha of 0.884. Factor analysis, with a KMO Measure of Sampling Adequacy of 0.898, and EFA revealed factor loadings ranging from 0.594 to 0.904. Items 1–3, 4–6, and 7–9 did not form distinct factors. Thus, all 9 items were retained as a single scale, as the removal of any item would have decreased the overall Cronbach's alpha (0.884), indicating the contribution of all items to the scale's reliability (Table 4).

Latent Class Analysis (LCA)

Based on the model fit indices, the three-class model was selected as the optimal solution in the Latent Class Analysis (LCA) (AIC = 44,029.623, BIC = 44,513.892, entropy = 0.916; Table 5). This model yielded score cut-off points that distinctly categorized participants into three latent classes: the 0-17 group, which included 964 individuals (49.9%); the 8-22 group, with 562 individuals (29.1%); and the 23-27 group, comprising 406 individuals (21.0%) (as illustrated in Fig 1).

DISCUSSION

This study developed and validated the Short-Video Application Addiction Screening Questionnaire (S-VAAQ), a screening tool designed to identify short-video application addiction among users who primarily consume short-form video content. Data were collected from a general population sample of individuals aged 13 years and older in Thailand (N = 1,932) to evaluate the psychometric properties of the S-VAAQ, which demonstrated good reliability and validity as a screening questionnaire.

The S-VAAQ is a 9-item self-report scale (total score range: 0–36) designed for rapid completion. Scores classify users into three risk groups: Low Risk (score <18), Moderate Risk (score 18-22), and High Risk (score >22). This classification framework facilitates early identification and intervention, ensuring that individuals at risk receive appropriate monitoring and clinical care.

The S-VAAQ was initially developed by adapting items from the GAME-S questionnaire, which is based on the ICD-11 criteria for gaming disorder encompassing three domains: Difficulty controlling engagement, prioritization over other activities, and continued use despite negative consequences. However, exploratory factor analysis (EFA) indicated that two items did not load onto their intended domains: Specifically, Item 3: ("I often get irritated when people tell me to stop watching short video clips") intended for the difficulty controlling engagement domain, was categorized under the continued despite negative consequences domain. This may reflect that irritation in response to warnings manifests as an interpersonal negative outcome. Similarly, Item 4: ("I often neglect or spend less time on my daily routines because of watching short video clips") originally assigned to prioritization over other activities, loaded under the difficulty controlling engagement domain.

TABLE 1. Demographic data.

Demographic data (n = 1932)	n	%
Level of Education		
Primary school	32	2
Lower secondary school	248	13
Upper secondary school / Vocational Certificate	395	20
Associate Degree / Higher Vocational Certificate	72	4
Bachelor's degree or higher	1185	61
Occupation		
Student	949	49
Government officer / State enterprise employee	383	20
Private company employee / Hired worker	335	17
Business owner / Entrepreneur	141	7
Freelancer / Self-employed	73	4
Unemployed / Retired	51	3
Marital status		
Single	1509	78
Married and living together	364	19
Married but living separately	31	2
Widowed / Divorced	28	1
Physical chronic illnesses		
No	1643	85
Yes	289	15
Psychiatric disease		
No	1834	95
Yes	98	5
Attention Deficit Hyperactivity Disorder (ADHD)	53	3
Depression	47	2
Anxiety / Panic Disorder	42	2
Bipolar Disorder	15	1
Learning / Intellectual Disabilities	6	0
Autism Spectrum Disorder	4	0
Substance Use Disorder	3	0
Eating disorder	1	0
Family structure in the past 12 months		
Living alone	219	11
Living with partner / friends / roommates	290	15
Nuclear family (parents and children living together)	946	49
Extended family (grandparents, parents, and children living together)	388	20
Skipped-generation family (grandparents and grandchildren living together)	53	3
Blended family (parents with stepchildren living together)	36	2

TABLE 2. Behavioral patterns and usage of smartphones, social media, and short-form video applications.

Behavioral and Usage of smartphone, social media and short-form video app data (n = 1932)	n	%
Purpose of smartphone use		
For using social media applications	1332	69
For other entertainment	278	14
For studying / working	189	10
For phone calls	100	5
For taking photos / recording videos	23	1
Purpose of social media use		
To chat / communicate (e.g., via Line)	796	41
To watch/share short-form videos (e.g., TikTok, YouTube Shorts, IG Stories)	695	36
To watch/share long-form videos (e.g., YouTube)	169	9
To view/share images (e.g., Instagram)	137	7
To read/share articles (e.g., Facebook, X)	124	6
Most frequently used short-form video app		
TikTok	953	49
Instagram reels/ story	379	20
Facebook reels	313	16
YouTube short	273	14
Others	5	0
Short-form videos viewing behavior		
Only watching	1472	76
Both watching and creating	454	23
Only creating	6	0
Perceived addiction to short-form videos		
Not addicted	527	27
Possibly addicted	1009	52
Addicted	396	20

TABLE 3. Content validity index (CVI) Scores of the S-VAAQ.

	Item 1	Item 2	Item 3	Item 4	Item 5	Item 6	Item 7	Item 8	Item 9
Relevance	1	1	1	1	1	1	1	1	1
Clarity	1	1	1	1	1	1	1	1	1
Simplicity	0.8	1	1	0.8	1	1	0.8	0.8	0.8

TABLE 4. Item-Level Factor Loadings and Reliability Analysis of the S-VAAQ.

Item	Factor 1	Factor 2	Factor 3	Corrected Item-Total Correlation	Cronbach's alpha if item delete	Mean	SD
Item 1		0.769	0.220	0.577	0.877	2.22	0.932
Item 2	0.205	0.834	0.209	0.631	0.873	2.45	1.033
Item 3	0.652	0.367		0.600	0.875	1.61	0.814
Item 4	0.469	0.594	0.284	0.713	0.865	2.02	0.961
Item 5		0.234	0.904	0.529	0.882	2.56	1.010
Item 6	0.414	0.386	0.638	0.716	0.865	2.11	0.950
Item 7	0.807	0.218	0.223	0.689	0.868	1.64	0.843
Item 8	0.736	0.286	0.230	0.683	0.868	1.81	0.911
Item 9	0.881			0.593	0.875	1.45	0.760

TABLE 5. Latent Class Analysis model for the S-VAAQ.

Model	AIC	BIC	Entropy
2-class	47026.086	47348.932	0.911
3-class	44029.623	44513.892	0.916
4-class	43022.733	43668.425	0.891

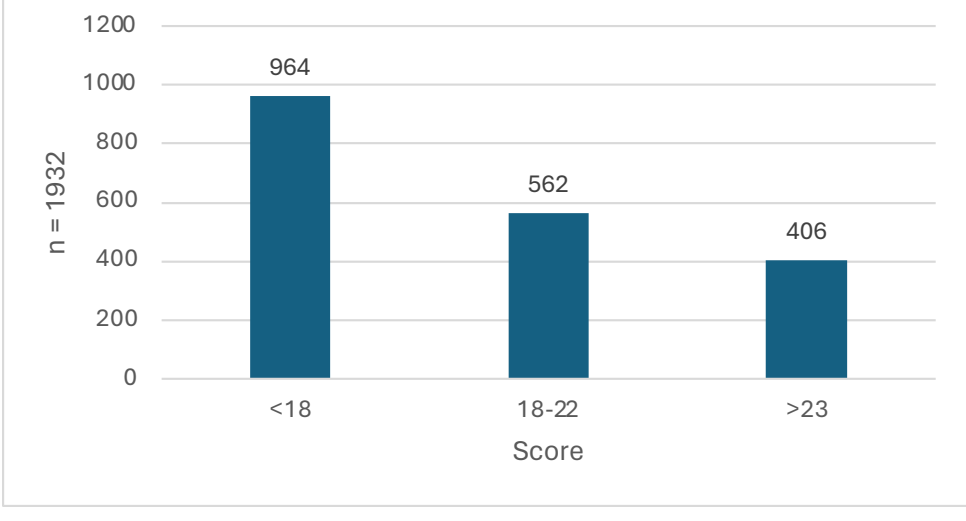

Fig 1. Cut-off points from the three-class Latent Class Analysis model of the S-VAAQ.

Similar ambiguity in interpretation is suggested as the reason for this unexpected loading.

Consequently, the researchers opted not to divide the S-VAAQ into separate domains but use a single total score instead. The internal consistency of the S-VAAQ was high, with a Cronbach's alpha of 0.884. Furthermore, the item-total correlation analyses indicated that the Cronbach's alpha if the item was deleted ranged from 0.865 to 0.882, which was lower than the overall Cronbach's alpha of 0.884. Therefore, no items were removed from the questionnaire.

Psychometrically, the S-VAAQ exhibits comparable reliability to existing instruments while offering distinct advantages. The S-VAAQ's Cronbach's alpha of 0.884 is similar to that of the PTTUS (0.83-0.90), however, the S-VAAQ is significantly more concise with only nine items compared to PTTUS's 16. Importantly, the S-VAAQ items specifically target viewing-related behaviors, aligning with the present study population where 76% of participants identified as being viewers only, whereas the PTTUS includes both content creators and viewers. When compared to the TTAS, the S-VAAQ's Cronbach's alpha (0.884) is slightly lower than the TTAS (0.911). Nevertheless, the fewer items in S-VAAQ (9 vs. 15), derived from only three core domains of game addiction, make it more practical for rapid self-screening. Furthermore, the S-VAAQ sample demonstrated superior representation of the general population due to equal male/female proportions and proportional sampling across short-video application usage age groups whereas the TTAS sample was disproportionately female and limited to ages of 16-54. Finally, while the S-VAAQ shares the same Cronbach's alpha (0.884) with SVAS, the S-VAAQ offers broader generalizability as SVAS was developed exclusively for an adolescent population.

This study has several notable strengths, including being the first in Thailand to develop a screening tool for short-video application addiction. The use of a large sample size, proportionally stratified across all user groups (starting from age 13, the minimum age for application use) and equal male/female ratio enhances the generalizability of findings. The S-VAAQ's brevity (9 items), self-report format, and straightforward language makes it well-suited for rapid self-screening, which aligns with the preferences of short-video users. The scale uses simple and understandable language, refined through focus group discussions involving participants aged 13 to over 55, including those with less than a high school education.

Limitations include a reliance on self-reported online data, which may introduce response bias. Also, the EFA results did not align with the original three-domain structure based on the ICD-11 model, limiting the tool's capacity to identify domain-specific impairments. Moreover, the sample was predominantly composed of individuals with a high school or higher education level.

This S-VAAQ questionnaire can serve as an effective screening tool for short-form video application addiction, allowing for early detection based on specific risk levels derived from the Latent Class Analysis (LCA) model.

1. Low Risk Group: Individuals with S-VAAQ scores between 0 and 17 are categorized into the Low Risk Group. This range corresponds to the lowest risk LCA class, suggesting that these participants are unlikely to be addicted to short-form video applications and generally do not require immediate intervention.

2. Moderate Risk Group: Scores ranging from 18 to 22 define the Moderate Risk Group. This level represents an elevated but subclinical level of short-form video application use disorder. Individuals in this group are strongly advised to increase self-awareness regarding their usage habits, and their patterns may warrant clinical attention or simple psychoeducational interventions to prevent progression to addiction.

3. High Risk Group: Finally, scores between 23 and 27 categorize participants into the High Risk Group. This range corresponds directly to the highest risk LCA class, indicating a high probability of meeting addiction criteria. Individuals identified in this group may require further psychiatric evaluation and intervention to address the potential disorder.

Future research should focus on improving the specificity of the screening tool, perhaps by refining the scoring thresholds or by integrating objective behavioral indicators, such as application usage duration and an assessment of psychosocial impact. Given the absence of direct diagnostic criteria for social media or short-video addiction, future work should also focus on developing standardized criteria that aligns more precisely with those standards.

CONCLUSION

The S-VAAQ is the first screening tool for short-video application addiction developed in Thailand and the first to comprehensively include users across all age groups, from the minimum allowable age through to adulthood, which successfully demonstrated good reliability and validity. This instrument is expected to be a valuable resource for screening short-form video addiction within the Thai population, thereby facilitating further research and the development of effective intervention strategies.

Data Availability Statement

The data underlying this study are not publicly available due to ethical and confidentiality constraints. However, de-identified data can be provided upon request to the corresponding author, pending approval from the institutional ethics review board. Relevant secondary data sources are referenced in the bibliography.

ACKNOWLEDGEMENTS

The research team sincerely thanks Tikumporn Hosiri, MD; Sirinadda Punyapa, MD; Pornjira Pariwatcharakul, MD; Tidarat Puranachaikere, MD; and Keerati Pattanaseri, MD for their expert evaluation of the content validity index (CVI). The authors also gratefully acknowledge Orawan Supapueng, PhD, and Ms. Narathip Sanguanpanit, Faculty of Medicine Siriraj Hospital, for their valuable statistical consultation and support.

DECLARATION

Grants and Funding Information

No funding was received for this study.

Conflict of Interest

The authors have no conflicts of interest to disclose.

Registration Number of Clinical Trial

Not applicable.

Author Contributions

Conceptualization and methodology, V.L, C.P., and W.A.; Investigation, V.L.; Formal analysis, V.L, W.A., and C.P; Visualization and writing – original draft, V.L ; Writing –review and editing, W.A., and C.P; Funding acquisition, W.A., and C.P; Supervision, W.A., and C.P; All authors have read and agreed to the final version of the manuscript.

Use of Artificial Intelligence

The authors used Gemini 2.5 Pro to assist with grammar correction and sentence refinement. All AI-assisted content was thoroughly validated and approved by the authors to ensure accuracy and compliance with academic and ethical standards.

Ethical Approval

This study was approved by the Institutional Review Board (IRB) of the Faculty of Medicine Siriraj Hospital (COA no.704/2024).

REFERENCES

1. Roj S. TikTok statistics and data for 2022 [Internet]. Thumbsup; 2022 [cited 2024 May 24]. Available from: https://www.thumbsup.in.th/tiktok-statistics-2022
2. TikTok users by country 2024 [Internet]. Statista; [cited 2024 May 24]. Available from: https://www.statista.com/statistics/1299807/number-of-monthly-unique-tiktok-users/
3. Sha P, Dong X. Research on adolescents regarding the indirect effect of depression, anxiety, and stress between TikTok use disorder and memory loss. Int J Environ Res Public Health [Internet]. 2021 [cited 2024 May 24];18(16):8820. Available from: https://pubmed.ncbi.nlm.nih.gov/34444569/
4. Ye JH, Wu YT, Wu YF, Chen MY, Ye JN. Effects of short video addiction on the motivation and well-being of Chinese vocational college students. Front Public Health [Internet]. 2022 [cited 2024 May 24];10:847672. Available from: http://dx.doi.org/10.3389/fpubh.2022.847672
5. Chanpen S, Pornnoppadol C, Vasupanrajit A, Dejatiwongse Na Ayudhya Q. An assessment of the validity and reliability of the Social-Media Addiction Screening Scale (S-MASS). Siriraj Med J [Internet]. 2023 [cited 2024 May 24];75(3):167–80. Available from: https://he02.tci-thaijo.org/index.php/sirirajmedj/article/view/261044
6. Andreassen CS, Torsheim T, Brunborg GS, Pallesen S. Development of a Facebook addiction scale. Psychol Rep [Internet]. 2012 [cited 2024 May 24];110(2):501–17. Available from: https://pubmed.ncbi.nlm.nih.gov/22662404/
7. Mu H, Jiang Q, Xu J, Chen S. Drivers and consequences of short-form video (SFV) addiction amongst adolescents in China: Stress-coping theory perspective. Int J Environ Res Public Health [Internet]. 2022 [cited 2024 May 24];19(21):14173. Available from: https://www.mdpi.com/1660-4601/19/21/14173
8. Zahra MF, Qazi TA, Ali AS, Hayat N, Hassan TU. How TikTok addiction leads to mental health illness? Examining the mediating role of academic performance using structural equation modeling. J Posit Sch Psychol [Internet]. 2022 [cited 2024 May 24];6(10):1490–502. Available from: https://journalppw.com/index.php/jpsp/article/view/13392
9. Lu L, Liu M, Ge B, Bai Z, Liu Z. Adolescent addiction to short video applications in the mobile Internet era. Front Psychol [Internet]. 2022 [cited 2024 May 24];13:893599. Available from: [http://dx.doi.org/10.3389/fpsyg.2022.893599
10. Galanis P, Katsiroumpa A, Moisoglou I, Konstantakopoulou O. The TikTok Addiction Scale: Development and validation. AIMS Public Health. 2024;11(4):1172–97.
11. Günlü A, Oral T, Yoo S, Chung S. Reliability and validity of the Problematic TikTok Use Scale among the general population. Front Psychiatry [Internet]. 2023 [cited 2024 May 24];14:1068431. Available from: [http://dx.doi.org/10.3389/fpsyt.2023.1068431
12. Miller M. 40+ TikTok stats digital marketers need to know [Internet]. Search Engine Journal. 2024 Apr 18 [cited 2025 Oct 3]. Available from: https://www.searchenginejournal.com/tiktok-stats/445449/
13. Jiang Z, Kang T, Chen Y, Chen W, Wu H. Validation of the Short Video Addiction Scale: a psychometric study among Chinese adolescents. Research Square [Preprint]. 2024 [cited 2024 Oct 3]. Available from: https://www.researchsquare.com/article/rs-6259796/v1
14. World Health Organization [Internet]. Gaming disorder; 2018 [cited 2018 Aug 4]. Available from: https://www.who.int/standards/classifications/frequently-asked-questions/gaming-disorder

15. China Internet Network Information Center (CNNIC). The 53rd Statistical Report on China's Internet Development. Beijing: CNNIC; 2024 Mar. p. 23. Available from: https://www.cnnic.com.cn/IDR/ReportDownloads/202405/P020240509518443205347.pdf
16. Iqbal M. TikTok revenue and usage statistics (2025). Business of Apps [Internet]. 2025 [cited 2025 Apr 18]. Available from: https://www.businessofapps.com/data/tik-tok-statistics/
17. Sangkhaphan T, Pornnoppadol C, Hataiyusuk S. The development of Gaming Disorder Scale (GAME-S). J Psychiatr Assoc Thailand. 2022;68(1):50–61.

Combining Histopathologic and Gene-Expression Profiling for Risk Stratification of Nodal Metastasis in Colorectal Cancer

Watsaphon Tangkullayanone, M.D.[1,2], Nutchavadee Vorasan, M.Sc.[3], Amphun Chaiboonchoe, Ph.D.[4], Atthaphorn Trakarnsanga, M.D.[2], Pariyada Tanjak, Ph.D.[2,5], Thanawat Suwatthanarak, Ph.D.[2,5], Woramin Riansuwan, M.D.[2], Kullanist Thanormjit, M.Sc.[2,5], Onchira Acharayothin, B.Sc.[2], Asada Methasate, M.D., Ph.D.[2], Yusuke Kinugasa, M.D., Ph.D.[8], Bhoom Suktitipat, M.D., Ph.D.[6,7], Vitoon Chinswangwatanakul, M.D., Ph.D.[2,5,*]

[1]Graduate School of Medical and Dental Sciences, Joint Degree Doctoral Program in Medical Sciences between Institute of Science Tokyo, Japan and Mahidol University, Bangkok, Thailand, [2]Division of General Surgery, Department of Surgery, Faculty of Medicine Siriraj Hospital, Mahidol University, Bangkok, Thailand, [3]Genetic Epidemiology Research Cluster, Research Division, Faculty of Medicine Siriraj Hospital, Mahidol University, Bangkok, Thailand, [4]Siriraj Center of Research Excellent for Systems Pharmacology, Department of Pharmacology, Faculty of Medicine Siriraj Hospital, Mahidol University, Bangkok, Thailand, [5]Siriraj Cancer Center, Faculty of Medicine Siriraj Hospital, Mahidol University, Bangkok, Thailand, [6]Department of Biochemistry, Faculty of Medicine Siriraj Hospital, Mahidol University, Bangkok, Thailand, [7]Integrative Computational BioScience (ICBS) Center, Mahidol University, Nakhon Pathom, Thailand, [8]Gastrointestinal Surgery, Institute of Science Tokyo, Bunkyo-ku, Japan.

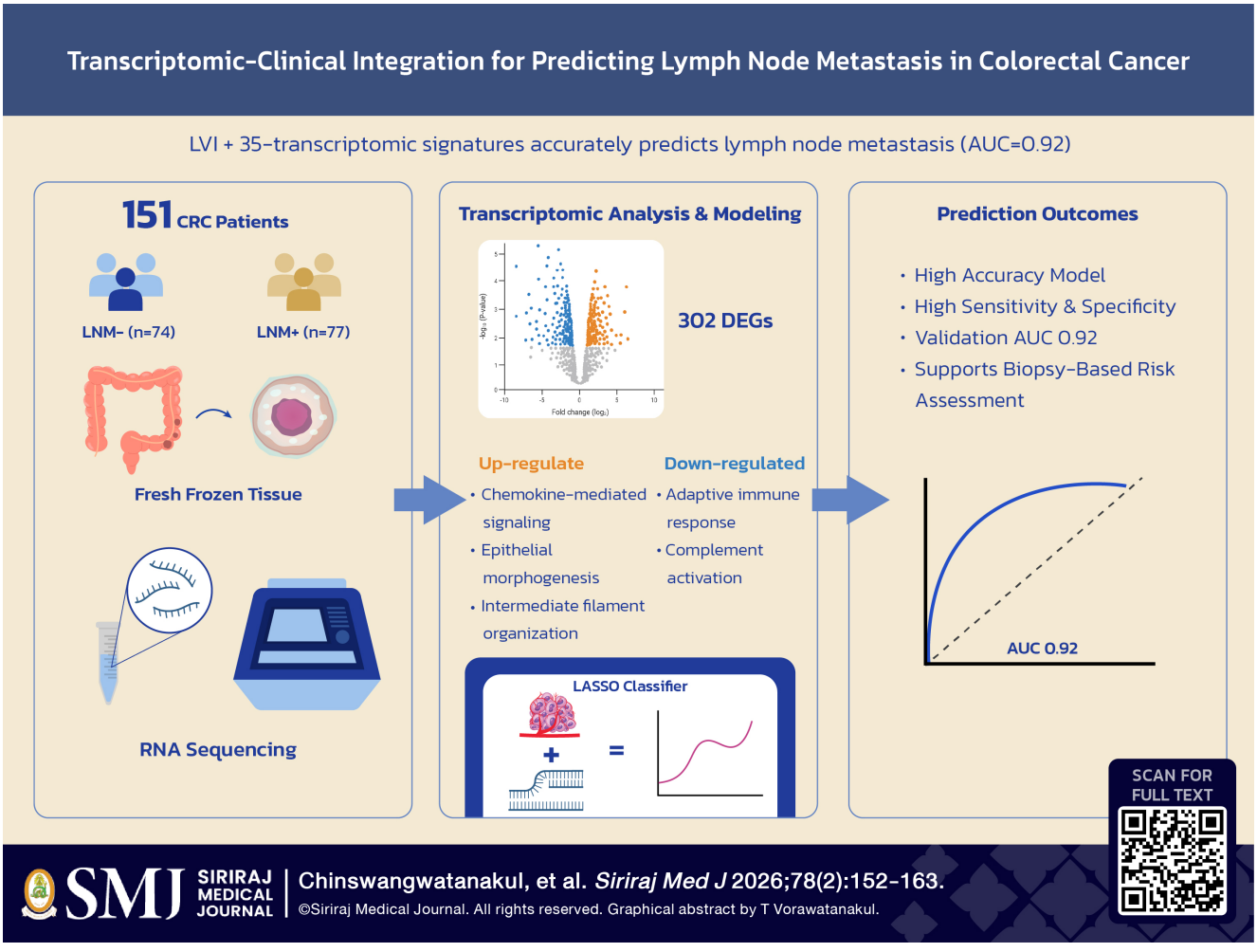

*Corresponding author: Vitoon Chinswangwatanakul
E-mail: vitoon.chi@mahidol.ac.th
Received 31 December 2025 Revised 13 January 2026 Accepted 13 January 2026
ORCID ID:http://orcid.org/0000-0001-9662-1669
https://doi.org/10.33192/smj.v78i2.279649

ABSTRACT

Objective: To identify gene-expression features associated with lymph node metastasis (LNM) in colorectal cancer (CRC) and to develop a transcriptomic-clinical predictive model for preoperative nodal assessment.

Materials and Methods: A total of 151 CRC tissue samples (74 LNM– and 77 LNM+) were analyzed using RNA sequencing. Differentially expressed genes (DEGs) were identified with DESeq2, and functional enrichment analyses were performed using the Database for Annotation, Visualization, and Integrated Discovery (DAVID). A Least Absolute Shrinkage and Selection Operator (LASSO) logistic regression model integrating gene-expression features with clinical variables was developed to predict LNM status. Model performance was evaluated using the area under the receiver operating characteristic curve (AUC), sensitivity, and specificity.

Results: A total of 302 DEGs were identified in LNM+ CRC, including 178 upregulated and 124 downregulated genes. Upregulated genes were enriched in chemokine-mediated signaling, epithelial morphogenesis, and intermediate filament organization, whereas downregulated genes were associated with adaptive immune response and complement activation. In multivariate analysis, lymphovascular invasion (LVI) was the only clinical variable independently associated with LNM. The optimized LASSO model, combining LVI with selected transcriptomic features, demonstrated excellent discriminatory performance (AUC ≈ 0.92). Key upregulated genes included *CCL21, CCL26, DEFB1, LST1, KANK4, TNNC1, PFDN6, TENM1, CST6,* and *PADI3,* while *IGHV2-26* was downregulated.

Conclusion: Integration of LVI with transcriptomic signatures enables accurate prediction of lymph node metastasis in CRC and supports biopsy-based risk assessment to guide clinical decision-making.

Keywords: Colorectal neoplasm; Lymphatic metastasis; RNA sequencing; Gene expression regulation; Logistic Models (Siriraj Med J 2026;78(2):152-163)

INTRODUCTION

Colorectal cancer (CRC) is one of the most prevalent malignancies of the gastrointestinal tract and ranks among the top three most commonly diagnosed cancers globally as reported in the GLOBOCAN 2020 database.[1] The global incidence of CRC is approximately 19.5 per 100,000 population and continues to increase despite advances in screening programs and treatment modalities. Mortality remains significant, with an estimated rate of 9 deaths per 100,000 population, underscoring the growing clinical burden of the disease.

The five-year overall survival rate for screen-detected CRC is approximately 83.4%.[2] Survival outcomes in CRC are strongly influenced by clinical staging, which is determined by tumor invasion depth (T stage) and lymph node involvement (N stage). According to the AJCC 8th edition[3], the presence of lymph node metastasis (LNM) marks the transition to Stage III, also known as locally advanced disease. While patients with Stage I and II CRC typically have excellent five-year survival rates—approaching 90%—this rate drops to around 80% in Stage III and falls below 50% in Stage IV disease. At Siriraj Hospital in Thailand, reported five-year survival rates for CRC are 89.1% for Stage I, 78.6% for Stage II, and 57.9% for Stage III disease.[4]

In clinical practice, LNM in CRC is evaluated using a combination of tumor characteristics and imaging findings. First, the depth of primary tumor invasion (T stage), typically assessed by endoscopic examination and preoperative imaging, is a key determinant of nodal involvement, with reported LNM rates increasing from 14.3% in T1 tumors to 25.6% in T2, 61.2% in T3, and 65.6% in T4 disease.[5] Second, direct assessment of lymph node status is performed using preoperative imaging, most commonly computed tomography (CT), which infers nodal metastasis based on lymph node size (>9 mm), morphology, margin characteristics, and nodal clustering. However, the diagnostic accuracy of CT remains limited (approximately 60–70%) and is subject to both false positive and false negative results.[6] Third, pathological features obtained from biopsy specimens, particularly lymphovascular invasion (LVI), are used as indicators of nodal spread. Although LVI is associated with an increased risk of LNM, its predictive value is constrained by the fact that histological LVI is identified in only about one-third of patients with confirmed nodal metastasis.[7,8]

Given the limitations of current diagnostic approaches, there is growing interest in integration of molecular biomarkers into the staging process. Transcriptomic profiling, particularly through RNA sequencing, has emerged as a powerful tool for identifying gene expression patterns associated with metastatic behavior. The differentially expressed genes (DEGs) analysis may reveal molecular

signatures linked to lymph node involvement, offering a path to more precise risk stratification.

In this study, we aim to characterize the biological functions and signaling pathways of DEGs and to establish a predictive model for LNM in CRC. By integrating RNA-sequencing–based gene expression profiles with relevant clinical variables, we applied the Least Absolute Shrinkage and Selection Operator (LASSO) regression to identify genes most strongly correlated with nodal involvement. The resulting gene signature is intended to improve the preoperative risk assessment and facilitate personalized management of patients with CRC.

MATERIALS AND METHODS

Patients aged 18 years or older with a histopathologically confirmed diagnosis of CRC who underwent upfront surgical resection at Siriraj Hospital between 2011 and 2024 were included. Diagnosis and preoperative staging were established by colonoscopic biopsy and contrast-enhanced CT imaging. During surgery, representative primary tumor tissue was collected and preserved as fresh frozen samples, while the entire specimen underwent standard pathological assessment. Patients were excluded if they had suspected hereditary CRC syndromes, multiple synchronous primary CRCs, received neoadjuvant chemotherapy or radiotherapy prior to surgery, or presented with distant metastatic disease at diagnosis, as defined by the American Joint Committee on Cancer (AJCC) Cancer Staging Manual, 8th Edition.[9]

There are 207 CRC cases in the tissue bank. After applying exclusion criteria, 2 samples from patients who had received neoadjuvant chemoradiation, 3 samples with synchronous tumors, and 9 samples with confirmed hereditary CRC were excluded. As this study focused on LNM, 40 stage IV samples were excluded. RNA-sequencing quality control identified two additional outlier samples, which were removed from the analysis. The final cohort comprised 151 samples, which 74 were the LNM-negative (LNM-) group and 77 were the LNM-positive (LNM+) group.

Total RNA was extracted from fresh CRC tissue specimens preserved in RNAlater using a previously described protocol[10] and purified with the RNeasy Mini Kit (Qiagen). RNA concentration, purity, and integrity were assessed using NanoDrop spectrophotometry and the Agilent 2100 Bioanalyzer; only samples with RNA integrity numbers (RIN) >7 and total RNA yield >1 μg were included. Messenger RNA was enriched using poly-T oligo–attached magnetic beads, followed by strand-specific library construction with dUTP incorporation. Library quality was evaluated by Qubit, qPCR, and Bioanalyzer profiling. Paired-end sequencing (2 × 150 bp) was performed on an Illumina NovaSeq platform, generating approximately 8 Gb of data per sample. Library preparation and sequencing were outsourced to Novogene Co. Ltd. (Singapore).

Statistical analysis

RNA-sequencing data pre-processing and transcript abundance quantification

Raw RNA-sequencing data (FASTQ format) were assessed for quality using FastQC. Adapter sequences and low-quality reads were trimmed using FastP, followed by post-filtering quality verification with FastQC and summary reporting using MultiQC. Quality-controlled reads were quantified using Salmon with pseudo-alignment against the GRCh38 human reference transcriptome. Transcript-level abundances were summarized at the gene level using the R package TXimport.[11-15]

Quality control and normalization

RNA-sequencing data from primary CRC tumors comprising 37,788 genes were analyzed. Quality control at the expression level was assessed using Relative Log Expression (RLE) plots. Samples whose median RLE deviated substantially from zero were considered outliers and excluded before analysis, yielding the final dataset used for downstream procedures. Low-count genes were removed before normalization and testing. We retained genes with ≥10 total reads across all samples and detectable expression in >30 samples. Normalization was performed using the median-of-ratios method in DESeq2, and variance stabilizing transformation (VST) was subsequently applied to normalized counts for downstream analyses.

DEGs and predictive modeling

The DEGs between patients with lymph node–positive and lymph node–negative CRC were tested using the Wald test in DESeq2 under a negative binomial framework. Multiple testing was controlled with the Benjamini–Hochberg false discovery rate (FDR); genes with FDR-adjusted $p < 0.05$ were considered statistically significant. For interpretability, we prespecified a threshold of $|\log_2 \text{fold change}| > 1$ to denote biologically meaningful effects.

Functional enrichment of the resulting 302 DEGs was conducted using the Database for Annotation, Visualization, and Integrated Discovery (DAVID).[16] Enrichment was assessed on multiple databases, including Gene Ontology (GO), Kyoto Encyclopedia of Genes and Genomes (KEGG), WikiPathways, and Reactome.

Statistical significance thresholds were set at p value < 0.05 and q value < 0.15 after correction for multiple testing by the Benjamini–Hochberg false discovery rate (FDR) method. Given the exploratory nature of pathway enrichment analysis, a less stringent FDR threshold (q < 0.15) was applied to identify biologically relevant pathways while minimizing false negative findings.

For downstream visualization and predictive modeling, the data were subsequently standardized to z-scores (per gene); when specified, the means and standard deviations (SDs) were estimated from the lymph node–negative reference group.

To develop a classifier for lymph node status, we used the LASSO logistic regression (glmnet package). The dataset was randomly partitioned into training (70%), testing (20%), and hold-out validation (10%) sets with stratification by outcome. The regularization parameter (λ) was selected via 10-fold cross-validation within the training set using the one-standard-error (1-SE) rule when applicable. Model performance was quantified in test and validation sets using the area under the receiver operating characteristic curve (AUC), sensitivity, and specificity. All modeling was performed in R 4.5.0.

We compared three regularized logistic regression approaches including Ridge (L2), Elastic Net ($\alpha \in [0,1]$), and LASSO (L1) using identical variable and the same outcome-stratified train/test/validation splits. For Elastic Net, α was tuned on a grid while λ was selected by 10-fold cross-validation. Model selection prioritized discrimination (AUC) and calibration on the test set, with parsimony considered when performance was comparable.

RESULTS

Baseline clinicopathological characteristics are summarized in Table 1. A total of 151 CRC samples were analyzed, including 74 LNM− and 77 LNM+ cases. Age, sex, and tumor location did not differ significantly between groups. In contrast, tumor invasion depth (T stage) was significantly higher in the LNM+ group (p < 0.001), with T3–T4 tumors predominating. LVI and perineural invasion (PNI) were strongly associated with LNM (both p < 0.001) and were largely absent in LNM− cases. Tumor differentiation was comparable between groups, with most tumors being moderately differentiated. Overall, T stage, LVI, and PNI were significantly associated with the presence of LNM, whereas other clinical features showed no significant differences.

Quality control of RNA-sequencing data from all CRC samples (37,788 genes) was performed using Relative Log Expression (RLE) plots (Fig S1).[17-19] Two samples with median RLE values deviating substantially from zero were excluded, leaving 151 samples for downstream analyses.

After sample QC and low-count filtering (retaining genes with ≥10 total reads and expression in >30 samples; 17,906 genes remained), differential expression was assessed in DESeq2. Using median-of-ratios normalization and Wald testing, we identified 302 DEGs in the primary tumors from the patients with lymph node–positive vs lymph node–negative CRC at FDR-adjusted p < 0.05 and $|\log_2$ fold change$| > 1$. Of these, 178 genes were upregulated and 124 were downregulated in lymph node–positive tumors. The overall distribution of effect sizes and significance is shown in the volcano plot (Fig 1) and the complete DEG list provided in Table S1.

Functional enrichment analysis of these DEGs using DAVID revealed distinct biological signatures between the two groups, as summarized in Table 2. The upregulated genes were mainly associated with epithelial morphogenesis, intermediate filament organization, and chemokine-mediated signaling, whereas the downregulated genes were enriched for pathways related to adaptive immune response and complement cascade.

For prediction, the 151 samples were partitioned with outcome stratification into training (n = 106; LNM−group = 51, LNM+ group = 55), test (n = 30; LNM−group = 18, LNM+ group = 12), and hold-out validation (n = 15; LNM− group = 5, LNM+ group = 10) sets (Fig 2). The candidate predictor set comprised 302 genes identified from the DEGs analysis (DESeq2; VST-transformed expression values standardized to per-gene z-scores; see Fig S2), along with the clinical covariates sex, age, primary tumor location, T stage, LVI, PNI, and tumor differentiation. Ten-fold cross-validation selected the penalty that minimized binomial deviance at λ_min = 0.01055471 ($\log \lambda \approx -4.55$) (Fig 3), yielding a 36-variable LASSO model (35 genes + LVI) with non-zero coefficients associated with lymph node positivity. Using this λ_min model, the classifier trained on per-gene z-standardized VST expression demonstrated excellent discrimination: in the training set, AUC was 1.00 with 100.0% sensitivity, 100.0% specificity, and 100.0% accuracy; in the independent test set, AUC was 0.93 with 91.7% sensitivity, 88.9% specificity, and 90.0% accuracy; and in the hold-out validation set, AUC was 0.92 with 90.0% sensitivity, 100.0% specificity, and 93.3% accuracy (Fig 4). For completeness, the one-standard-error solution is reported in Table 3 as a parsimonious comparator, but all primary performance estimates refer to the λ_min (35 genes + LVI) model. Non-zero coefficients for the λ_min model are listed in Table 3.

We compared LASSO, Ridge, and Elastic Net logistic

TABLE 1. Baseline characteristics of the patients according to lymph node status.

Characteristic	LNM− (n=74)	LNM+ (n=77)	p-values
Age, yr (mean ±SD)	66.89 ± 12.70	63.92 ± 11.60	0.135
Male, n (%)	44 (59.5)	38 (49.4)	0.213
Primary tumor location, n (%)			0.332
Right colon	11 (14.9)	10 (13.0)	
Transverse colon	4 (5.4)	2 (2.6)	
Left colon	31 (41.9)	25 (32.5)	
Rectum	28 (37.8)	40 (51.9)	
T stage, n (%)			<0.001
T1	6 (8.1)	1 (1.3)	
T2	31 (41.9)	9 (11.7)	
T3	32 (43.2)	53 (68.8)	
T4a	3 (4.1)	9 (11.7)	
T4b	2 (2.7)	5 (6.5)	
LVI, n (%)			<0.001
No	69 (93.2)	48 (62.3)	
Yes	5 (6.8)	29 (37.7)	
PNI, n (%)			<0.001
No	68 (91.9)	53 (68.8)	
Yes	6 (8.1)	24 (31.2)	
Tumor differentiation, n (%)			0.126
Well differentiated	14 (18.9)	5 (6.5)	
Moderately differentiated	58 (78.4)	67 (87.0)	
Poorly differentiated	1 (1.4)	1 (1.3)	
Signet-ring cell	0 (0)	2 (2.6)	
Mucinous	1 (1.4)	2 (2.6)	

*p-values are based on the t-test for continuous variables and the χ^2 test for categorical variables.

regression using identical features and outcome-stratified train/test/validation splits. LASSO provided the most balanced and consistent discrimination across held-out sets, achieving an AUC of 0.93 in the test set (sensitivity 91.7%, specificity 88.9%) and 0.92 in the validation set (sensitivity 90.0%, specificity 100.0%), while maintaining perfect training performance (AUC 1.00) (Fig 4). Ridge regression yielded a slightly higher test AUC (0.95) but produced a non-sparse solution that retained all features; test specificity (88.9%) and sensitivity (100.0%) were comparable, and validation AUC was 1.00 (sensitivity 90.0%, specificity 100.0%) (Fig S4). Elastic Net produced a test AUC of 0.92 with sensitivity (91.7%) at specificity (83.3%), and a validation AUC of 0.92 (sensitivity 90.0%, specificity 100.0%) (Fig S6). Considering sensitivity, specificity, and AUC jointly on the independent test and validation sets together with model sparsity and interpretability we selected LASSO as the final classifier.

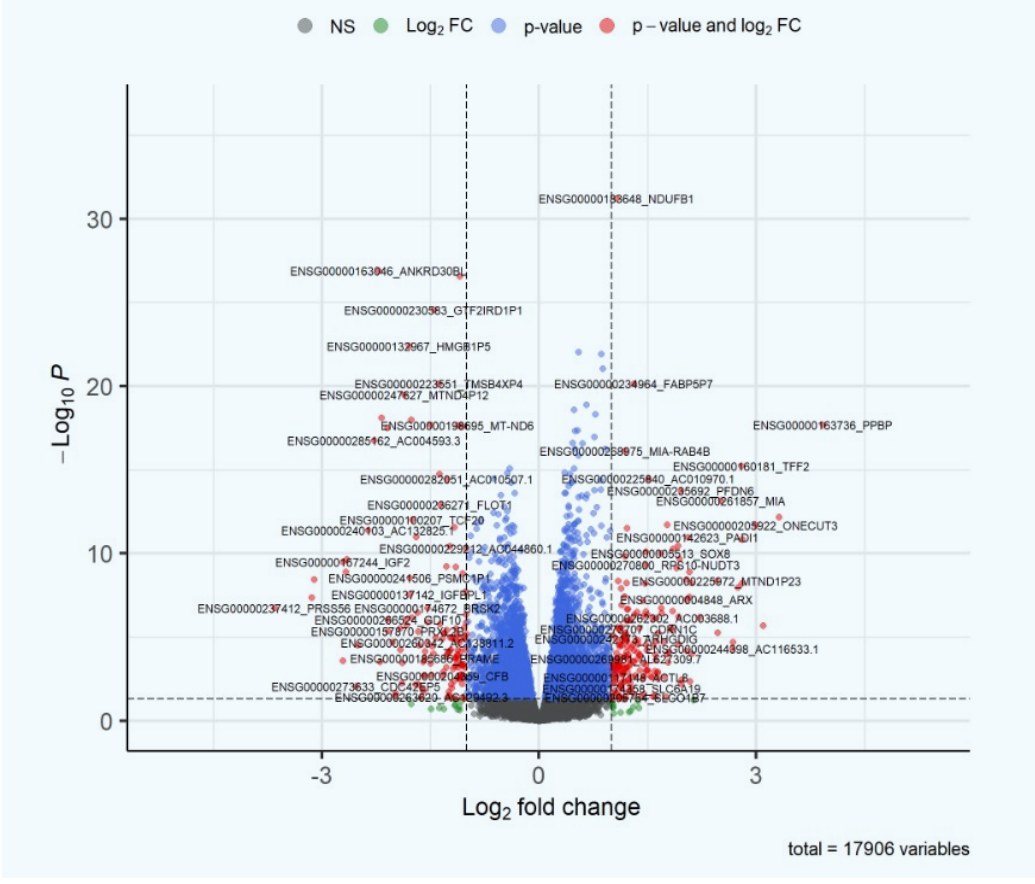

Fig 1. Volcano plot displaying differential expression between lymph node–positive and lymph node–negative CRC (DESeq2, Wald test). The x-axis shows $\log_2$ fold change (LNM+ vs LNM–) and the y-axis shows $-\log_{10}$ (FDR-adjusted P). The points in red indicate significantly DEGs ($|\log_2 FC| > 1$, FDR < 0.05; n = 302), and the points in blue represent genes with FDR < 0.05 but fold changes within ±1 (less than two-fold change). Non-significant genes are shown in grey.

TABLE 2. Functional Pathways and Representative Genes in LNM+ CRC.

Upregulation in LNM+ CRC	Representative Genes	Downregulation in LNM+ CRC	Representative Genes
Pancreatic cancer subtypes	SCEL, TFF2, KRT7, CTSE, CST6, KRT6A	Adaptive immune response	FGB, FGA, IGHV3-72, IGKV3-7, IGHV2-26, IGKV1D-13, IGKV1D-12, IGHG2, IGKV6D-21, TRBC2, IL17F, IL17A, IGKV2D-24
Morphogenesis of the epithelium	KRT16, SOX8, SOX10, KRT6A	Complement system	FGB, FGA, CFHR2, CFB, CPN1, C2
Chemokine-mediated signaling	CCL13, CCL21, TFF2, PPBP, CCL26	Regulation of complement cascade	IGHG2, CFHR2, CFB, IGKV1D-12, CPN1, C2
Intermediate filament organization	KRT16, KRT7, KRT6B, KRT6A, PRPH	Complement cascade	IGHG2, CFHR2, CFB, IGKV1D-12, CPN1, C2
Cell maturation	CCL21, REN, SOX8, SOX10	Complement and coagulation cascades	FGB, FGA, CFHR2, CFB, C2

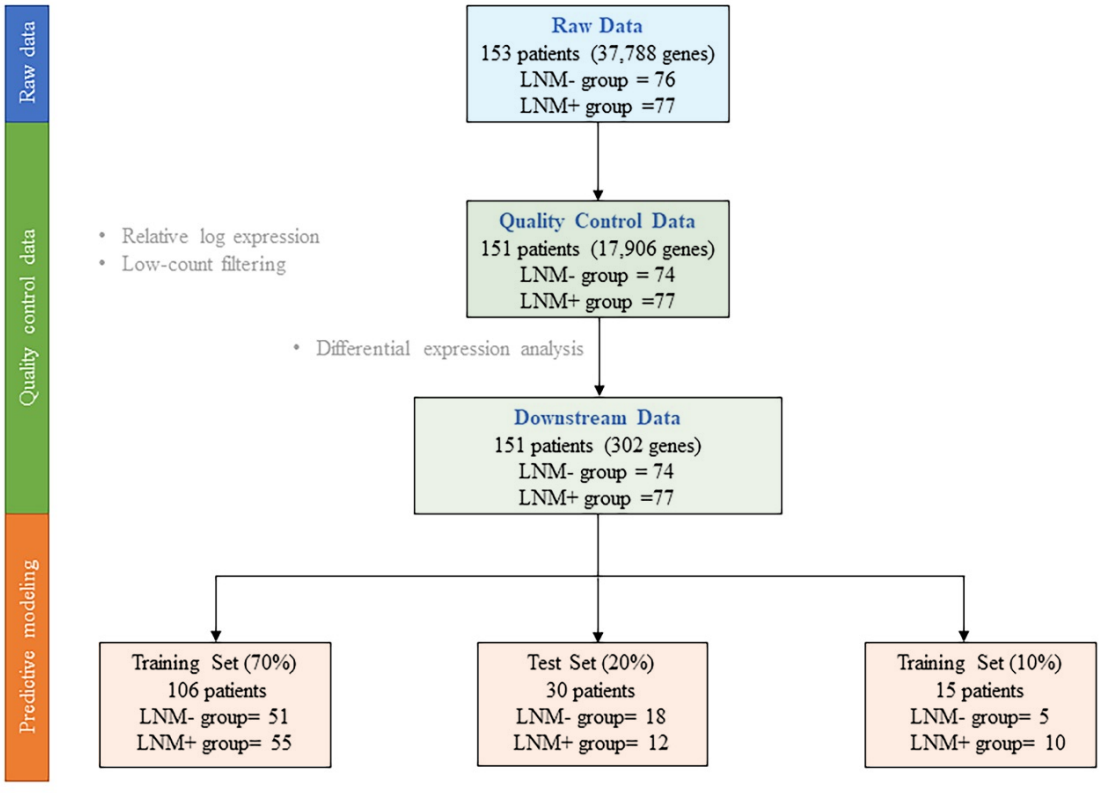

Fig 2. Diagram dataset split for predictive modeling

The full cohort (n = 151 tumors; 17,906 genes after low-count filtering) was partitioned by outcome into training (70%, n = 106; LNM−group = 51, LNM+ group = 55), test (20%, n = 30; LNM−group = 18, LNM+-group = 12), and hold-out validation (10%, n = 15; LNM− group = 5, LNM+ group = 10) sets using stratified random sampling.

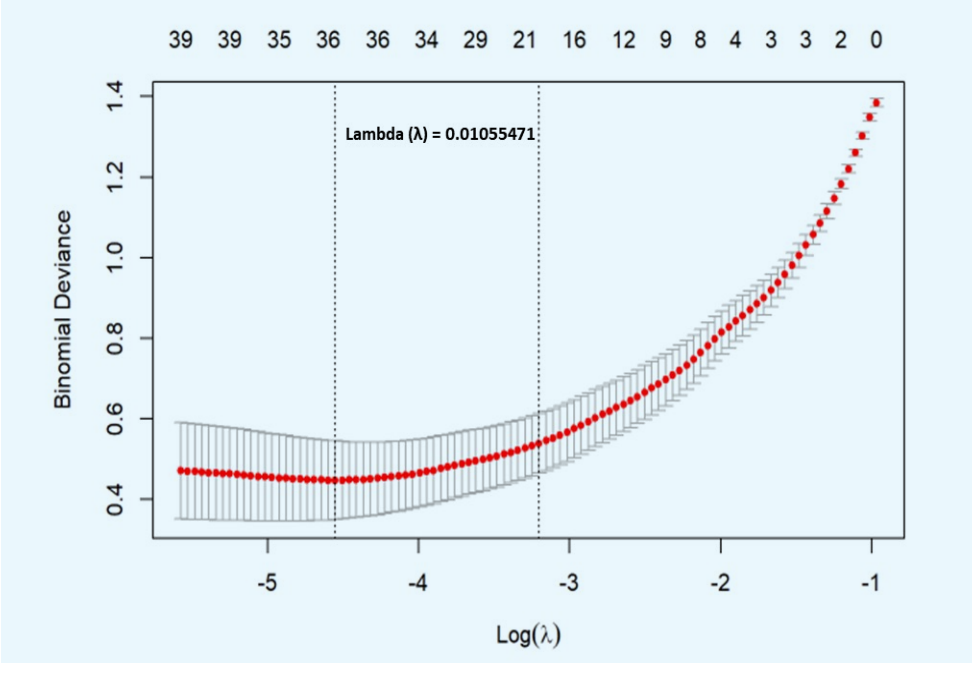

Fig 3. Ten-fold cross-validation for the LASSO logistic model.

Ten-fold cross-validation curve showing mean binomial deviance (red points) ± 1 SE (gray bars) across log(λ) values. The vertical dotted lines mark λ_min (left) and λ_1SE (right). The selected penalty at λ_min = 0.01055471 (log λ ≈ −4.55) minimizes deviance. The numbers along the top indicate the number of non-zero coefficients in the model at each λ.

TABLE 3. Final LASSO genes and clinical variable to predict lymph-node positive status.

Type	Regulation	Ensembl ID	Gene symbol/variable	Coefficient (β)
Clinical			LVI	1.367
Gene	Downregulation	ENSG00000285162	AC004593.3	-0.659
Gene		ENSG00000244694	PTCHD4	-0.396
Gene		ENSG00000205578	POM121B	-0.278
Gene		ENSG00000066032	CTNNA2	-0.266
Gene		ENSG00000143627	PKLR	-0.225
Gene		ENSG00000170892	TSEN34	-0.153
Gene		ENSG00000177238	TRIM72	-0.151
Gene		ENSG00000262771	SSBP1	-0.124
Gene		ENSG00000196656	AC004057.1	-0.096
Gene		ENSG00000167244	IGF2	-0.057
Gene		ENSG00000147255	IGSF1	-0.049
Gene		ENSG00000135744	AGT	-0.044
Gene		ENSG00000282344	IGHV2.26	-0.042
Gene		ENSG00000259848	AC097374.1	-0.025
Gene	Upregulation	ENSG00000270136	MINOS1.NBL1	0.551
Gene		ENSG00000174473	GALNTL6	0.526
Gene		ENSG00000276725	CEP170	0.519
Gene		ENSG00000226182	LST1	0.438
Gene		ENSG00000267022	AC067968.1	0.429
Gene		ENSG00000278622	TSEN34	0.392
Gene		ENSG00000006606	CCL26	0.290
Gene		ENSG00000114854	TNNC1	0.284
Gene		ENSG00000204542	C6orf15	0.280
Gene		ENSG00000280571	AC006059.2	0.270
Gene		ENSG00000283707	AC275455.1	0.239
Gene		ENSG00000175315	CST6	0.151
Gene		ENSG00000132854	KANK4	0.132
Gene		ENSG00000268975	MIA.RAB4B	0.096
Gene		ENSG00000137077	CCL21	0.073
Gene		ENSG00000164825	DEFB1	0.065
Gene		ENSG00000142619	PADI3	0.057
Gene		ENSG00000009694	TENM1	0.054
Gene		ENSG00000206283	PFDN6	0.042
Gene		ENSG00000234964	FABP5P7	0.027
Gene		ENSG00000178343	SHISA3	0.022

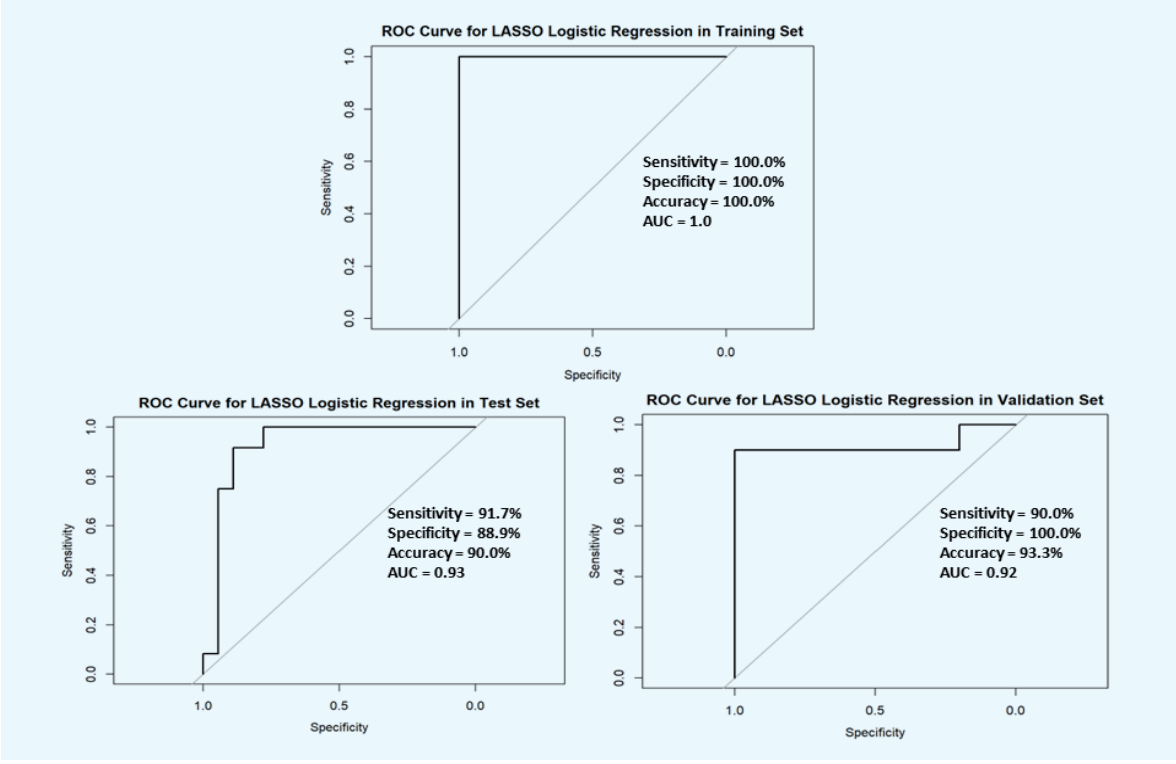

Fig 4. ROC curves for the 35 genes + LVI LASSO classifier
Receiver operating characteristic (ROC) curves for the LASSO logistic regression model selected at λ_min = 0.01055471, evaluated in the training (top), test (bottom-left), and hold-out validation (bottom-right) sets. Performance summaries are shown within each panel.

DISCUSSION

LVI is a well-established histopathological marker of aggressive colorectal cancer and was significantly associated with lymph node metastasis (LNM) in our cohort. After integration into a multivariate LASSO model with transcriptomic variables, LVI remained the only independent pathological predictor, underscoring its role as a critical early step in lymphatic dissemination. Functional analysis of 302 differentially expressed genes revealed that LNM-positive tumors were enriched for pathways related to chemokine signaling, epithelial morphogenesis, and cytoskeletal organization, while downregulated genes were associated with adaptive immune responses and complement activation. These findings suggest that nodal metastasis in CRC arises from coordinated epithelial remodeling alongside suppression of antitumor immune mechanisms.

Among these, Sciellin (SCEL) promotes cancer cell stiffness and tumor colonization, partly through activation of the Wnt/β-catenin pathway and enhancement of mesenchymal-to-epithelial transition (MET). Elevated SCEL expression in late-stage CRC suggests its involvement in tumor progression.[20] Chemokine-mediated signaling directs lymphocyte trafficking to lymph nodes, and it has been hypothesized that cancer cells may exploit this mechanism to invade lymphatic tissue.[21] In this pathway, CCL21 and CCL26 (C-C motif chemokine ligand 21 and 26) are implicated. CCL21 promotes nodal spread through matrix metalloproteinase-9 (MMP9) activation and extracellular matrix remodeling[22,23], thereby enhancing cancer cell migration.[24] Additionally, increased expression of epithelial markers such as Keratin (KRT) or cytokeratin (CK) has been associated with tumor progression, increased migratory capacity, and epithelial–mesenchymal transition (EMT).[25] The transcription factor SOX8 (SRY-box) further contributes to aggressive tumor behavior by activating Wnt/β-catenin signaling, leading to enhanced proliferation, reduced apoptosis, and increased EMT activity.[26]

Tumor-infiltrating B lymphocytes (TIBLs) are associated with favorable outcomes in CRC, and downregulation of IGHV2-26 may reflect reduced immune infiltration and enhanced immune evasion.[27] Additionally, diminished expression of the complement cascade may impair immune surveillance and complement-dependent cytotoxicity, facilitating LNM.[28]

The LASSO regression model identified a concise panel of 35 genes together with LVI as an independent clinical predictor of lymph-node metastasis. Although the selected genes did not fully overlap with the DAVID-

enriched set, many shared functional relevance with pathways involved in chemokine signaling, epithelial remodeling, cytoskeletal dynamics, and immune regulation. This complementarity reflects the distinct aims of the two analyses: DAVID reveals global biological themes, while LASSO isolates the smallest gene set that best predicts metastatic potential.

Among the upregulated genes, several were linked to chemokine-mediated signaling and immune modulation. CCL21 and CCL26 may guide tumor-cell migration toward lymphatic channels through MMP9-dependent matrix remodeling. DEFB1 (Defense beta1), an innate-immunity gene with context-specific oncogenic or suppressive roles, correlates with immune-checkpoint activation and poorer outcomes.[29,30] LST1 (Leukocyte specific transcript 1) mediates inflammatory crosstalk between tumor and stromal cells, promoting invasion and proliferation.[31,32]

KANK4 (KN motif and ankyrin repeat domains 4)[33,34], TNNC1 (Troponin C1)[35-37], PFDN6 (Prefoldin 6)[38], and TENM1 (Teneurins 1)[39], regulate cytoskeletal organization and epithelial structure, supporting increased motility and adhesion changes characteristic of metastatic cells.

PADI3 (Protein arginine deaminase 3)[40,41] and CST6 (Cystatin 6)[42,43] participate in EMT control; their dysregulation may favor metastatic colonization. GALNT6 (Polypeptide N-acetylgalactosaminyltransferase 6)[44] promotes proliferation and migration by altering mucin glycosylation and epithelial polarity, while TSEN34 and CEP170[45]—involved in RNA processing and cell-division control—likely reflect heightened proliferative activity in advanced tumors.

Among the downregulated genes, several act as tumor suppressors or immune mediators. TRIM72 (Tripartite motif containing 72)[46] and PTCHD4 (Patched domain containing 4)[47,48], a negative regulator of Hedgehog (HH) signaling. Loss of Patched-mediated inhibition may lead to HH signaling activation and promote EMT induction. Reduced CTNNA2 (Catenin alpha 2) disrupts epithelial adhesion and favors mesenchymal transformation.[49] The suppression of IGHV2-26, a key immunoglobulin heavy-chain gene, mirrors the weakened adaptive-immune and complement pathways observed in the DAVID analysis.

Overall, our findings highlight the central role of LVI in allowing tumor cells to access the lymphatic system and spread to lymph nodes. Lymph-node–positive CRC demonstrated increased chemokine signaling, cytoskeletal remodeling, EMT, and reduced immune activity, which are biological processes that support metastatic progression. The genes selected by the LASSO model represent these pathways and together form an expression pattern that can help estimate the likelihood of nodal involvement. This study has strengths, including the integration of gene-expression data with a routinely assessed pathological feature, LVI, producing a model that may be usable in real clinical decision-making. However, the study also has limitations. Samples were obtained from a single center, and some genes in the model have not yet been well studied in CRC. Some histopathologic features incorporated into the model, including tumor budding and LVI, are known to be subject to inter-observer variability. These parameters were derived from routine pathology reports assessed by a single pathologist, rather than independent review by multiple observers. This may introduce variability in feature classification and represents a limitation of the study. The proposed model is intended for preoperative risk stratification using colonoscopic biopsy specimens, all transcriptomic data were generated from surgically resected tumor tissues. Therefore, external validation using matched biopsy and resection samples will be essential to determine the generalizability of this model and to establish its applicability for preoperative clinical decision-making. In addition, future studies should evaluate whether a targeted expression panel derived from the model genes, such as RT-qPCR- or immunohistochemistry (IHC)-based assay can maintain predictive performance.

CONCLUSIONS

Combining LVI with transcriptomic profiling provides an effective approach to predict lymph-node metastasis in CRC. The resulting gene-based model reflects coordinated activation of chemokine signaling, cytoskeletal remodeling, and EMT, accompanied by immune suppression, and demonstrates strong potential for early nodal risk assessment. However, further validation in preoperative biopsy samples is required to confirm its real-world clinical utility. In addition, optimization of the gene set into a targeted, cost-effective assay suitable for routine pathology workflows will be necessary to support future clinical translation.

Data Availability Statement

The authors affirm that the data supporting the findings of this study are included within the article and its supplementary materials.

ACKNOWLEDGEMENTS

The authors thank all individuals and departments who contributed to this study and are grateful to Dr. Mark Simmerman for English language editing.

DECLARATIONS

Grants and Funding Information

This research study was funded by (i) Health Systems Research Institute (HSRI) of Thailand (63-117, 66-083) and (ii) Foundation for Cancer Care, Siriraj Hospital (R016241047).

Conflict of Interest

The authors declare no competing interests.

Registration Number of Clinical Trial

Not applicable.

Author Contributions

Conceptualization and methodology, W.T., P.T., T.S., B.S., and V.C. ; Investigation, W.T., P.T., T.S., A.T., W.R., A.M., K.T., and O.A. ; Formal analysis, W.T., A.C., P.T., T.S., N.V., and B.S. ; Visualization and writing – original draft, W.T. and N.V. ; Writing – review and editing, P.T., T.S., B.S., Y.K., and V.C. ; Funding acquisition, P.T. and V.C. ; Supervision, V.C. All authors have read and agreed to the final version of the manuscript.

Use of Artificial Intelligence

No artificial intelligence tools or technologies were utilized in the writing, analysis, or development of this research.

Supplementary Information

The online version contains supplementary material are available from the corresponding author on reasonable request.

Ethical Approval

This study was approved by the Siriraj Institutional Review Board (COA No. Si 105/2021 and Si 156/2011) and conducted in accordance with the Declaration of Helsinki. Written informed consent was obtained from all participants.

REFERENCES

1. Sung H, Ferlay J, Siegel RL, Laversanne M, Soerjomataram I, Jemal A, et al. Global Cancer Statistics 2020: GLOBOCAN Estimates of Incidence and Mortality Worldwide for 36 Cancers in 185 Countries. CA Cancer J Clin. 2021;71(3):209-49.
2. Cardoso R, Guo F, Heisser T, De Schutter H, Van Damme N, Nilbert MC, et al. Overall and stage-specific survival of patients with screen-detected colorectal cancer in European countries: A population-based study in 9 countries. Lancet Reg Health Eur. 2022;21:100458.
3. Weiser MR. AJCC 8th Edition: Colorectal Cancer. Ann Surg Oncol. 2018;25(6):1454-5.
4. Mongkhonsupphawan A, Sethalao N, Riansuwan W. Long-term Oncologic Outcomes After Curative Surgery in Stage I–III Thai Colorectal Cancer Patients. Siriraj Med J. 2022;74(11):739-46.
5. Lohsiriwat V, Rungteeranont C, Saigosoom N. Incidence and Pattern of Nodal Metastasis in Colon and Rectal Cancer: a Study of 1,012 Cases from Thailand. Siriraj Med J. 2020;72(5):386-90.
6. Hong EK, Landolfi F, Castagnoli F, Park SJ, Boot J, Van den Berg J, et al. CT for lymph node staging of Colon cancer: not only size but also location and number of lymph node count. Abdom Radiol (NY). 2021;46(9):4096-105.
7. Wang X, Cao Y, Ding M, Liu J, Zuo X, Li H, Fan R. Oncological and prognostic impact of lymphovascular invasion in Colorectal Cancer patients. Int J Med Sci. 2021;18(7):1721-9.
8. Zhang L, Deng Y, Liu S, Zhang W, Hong Z, Lu Z, et al. Lymphovascular invasion represents a superior prognostic and predictive pathological factor of the duration of adjuvant chemotherapy for stage III colon cancer patients. BMC Cancer. 2023;23(1):3.
9. Weiser MR. AJCC 8th Edition: Colorectal Cancer. Ann Surg Oncol. 2018;25(6):1454-5.
10. Acharayothin O, Thiengtrong B, Juengwiwattanakitti P, Anekwiang P, Riansuwan W, Chinswangwatanakul V, et al. Impact of Washing Processes on RNA Quantity and Quality in Patient-Derived Colorectal Cancer Tissues. Biopreserv Biobank. 2023;21(1):31-7.
11. Bioinformatics B. FastQC: a quality control tool for high throughput sequence data. 2011.
12. Ewels P, Magnusson M, Lundin S, Käller M. MultiQC: summarize analysis results for multiple tools and samples in a single report. Bioinformatics. 2016;32(19):3047-8.
13. Patro R, Duggal G, Love MI, Irizarry RA, Kingsford C. Salmon provides fast and bias-aware quantification of transcript expression. Nat Methods. 2017;14(4):417-9.
14. Chen S, Zhou Y, Chen Y, Gu J. fastp: an ultra-fast all-in-one FASTQ preprocessor. Bioinformatics. 2018;34(17):i884-i90.
15. Chen S. Ultrafast one-pass FASTQ data preprocessing, quality control, and deduplication using fastp. iMeta. 2023;2(2):e107.
16. Sherman BT, Hao M, Qiu J, Jiao X, Baseler MW, Lane HC, et al. DAVID: a web server for functional enrichment analysis and functional annotation of gene lists (2021 update). Nucleic Acids Res. 2022;50(W1):W216-w21.
17. Peixoto L, Risso D, Poplawski SG, Wimmer ME, Speed TP, Wood MA, Abel T. How data analysis affects power, reproducibility and biological insight of RNA-seq studies in complex datasets. Nucleic Acids Res. 2015;43(16):7664-74.
18. Gandolfo LC, Speed TP. RLE plots: Visualizing unwanted variation in high dimensional data. PLoS One. 2018;13(2):e0191629.
19. Molania R, Gagnon-Bartsch JA, Dobrovic A, Speed TP. A new normalization for Nanostring nCounter gene expression data. Nucleic Acids Res. 2019;47(12):6073-83.
20. Chou CK, Fan CC, Lin PS, Liao PY, Tung JC, Hsieh CH, et al. Sciellin mediates mesenchymal-to-epithelial transition in colorectal cancer hepatic metastasis. Oncotarget. 2016;7(18):25742-54.
21. Mashino K, Sadanaga N, Yamaguchi H, Tanaka F, Ohta M, Shibuta K, et al. Expression of Chemokine Receptor CCR7 Is Associated with Lymph Node Metastasis of Gastric Carcinoma1. Cancer Res. 2002;62(10):2937-41.
22. Li J, Sun R, Tao K, Wang G. The CCL21/CCR7 pathway plays

a key role in human colon cancer metastasis through regulation of matrix metalloproteinase-9. Dig Liver Dis. 2011;43(1):40-7.
23. Zou Y, Chen Y, Wu X, Yuan R, Cai Z, He X, et al. CCL21 as an independent favorable prognostic factor for stage III/IV colorectal cancer. Oncol Rep. 2013;30(2):659-66.
24. Pezeshkian Z, Nobili S, Peyravian N, Shojaee B, Nazari H, Soleimani H, et al. Insights into the Role of Matrix Metalloproteinases in Precancerous Conditions and in Colorectal Cancer. Cancers. 2021;13(24):6226.
25. Hosseinalizadeh H, Hussain QM, Poshtchaman Z, Ahsan M, Amin AH, Naghavi S, et al. Emerging insights into keratin 7 roles in tumor progression and metastasis of cancers. Front Oncol. 2023;13:1243871.
26. Li C, Cheng B, Yang X, Tong G, Wang F, Li M, et al. SOX8 promotes tumor growth and metastasis through FZD6-dependent Wnt/β-catenin signaling in colorectal carcinoma. Heliyon. 2023;9(12):e22586.
27. Fagarasan G, Fagarasan V, Bintintan VV, Dindelegan GC. The Role of Tumor-Infiltrating B Lymphocytes in Colorectal Cancer Patients: A Systematic Review of Immune Landscape Evolution. Cancers (Basel). 2025;17(18).
28. Afshar-Kharghan V. The role of the complement system in cancer. J Clin Invest. 2017;127(3):780-9.
29. Agoston EI, Acs B, Herold Z, Fekete K, Kulka J, Nagy A, et al. Deconstructing Immune Cell Infiltration in Human Colorectal Cancer: A Systematic Spatiotemporal Evaluation. Genes (Basel). 2022;13(4).
30. Lo JH, Battaglin F, Baca Y, Xiu J, Brodskiy P, Algaze S, et al. DEFB1 gene expression and the molecular landscape of colorectal cancer (CRC). J Clin Oncol. 2022;40(16 Suppl):3523.
31. Weidle UH, Rohwedder I, Birzele F, Weiss EH, Schiller C. LST1: A multifunctional gene encoded in the MHC class III region. Immunobiology. 2018;223(11):699-708.
32. Islam MS, Gopalan V, Lam AK, Shiddiky MJA. Current advances in detecting genetic and epigenetic biomarkers of colorectal cancer. Biosens Bioelectron. 2023;239:115611.
33. Bjorling E, Oksvold P, Forsberg M, Lund J, Ponten F, Uhlén M. Human protein atlas, version 2. Molecular & Cellular Proteomics. 2006;5(10):S328-S.
34. Tadijan A, Samarzija I, Humphries JD, Humphries MJ, Ambriovic-Ristov A. KANK family proteins in cancer. Int J Biochem Cell Biol. 2021;131:105903.
35. Yin JH, Elumalai P, Kim SY, Zhang SZ, Shin S, Lee M, et al. TNNC1 knockout reverses metastatic potential of ovarian cancer cells by inactivating epithelial-mesenchymal transition and suppressing F-actin polymerization. Biochem Biophys Res Commun. 2021;547:44-51.
36. Fang C, Zhang X, Li C, Liu F, Liu H. Troponin C-1 Activated by E2F1 Accelerates Gastric Cancer Progression via Regulating TGF-beta/Smad Signaling. Dig Dis Sci. 2022;67(9):4444-57.
37. Shang B, Qiao H, Wang L, Wang J. In-depth study of pyroptosis-related genes and immune infiltration in colon cancer. PeerJ. 2024;12:e18374.
38. Xu F, Kong L, Sun X, Hui W, Jiang L, Han W, et al. PFDN6 contributes to colorectal cancer progression via transcriptional regulation. eGastroenterology. 2024;2(2):e100001.
39. Peppino G, Ruiu R, Arigoni M, Riccardo F, Iacoviello A, Barutello G, et al. Teneurins: Role in Cancer and Potential Role as Diagnostic Biomarkers and Targets for Therapy. Int J Mol Sci. 2021;22(5):2321.
40. De Smedt L, Palmans S, Andel D, Govaere O, Boeckx B, Smeets D, et al. Expression profiling of budding cells in colorectal cancer reveals an EMT-like phenotype and molecular subtype switching. Br J Cancer. 2017;116(1):58-65.
41. Chang X, Chai Z, Zou J, Wang H, Wang Y, Zheng Y, et al. PADI3 induces cell cycle arrest via the Sirt2/AKT/p21 pathway and acts as a tumor suppressor gene in colon cancer. Cancer Biol Med. 2019;16(4):729-42.
42. Xu D, Ding S, Cao M, Yu X, Wang H, Qiu D, et al. A Pan-Cancer Analysis of Cystatin E/M Reveals Its Dual Functional Effects and Positive Regulation of Epithelial Cell in Human Tumors. Front Genet. 2021;12:733211.
43. Zhu X, Zhao L, Hu P. Predictive Values of Homeobox Gene A-Antisense Transcript 3 (HOXA-AS3), Cystatin 6 (CST6), and Chromobox Homolog 4 (CBX4) Expressions in Cancer Tissues for Recurrence of Early Colon Cancer After Surgery. Int J Gen Med. 2024;17:1-8.
44. Peng X, Chen X, Zhu X, Chen L. GALNT6 Knockdown Inhibits the Proliferation and Migration of Colorectal Cancer Cells and Increases the Sensitivity of Cancer Cells to 5-FU. J Cancer. 2021;12(24):7413-21.
45. Nunes L, Li F, Wu M, Luo T, Hammarström K, Torell E, et al. Prognostic genome and transcriptome signatures in colorectal cancers. Nature. 2024;633(8028):137-46.
46. Faleti OD, Gong Y, Long J, Luo Q, Tan H, Deng S, et al. TRIM72 inhibits cell migration and epithelial-mesenchymal transition by attenuating FAK/akt signaling in colorectal cancer. Heliyon. 2024;10(18):e37714.
47. Chung JH, Larsen AR, Chen E, Bunz F. A PTCH1 homolog transcriptionally activated by p53 suppresses Hedgehog signaling. J Biol Chem. 2014;289(47):33020-31.
48. Rossi M, Banskota N, Shin CH, Anerillas C, Tsitsipatis D, Yang JH, et al. Increased PTCHD4 expression via m6A modification of PTCHD4 mRNA promotes senescent cell survival. Nucleic Acids Res. 2024;52(12):7261-78.
49. Vite A, Li J, Radice GL. New functions for alpha-catenins in health and disease: from cancer to heart regeneration. Cell Tissue Res. 2015;360(3):773-83.

Selective Fetal Growth Restriction in Monochorionic Twin Pregnancy: A Review of Current Literature on Diagnostic and Therapeutic Updates

Fransiscus Octavius Hari Prasetyadi, M.D.[1,3,*], Cecilia Putri Tedyanto, M.D.[2], Vashti Saraswati, M.D.[4]

[1]Department of Obstetrics and Gynecology, Faculty of Medicine, Universitas Hang Tuah, Surabaya, Indonesia, [2]Faculty of Medicine, Universitas Katolik Widya Mandala Surabaya, Surabaya, Indonesia, [3]Division of Maternal-Fetal Medicine, Department of Obstetrics and Gynecology, Dr. Ramelan Naval Central Hospital, Surabaya, Indonesia, [4]Department of Obstetrics and Gynecology, Dr. Soetomo Academic General Hospital, Universitas Airlangga, Surabaya, Indonesia.

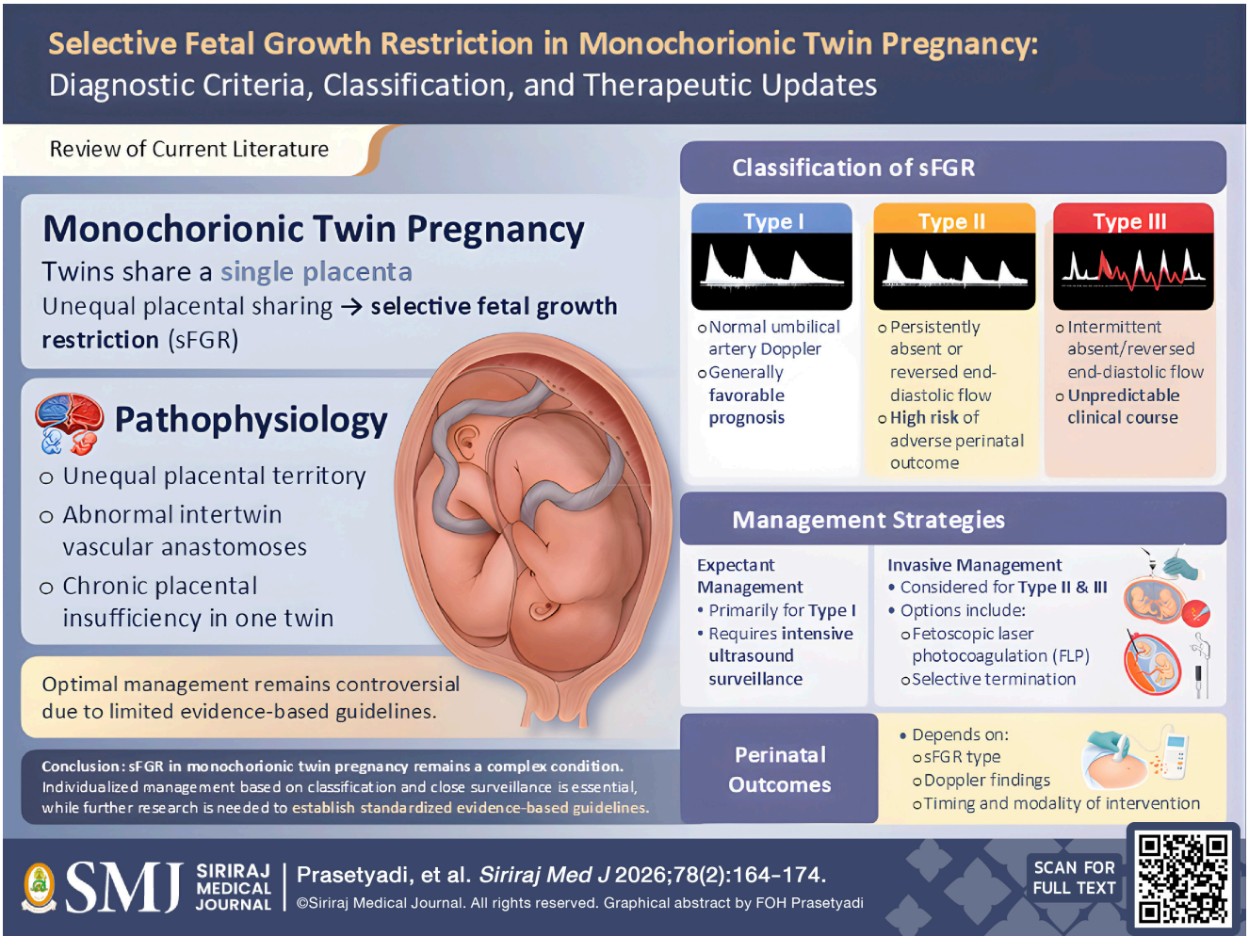

**Corresponding author: Fransiscus Octavius Hari Prasetyadi*
E-mail: frans.ohp@hangtuah.ac.id
Received 5 October 2025 Revised 15 January 2026 Accepted 15 January 2026
ORCID ID:http://orcid.org/0009-0003-1786-4809
https://doi.org/10.33192/smj.v78i2.278098

ABSTRACT

Monochorionicity refers to the condition in which twins share a single placenta. Selective fetal growth restriction (sFGR) in monochorionic (MC) twin pregnancy poses significant challenges due to its association with high risks of perinatal mortality and morbidity. Managing sFGR poses a particular challenge, as affected pregnancies require more frequent monitoring compared to uncomplicated singleton or twin pregnancies. Expectant management is typically applied for type I cases, which generally have favorable outcomes. In contrast, more severe cases (type II and III) may require invasive management, such as fetoscopic laser photocoagulation (FLP) or selective termination. However, how to best manage this complicated pregnancy remains debated, as no evidence-based guidance is currently available. This review aims to summarize the underlying pathophysiology, various diagnostic criteria, classification systems, and current management strategies for sFGR. These include the perinatal outcomes associated with expectant and invasive management in sFGR.

Keywords: Selective fetal growth restriction; monochorionic twin pregnancy; twins; birthweight discordance; fetal therapy (Siriraj Med J 2026;78(2):164-174)

INTRODUCTION

Monochorionic (MC) twin pregnancies account for approximately 30% of all twin pregnancies, with two-thirds of those MC twin pregnancies being monochorionic diamniotic (MCDA).[1] MC refers to the presence of a shared placenta between the twins, which is associated with significantly higher perinatal morbidity and mortality compared to dichorionic (DC) twins.[2] Several adverse perinatal outcomes are mainly attributable to complications related to MC, such as selective fetal growth restriction (sFGR).[3-6]

sFGR is characterized by discrepant growth between twins, resulting from unequal placental sharing.[4,5] The natural history of sFGR is influenced not only by its unique placental distribution but also by vascular anastomosis between the two fetuses.[7-9] sFGR ranges between 12 and 25% in MC twin pregnancies, depending on the diagnostic criteria.[4,6,9] More recent literature states that this particular complication occurs in approximately 10-15% of cases.[5,10]

Several adverse perinatal outcomes could result from sFGR, such as intrauterine fetal demise (IUFD), preterm birth (PTB), neonatal death (NND), and neurodevelopmental impairment (NDI).[3-6] Managing sFGR poses a certain challenge, as affected pregnancies require more frequent monitoring compared to uncomplicated singleton or twin pregnancies.[7,9,11] Moreover, if the sFGR dies in utero, the usually co-twin may suffer from brain damage or death in utero too. Proper management is necessary to avoid sFGR or prevent adverse events in the co-twin. A recent survey also highlighted significant variations in diagnosing and managing sFGR in MC twin pregnancies, emphasizing the urgent need for standardized guidelines.[12-14] Therefore, this review aims to discuss current practices in diagnosing and managing sFGR in MC twins, as well as address the ongoing lack of consensus and recommendations for optimal management in achieving better perinatal outcomes for sFGR in MC twin pregnancies.

Methodology

A comprehensive literature review was conducted following an extensive search of electronic databases, including PubMed/MEDLINE, Scopus, and Web of Science. The search strategy was performed using different combinations of keywords: selective fetal growth restriction, monochorionic, twin, and pregnancy. Studies published in a wide range of date publication that investigating the efficacy, safety, and perinatal outcomes of both expectant or invasive management for sFGR were also considered. Additionally, guidelines such as the Royal College of Obstetricians and Gynaecologists (RCOG), American College of Obstetricians and Gynecologists (ACOG), and International Society of Ultrasound in Obstetrics and Gynecology (ISUOG) were consulted to ensure comprehensive coverage of current recommendations and best practices in sFGR management.

Definition and Diagnostic Criteria of sFGR

Using varying criteria for diagnosing sFGR poses a challenge when conducting comparative studies to establish evidence-based management guidelines. Khalil et al. in 2016 define sFGR based on estimated fetal weight (EFW), where EFW is below the 10th centile for DC twins and both of EFW below the 10th centile with discordance of at least 25% for MC twins.[15] Experts then in 2019 have reached a consensus on sFGR diagnosis in MC twin

pregnancies criteria based on one of the following: (1) EFW of one twin below the 3rd centile or (2) at least two of the following four criteria: EFW of one twin below the 10th centile, abdominal circumference (AC) of one twin below the 10th centile, EFW discordance more than equal to 25%, or an umbilical artery pulsatility index (UA-PI) of the smaller twin above the 95th centile.[16] More recently, in January 2025, the previously reported guideline updated the consensus with the same diagnostic criteria, along with reaffirmation of the importance of ultrasound examination and monitoring in twin pregnancies to detect sFGR early.[17] Table 1 summarizes the practical guidelines and clinical consensus updates for the diagnostic criteria of sFGR.

The widely accepted classification of sFGR was proposed by Gratacós et al. in 2007, which divides sFGR into three types based on the umbilical artery (UA) Doppler findings of the smaller twin or co-twin. Type I is when there is positive end-diastolic flow (EDF) of both twins, type II is when there is persistent absent or reversed end-diastolic flow (AREDF) of the co-twin, and type III is when there is intermittent AREDF of the co-twin.[14]

Pathophysiology of sFGR

The pathophysiology, diagnosis, and classification of sFGR are illustrated in Fig 1. The majority of MC twins have placental vascular anastomoses, including arterio-venous (AV), arterio-arterial (AA), and veno-venous (VV). Unequitable placental sharing and intertwin vascular connections can lead to disparities in fetal nutrient and oxygen supply, contributing to sFGR.[16,18,19] This complexity is commonly associated with velamentous or eccentric umbilical cord insertion in the growth-restricted fetus and can be readily confirmed by a postpartum placental angioarchitecture study.[7] These findings influence the natural history of the smaller twin and explain why it differs from that of FGR in singleton pregnancy and DC twins.[16,20]

The degree of placental territory (PT) discordance and the number and types of vascular anastomoses in sFGR determine its clinical picture. The predominant direction and extent of blood flow exchange may impose advantageous or detrimental effects on the smaller twin. Substantial variations exist among similar cases, and thus, similar EFW discordance with the same diagnosis may exhibit varying clinical manifestations and outcomes.[16,21] The greater discordance in placental territory may be attributed to the earlier onset of sFGR, and large AA anastomoses are expected to be more prevalent.[22]

The UA is strongly influenced by intertwin blood flow exchange as reflected in its Doppler flow pattern. This parameter is considered one of the most reliable indicators for assessing the hemodynamic status of a fetus with growth restriction. A characteristic feature of MC twins, in contrast to other types of pregnancies,

TABLE 1. Updated practice guideline and consensus of the diagnostic criteria for selective fetal growth restriction in monochorionic twin pregnancies

Author	Year	Criteria Reference	Diagnostic Criteria
Khalil et al. [14]	2016	EFW	a. DC twins: EFW below the 10th centile b. MC twins: EFW below the 10th centile AND discordance of EFW more than or equal to 25%
Khalil et al. [15]	2019	AC, EFW, and UA-PI	(1) EFW of one twin below the 3rd centile OR (2) At least two of the following four criteria: a. EFW of one twin below the 10th centile b. AC of one twin below the 10th centile c. EFW discordance more than equal to 25% d. UA-PI of the smaller twin above the 95th centile
Khalil et al. [16]	2025	Same as previous	Same as previous with a reaffirmation of the importance of ultrasound examination for early detection of sFGR in twin pregnancies

Abbreviations: AC: Abdominal Circumference; EDF: End-Diastolic Flow; EFW: Estimated Fetal Weight; UA-PI: Umbilical Artery Pulsatility Index

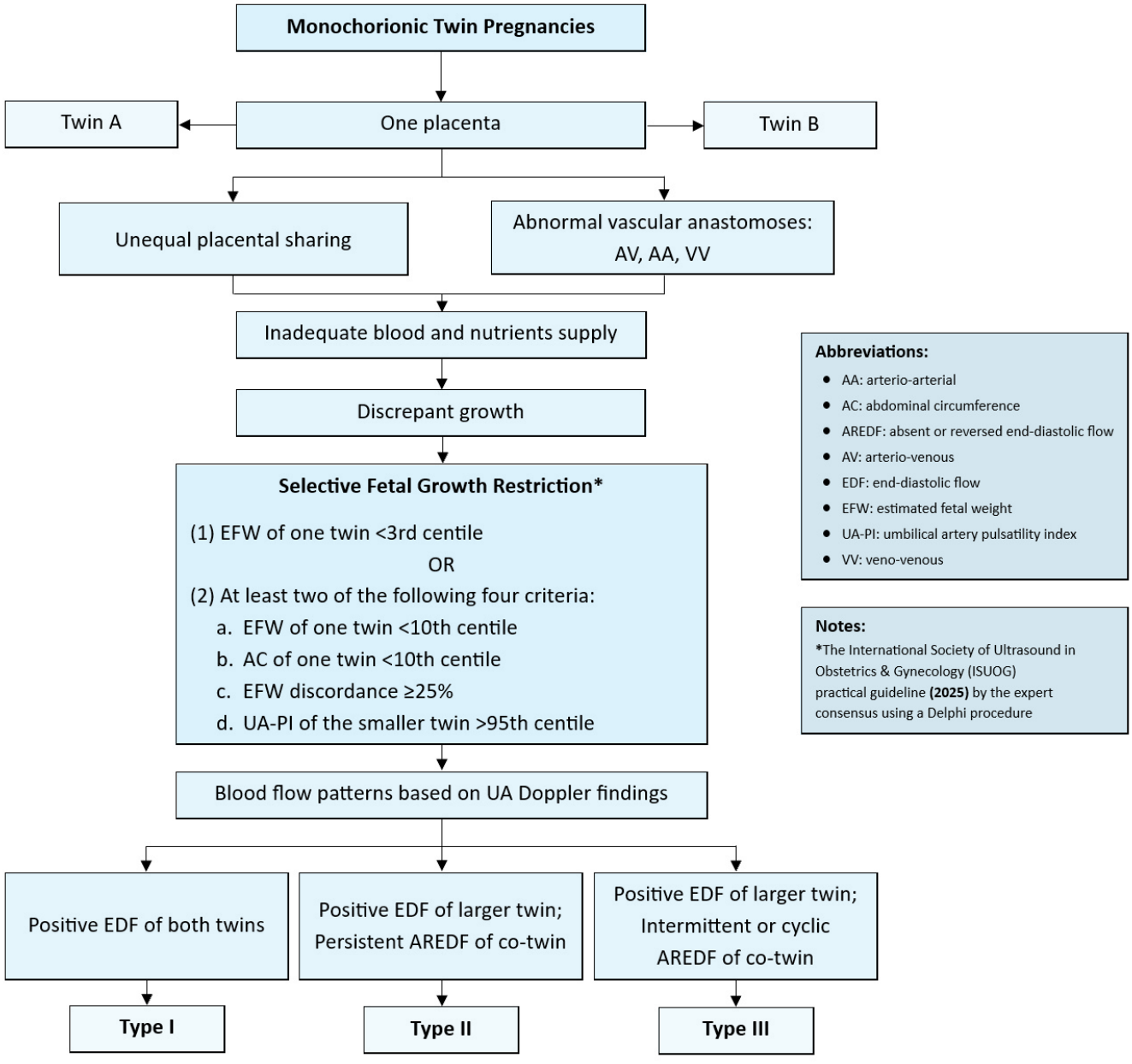

Fig 1. Pathophysiology, diagnosis, and classification of sFGR

is that the Doppler patterns mentioned can be detected very early in gestation and typically persist without significant alterations until delivery.[15] Nevertheless, a study by Batsry et al. indicated that the UA Doppler pattern may change during pregnancy, which can subsequently impact perinatal outcomes.[23]

The configuration of vascular anastomoses varied among the different study cohorts. Type I cases exhibited a proportion of anastomoses similar to that observed in uncomplicated cases. Type II cases demonstrated a lower frequency of large AA anastomoses, whereas type III cases had a significantly higher proportion of AA anastomoses, especially large AAs (more than 2 mm). These findings explain why type I has a good prognosis with a dual survival rate exceeding 90%. In contrast, type II carries the worst prognosis, and type III has an unpredictable outcome with a potentially high risk of intrauterine death.[7,24]

In addition to the more common findings of high PT discordance, large AA anastomoses, and velamentous cord insertion, type III cases also exhibit a higher prevalence of closely positioned cord insertions. In such cases, the smaller twin practically relies upon its blood supply from its co-twin via a large AA anastomosis that functions similarly to an AV anastomosis. This type of anastomosis allows a precarious hemodynamic balance that may

potentially lead to episodes of feto-fetal transfusion, which eventually puts both twins at risk of unpredictable demise and brain damage, especially to the larger twin.[7,16,25]

Expectant Management of sFGR

Several factors, such as gestational age (GA) at diagnosis, whether it is early- or late-onset, and parental preferences, should be taken into consideration in making decisions on how to manage this particular complication of MC twins clinically. However, it primarily relies on the findings from Doppler examinations and the specific type of sFGR.[26,27]

Expectant management (EM) involves intensive monitoring through serial ultrasound assessments and Doppler studies to detect fetal compromise. The goal is to prolong gestation while minimizing risks to both twins. The majority of studies recommend weekly outpatient monitoring. More frequent examinations are conducted if any clinical signs of worsening progression are observed.[8,9,28,29]

In addition to fetal biometry, Doppler examination of UA, mid-cerebral artery (MCA), and ductus venosus (DV), as well as assessments of amniotic fluid, bladder visualization, and biophysical profile (BPP), are considered key parameters in the evaluation process.[3-6] Batsry et al. performed non-stress tests twice a week, starting at 32 weeks of gestation for type I cases, continuing until termination of pregnancy at 34-35 weeks.[23] They hospitalized types II and III cases at 26-28 weeks of gestation to allow even closer surveillance. They also routinely carried out fetal brain magnetic resonance imaging (MRI) at 28-30 weeks of gestation and scheduled delivery at 31-32 weeks of gestation.

Systematic reviews have reported variations in diagnostic criteria and management options across studies, as well as other factors that may contribute to potential publication bias, such as small sample sizes, heterogeneous populations, and retrospective or non-randomized study designs.[30-32] Most of the limited number of studies recommend EM for type I sFGR with good clinical outcomes.[33,34] However, in a recent survey exploring how clinicians diagnose and manage sFGR, 79.8% of them would manage early-onset type I cases expectantly. For type II and III cases, 19.3% and 35.7% of clinicians, respectively, would opt for EM.[12]

Perinatal Outcomes Associated with Expectant Management in sFGR

(Prematurity)

It is evident that complicated pregnancies, including sFGR, are often associated with early termination, which increases the risk of prematurity. Prematurity itself poses significant consequences in terms of perinatal mortality and morbidity. The risks of respiratory distress syndrome, neonatal intensive care unit (NICU) admission, cerebral injuries, retinopathy, necrotizing enterocolitis, and sepsis undoubtedly carry significant challenges for clinicians managing sFGR. The risk of death of one or both twins has been reported in studies involving EM, which at the same time provides an opportunity to observe the natural history of the disease.[3,4,7-9]

(Survival Rates)

EM for sFGR in MC twins has resulted in poor perinatal outcomes, especially when UA abnormalities are present. The survival rate of smaller twins ranged from 58% to 89%.[34-37] A small rate of IUFD was also observed for the smaller and larger twins. When categorized into early- and late-onset sFGR, EM of early-onset cases led to lower survival rates for one or both twins. At the same time, the postnatal prognosis remained similar among live-born infants.[28,35]

(Gestational Age at Delivery)

A study of 75 MC twin pregnancies by Aquino et al. reported that type I sFGR cases were diagnosed at a later GA with less discordance in EFW.[29] These cases had significantly later GA at delivery (34.3 weeks) and higher neonatal birth weights when managed expectantly. The mean GA at delivery for type II and type III cases was 27.8 weeks and 28.3 weeks, respectively. Neonatal death was observed at a rate of 1.33%.

Another study by Sobhani et al. evaluated 73 MC twin pregnancies with an EFW discordance of 20% or more.[38] The study found no significant difference in overall adverse pregnancy outcomes between cases that developed sFGR and those that did not. Dual survival did not differ between the two groups, with a mean GA at delivery of 33 weeks. A key finding of the study was that for every additional 10% increase in EFW discordance, the likelihood of developing sFGR was nearly three times higher. However, this association did not reach statistical significance even after adjusting for multiple influential factors.

(Neurodevelopmental Outcomes)

The long-term neurodevelopmental outcomes of complicated pregnancies should not be overlooked, as they have clinical, psychological, and financial implications. EM is currently considered the standard approach for the early stages of any phenotype of complicated twin pregnancy, such as type I sFGR, with intervention considered only

if there are signs of progression suggesting an increased risk of demise or disability. Survivors who experienced the loss of a co-twin have been reported to have a 20-26% incidence of neurological impairment.[39,40]

The neurological outcomes in many studies include cerebral palsy and NDI, which is defined as a score below a certain threshold on standard evaluation tools, as well as bilateral deafness or blindness. Brain imaging, either by ultrasound or magnetic resonance imaging (MRI), is typically performed during the neonatal period (i.e., at a corrected GA of 40 weeks) to detect intraventricular haemorrhage (IVH) and cystic periventricular leukomalacia (PVL). [10]

A recent study on the survivors of various complicated MC twin pregnancies- including twin-twin transfusion syndrome (TTTS), sFGR, twin anemia-polycythemia sequence (TAPS), twin reversed arterial perfusion (TRAP) sequence, and single IUFD-concluded that adverse neurodevelopmental outcomes were independent of prematurity.[39] However, in sFGR cases, neurological injury is primarily linked to abnormal Doppler results, sIUFD, and a lower GA at delivery, with an estimated incidence of approximately 10%.[41] Regarding neurological outcomes, EM of severe forms of sFGR showed poor results.[42] Colmant et al. reported that 21% of type II sFGR survivors exhibited NDI at 6 years of age.[36] In a systematic review by Townsend et al., which included 16 observational studies, the risk of IUFD in sFGR pregnancies managed expectantly was reported as 3.1%, 16.6%, and 13.2% for types I, II, and III, respectively. No cases of type I had NND, whereas the NND rates for types II and III were 6.4% and 6.8%, respectively. Survivors without NDI were reported at 97.9%, 89.3%, and 61.9% for types I, II, and III, respectively. These data suggest that type I cases are best managed by EM. At the same time, this led to the consideration of performing invasive procedures for the other types, aimed at improving perinatal outcomes.[31]

Regarding long-term neurological outcomes, studies monitored surviving infants using comparable clinical parameters but over different follow-up periods. Most of these studies are retrospective and lack proper control groups, making them highly susceptible to bias.[31,40,41] One key advantage of EM is its non-invasive nature and its ability to allow the natural progression of pregnancy while avoiding risks associated with surgical interventions, such as preterm pre-labour rupture of membranes and infections. On the other hand, considering the pathophysiology of sFGR in MC twin pregnancies, EM may lead to a high risk of fetal demise or neurological injury in severe cases, as well as an increased risk of preterm delivery.

Invasive Management of sFGR

Invasive management (IM) aims to address the underlying pathophysiology of sFGR by either separating the vascular connections between twins, using fetoscopic laser photocoagulation (FLP), or selectively terminating the smaller twin using bipolar cord occlusion (BCO) or radiofrequency ablation (RFA), to improve outcomes for the normally growing co-twin.[20,21,26,27,43] Earlier studies applied these invasive procedures to all types of sFGR. This was also reported in a recent survey of clinicians, which showed that even for type I cases, a small portion of respondents would opt for intervention. However, most clinicians would reserve invasive procedures for more severe cases.[12]

A recent meta-analysis comprising 27 studies and 354 MC twin pregnancies evaluated both EM and IM across all types of sFGR. In cases of type I sFGR, the IUFD rate of the smaller twin following IM was 12%, whereas similar cases managed expectantly had an IUFD rate of only 2%. For type II sFGR, IM was associated with higher mortality but lower morbidity in terms of neurological outcomes compared to EM. In type III sFGR cases, IM resulted in higher mortality and morbidity in comparison to EM.[44]

Perinatal Outcomes Associated with Fetoscopic Laser Photocoagulation in sFGR

FLP involves coagulating the shared placental vessels to eliminate intertwin vascular connections, thereby addressing the underlying cause of sFGR. A 2001 study by Quintero et al. was among the first to evaluate the feasibility of applying FLP for sFGR.[45] Nevertheless, performing laser therapy for sFGR is technically more challenging due to the absence of the oligo-polyhydramnios sequence seen in TTTS.[12,33] Ishii et al. and Yamamoto et al. have reported FLP management for type II and III sFGR in cases where the smaller twin had oligohydramnios.[10,46]

(Survival Rates)

FLP has been associated with improved survival rates for the normally grown twin, especially in type II and III sFGR. However, the survival rate of the smaller twin remains lower compared to EM.[12,30-33] This phenomenon can be logically explained by examining the underlying pathophysiology of sFGR, particularly in type III cases, where the smaller twin, typically with a tiny placental territory, relies on its co-twin for vascular supply via a large anastomosis.[16,22]

(Gestational Age at Delivery)

Quintero et al. conducted a prospective randomized

study comparing EM with FLP for type II sFGR.[33] Neurodevelopmental outcomes at approximately 70-75 months were not significantly different between the two groups; however, the FLP group had a significantly later GA at birth (33.4 weeks versus 28.3 weeks, p=0.0039). This outcome was associated with the expense of a higher mortality rate of the smaller twin in the FLP group (70%), all of which occurred during the fetal period. Overall, this study was limited by its small sample size. Given the later GA at delivery in the FLP group, it could be expected that a much larger cohort would also show reduced NDI. Their previous similar study initiated the use of FLP for managing sFGR, but this was conducted before the publication of the Gratacós criteria for classifying sFGR.[45]

Another study conducted in a country where FLP is the only alternative to EM was reported by Miyadahira et al.[47] Type II (n=36) and III (n=31) sFGR cases were included. Only those with absent or reversed a-waves of ductus venosus, used as clinical worsening parameters, were assigned to FLP treatment: 83% of type II and 29% of type III cases. Perinatal outcomes were not significantly different between the EM and FLP groups; however, they were not directly comparable, as no cases in the EM group showed an abnormal Doppler waveform of the ductus venosus. Other studies have presented similar results, which could contribute to further research to determine whether interventions should be reserved only for cases that worsen.[30-33,48]

(Neurodevelopmental Outcomes)

Isolated oligohydramnios of the smaller twin in sFGR has not been frequently discussed in the literature. Yamamoto et al. proposed considering it as a clinical parameter indicating worsening sFGR in MC twin pregnancies.[10] This might alleviate some of the technical challenges in performing FLP for sFGR, particularly since the normally grown twin does not have polyhydramnios, as seen in TTTS. Another potentially beneficial situation is that the flapping intertwin membrane would pose less of an obstacle in visualizing the placental anastomotic vessels. Amnioinfusion into the normally grown twin's sac may be helpful when necessary. They reported neurological impairment at 3 years of age in 4.5% of the smaller twins and 11.6% of the larger twins, leading to the conclusion that FLP could be a beneficial management option in severe forms of sFGR, particularly when accompanied by oligohydramnios in the smaller twin.

Many studies indicate that higher survival rates without neurological impairment for larger twins in severe forms of sFGR treated with FLP often come at the expense of an increased IUFD rate in the smaller twin. These findings suggest that the unequal distribution of placental territory could not be resolved solely by interrupting the intertwin vascular connections. Nonetheless, FLP considerably lowers the likelihood of fetal demise and the risk of acute brain injury in the larger twin due to acute feto-fetal transfusion.[33,36,45,49]

The coexistence of or superimposed TTTS in sFGR can be identified when the diagnosis of sFGR is made before that of TTTS. Studies have reported that such cases are more frequent in early-onset than in late-onset sFGR and carry a worse prognosis than sFGR without TTTS. These cases would ideally be treated with FLP, as it has become the standard of care for TTTS.[9,50,51] Nevertheless, defining which precedes the other may not be possible. A systematic review comparing TTTS cases with and without sFGR treated with FLP revealed that the coexistence of both conditions had a 50% increase in fetal loss and neurological morbidity. These adverse perinatal outcomes were significantly more prevalent in the donor twin.[52] The potential risks associated with the FLP procedure, such as preterm pre-labour rupture of membranes (PPROM), separation of the chorioamniotic membrane, accidental septostomy, uterine hemorrhage, placental abruption, and clinical chorioamnionitis, must be thoroughly discussed with parents or couples in advance.[9]

Perinatal Outcomes Associated with Selective Termination in sFGR

Selective termination via BCO, RFA, or more rarely, microwave ablation (MWA) has been recommended for consideration in severe cases of sFGR where the survival of the smaller twin is unlikely and poses a significant risk to its co-twin. This technique aims to prevent acute feto-fetal transfusion following episodes of hypotension or the demise of the smaller twin, thereby improving survival and neurological outcomes for the larger twin.[31,36]

Parra-Cordero et al. reported a series of 90 type II and III sFGR cases managed with BCO.[53] They found that 92.9% of cases resulted in more than 32 weeks of delivery, with a 93.3% survival rate for the larger twin. Townsend et al. reported in their meta-analysis that type I sFGR cases managed by selective termination, either by RFA or BCO, resulted in 100% survival, with no NDI found among these neonates. In type II sFGR, IUFD, and NND of the larger twin, the rates were 5% and 3.7%, respectively. The majority (90.6%) of survivors had no NDI. Selective termination for type III resulted in a 5.2% NND rate of the larger twin, with 98.8% of survivors having no NDI.[31] In terms of long-term neurodevelopmental outcomes

at 6 years of age, 24% of surviving larger twins had NDI.[36] In cases where TTTS coexists with sFGR, which is expected to lead to worse perinatal outcomes, selective termination did not result in a significant difference compared to sFGR cases alone.[54]

The management of sFGR involves complex decision-making, particularly when considering invasive interventions such as selective termination. Given the emotional toll of these decisions, psychological support for parents is crucial. However, this option is not always feasible or available, as it raises ethical concerns and may not be acceptable to all patients or healthcare providers. In some countries, selective termination is illegal, making this type of management unavailable.[55-57]

Current Guidelines and Future Directions

The application of the Delphi procedure-based consensus and Gratacós classification in more recent studies has been a significant game-changer, leading to greater consistency in diagnosing sFGR.[16,17] This uniformity is likely to reduce potential bias in gathering further evidence-based comparative data, particularly regarding the natural history of the disease. However, questions remain regarding the use of the Gratacós classification in managing sFGR. GA at diagnosis, ductus venosus Doppler findings, and the presence of superimposed TTTS may impact prognosis. The potential alterations in the smaller twin's UA Doppler waveform along the course of pregnancy lead to variations in determining which data should be used as the basis for diagnosis, whether the first, the most frequent, or the last findings before IUFD or termination of pregnancy.[19,23,29,32,58] Therefore, it is reasonable to propose modifications to the classification by incorporating these parameters, followed by validation studies.[59]

Several limitations were observed in the overall included studies. First, variation in surveillance protocols across studies influences the outcomes of the management approaches. Variations in management protocols across centres, along with the diverse diagnostic criteria used in previous studies, should prompt a large, well-designed multicentre study. Second, the GA at diagnosis also affects the selection of management between EM and IM; therefore, it also affects the management outcomes. As previously mentioned, management has largely relied on expert opinions, as there is still no consensus. The lack of robust evidence to create reliable guidelines is understandable, given the rarity and complexity of the disease. Guidelines from prominent scientific organizations, such as the ACOG, RCOG, and ISUOG, clearly emphasize this issue.[17,60-62] There was also a limitation regarding the management approaches, especially in an operator-dependent procedure such as FLP. The outcomes of this management approach depend on the center's ability and expertise.

EM means closely monitoring the pregnancy and terminating it in a timely manner when deterioration occurs. In other words, no active intervention is undertaken despite a 15% risk of fetal demise and 26% risk of neurological injury in the surviving co-twin. These potential risks pose ethical challenges and psychological burdens to parents.[36,63]

IM consists of FLP and selective termination. FLP has not been proven to be significantly effective. To date, no large, robust, randomized trial has compared all management options for sFGR. Another challenge in performing FLP is that it is technically more difficult than its use for TTTS, which is considered the standard treatment. Selective termination of the smaller twin allows the larger twin to develop normally, but, as mentioned before, it may not be an option for some parents and clinicians. It may be perceived as the 'deliberate killing' of the unfortunate twin and immediately eliminates its chance of survival.[64,65]

CONCLUSIONS

The management of MC twins affected by sFGR remains a challenging clinical scenario. It relies primarily on expert opinion, which significantly impacts the likelihood of adverse perinatal outcomes. EM is appropriate for milder forms of sFGR (type I), while IM or interventions are warranted in severe cases to optimize outcomes for the normally grown twin. Early delivery can reduce mortality, but it is also linked to increased short- and long-term morbidity. Individualized care, guided by the type of sFGR and parental preferences, is essential for achieving the best possible outcomes. Despite these challenges, further studies are needed to refine management strategies and explore additional innovative therapeutic options. Robust, well-designed multicenter RCTs comparing EM versus IM strategies are essential, as are further investigations into the long-term neurodevelopmental outcomes of survivors using more uniform parameters.

Data Availability Statement

The data underlying this study are available in the published article.

ACKNOWLEDGEMENT

None

DECLARATIONS

Grants and Funding Information

This study received no external funding.

Conflict of Interest

The authors report no conflict of interest in this study.

Registration number of clinical trial

Not applicable.

Author Contributions

Conceptualization, writing – original draft, FOHP.; Writing – review & editing, FOHP, CPT, VS. All authors have read and agreed to the final version of the manuscript.

Use of artificial intelligence

This study does not use any artificial intelligence assistant.

REFERENCES

1. Kanokpongsakdi S. Pre-operative diagnosis of alive twin tubal pregnancy. Siriraj Med J. 2020;62(2):71-72.
2. Vitthala S, Gelbaya TA, Brison DR, Fitzgerald CT, Nardo LG. The risk of monozygotic twins after assisted reproductive technology: a systematic review and meta-analysis. Hum Reprod Update. 2009;15(1):45-55.
3. Lewi L. Monochorionic diamniotic twin pregnancies. Am J Obstet Gynecol MFM. 2022;4(2S):100501.
4. Lewi L, Gucciardo L, Huber A, Jani J, Van Mieghem T, Doné E, et al. Clinical outcome and placental characteristics of monochorionic diamniotic twin pairs with early- and late-onset discordant growth. Am J Obstet Gynecol. 2008;199(5):511.e1-7.
5. Lewi L, Jani J, Blickstein I, Huber A, Gucciardo L, Van Mieghem T, et al. The outcome of monochorionic diamniotic twin gestations in the era of invasive fetal therapy: a prospective cohort study. Am J Obstet Gynecol. 2008;199(5):514.e1-8.
6. Valsky DV, Eixarch E, Martinez JM, Gratacós E. Selective intrauterine growth restriction in monochorionic diamniotic twin pregnancies. Prenat Diagn. 2010;30(8):719-26.
7. Lewi L, Deprest J, Hecher K. The vascular anastomoses in monochorionic twin pregnancies and their clinical consequences. Am J Obstet Gynecol. 2013;208(1):19-30.
8. Lewi L, Gucciardo L, Van Mieghem T, de Koninck P, Beck V, Medek H, et al. Monochorionic diamniotic twin pregnancies: natural history and risk stratification. Fetal Diagn Ther. 2010; 27(3):121-33.
9. Curado J, Sileo F, Bhide A, Thilaganathan B, Khalil A. Early- and late-onset selective fetal growth restriction in monochorionic diamniotic twin pregnancy: natural history and diagnostic criteria. Ultrasound Obstet Gynecol. 2020;55(5):661-6.
10. Yamamoto R, Ozawa K, Wada S, Sago H, Nagasaki S, Takano M, et al. Infant outcome at 3 years of age of monochorionic twins with Type-II or -III selective fetal growth restriction and isolated oligohydramnios that underwent fetoscopic laser photocoagulation. Ultrasound Obstet Gynecol. 2024;63:758-63.
11. Bennasar M, Eixarch E, Martinez JM, Gratacós E. Selective intrauterine growth restriction in monochorionic diamniotic twin pregnancies. Semin Fetal Neonatal Med. 2017;22(6):376-82.
12. Prasad S, Khalil A, Kirkham JJ, Sharp A, Woolfall K, Mitchell TK, et al; FERN Study Team. Diagnosis and management of selective fetal growth restriction in monochorionic twin pregnancies: A cross-sectional international survey. BJOG. 2024;131(12):1684-93.
13. Sorrenti S, Khalil A, D'Antonio F, D'Ambrosio V, Zullo F, D'Alberti E, et al. Counselling in Fetal Medicine: Complications of Monochorionic Diamniotic Twin Pregnancies. J Clin Med. 2024;13(23):7295.
14. Gratacós E, Lewi L, Muñoz B, Acosta-Rojas R, Hernandez-Andrade E, Martinez JM, et al. A classification system for selective intrauterine growth restriction in monochorionic pregnancies according to umbilical artery Doppler flow in the smaller twin. Ultrasound Obstet Gynecol. 2007;30(1):28-34.
15. Khalil A, Rodgers M, Baschat A, Bhide A, Gratacos E, Hecher K, et al. ISUOG Practice Guidelines: role of ultrasound in twin pregnancy. Ultrasound Obstet Gynecol. 2016;47(2):247-63.
16. Khalil A, Beune I, Hecher K, Wynia K, Ganzevoort W, Reed K, et al. Consensus definition and essential reporting parameters of selective fetal growth restriction in twin pregnancy: a Delphi procedure. Ultrasound Obstet Gynecol. 2019;53(1):47-54.
17. Khalil A, Sotiriadis A, Baschat A, Bhide A, Gratacós E, Hecher K, et al. ISUOG Practice Guidelines (updated): role of ultrasound in twin pregnancy. Ultrasound Obstet Gynecol. 2025;65(2):253-76.
18. Lewi L, Cannie M, Blickstein I, Jani J, Deprest J. Placental sharing and birth weight in monochorionic twins: the critical role of 'life supporting' vascular anastomoses. J Soc Gynecol Invest. 2006;13(Suppl):A76.
19. Groene SG, Openshaw KM, Jansén-Storbacka LR, Slaghekke F, Haak MC, Heijmans BT, et al. Impact of placental sharing and large bidirectional anastomoses on birthweight discordance in monochorionic twins: a retrospective cohort study in 449 cases. Am J Obstet Gynecol. 2022;227(5):755.e1-e10.
20. Townsend R, Khalil A. Fetal growth restriction in twins. Best Pract Res Clin Obstet Gynaecol. 2018;49:79-88.
21. Kozinszky Z, Surányi A. The High-Risk Profile of Selective Growth Restriction in Monochorionic Twin Pregnancies. Medicina (Kaunas). 2023;59(4):648.
22. Wang X, Li L, Yuan P, Zhao Y, Wei Y. Placental characteristics in different types of selective fetal growth restriction in monochorionic diamniotic twins. Acta Obstet Gynecol Scand. 2021;100(9):1688-93.
23. Batsry L, Matatyahu N, Avnet H, Weisz B, Lipitz S, Mazaki-Tovi S, et al. Perinatal outcome of monochorionic diamniotic twin pregnancy complicated by selective intrauterine growth restriction according to umbilical artery Doppler flow pattern: single-center study using strict fetal surveillance protocol. Ultrasound Obstet Gynecol. 2021;57(5):748-55.
24. Spekman JA, Ros E, Lewi L, Slaghekke F, Verweij EJTJ, Noll ATR, et al. Proximate cord insertion in monochorionic twins with selective fetal growth restriction. Am J Obstet Gynecol MFM. 2025;7(2):101598.
25. Murakoshi T, Quintero RA, Bornick PW, Allen MH. In vivo endoscopic assessment of arterioarterial anastomoses: insight into their hemodynamic function. J Matern Fetal Neonatal

Med. 2003;14(4):247-55.
26. Mazer Zumaeta A, Gil MM, Rodriguez-Fernandez M, Carretero P, Ochoa JH, Casanova MC, et al. Selective fetal growth restriction in monochorionic diamniotic twins: diagnosis and management. Maternal Fetal Med. 2022;4(4):268-75.
27. Chalouhi GE, Marangoni MA, Quibel T, Deloison B, Benzina N, Essaoui M, et al. Active management of selective intrauterine growth restriction with abnormal Doppler in monochorionic diamniotic twin pregnancies diagnosed in the second trimester of pregnancy. Prenat Diagn. 2013;33(2):109-15.
28. Wang Y, Shi H, Wang X, Yuan P, Wei Y, Zhao Y. Early- and late-onset selective fetal growth restriction in monochorionic twin pregnancy with expectant management. J Gynecol Obstet Hum Reprod. 2022;51(4):102314.
29. Aquino C, Rodrigues Baião AE, de Carvalho PRN. Perinatal Outcome of Selective Intrauterine Growth Restriction in Monochorionic Twins: Evaluation of a Retrospective Cohort in a Developing Country. Twin Res Hum Genet. 2021;24(1):37-41.
30. Buca D, Pagani G, Rizzo G, Familiari A, Flacco ME, Manzoli L, et al. Outcome of monochorionic twin pregnancy with selective intrauterine growth restriction according to umbilical artery Doppler flow pattern of smaller twin: systematic review and meta-analysis. Ultrasound Obstet Gynecol. 2017;50(5):559-68.
31. Townsend R, D'Antonio F, Sileo FG, Kumbay H, Thilaganathan B, Khalil A. Perinatal outcome of monochorionic twin pregnancy complicated by selective fetal growth restriction according to management: systematic review and meta-analysis. Ultrasound Obstet Gynecol. 2019;53(1):36-46.
32. El Emrani S, Groene SG, Verweij EJ, Slaghekke F, Khalil A, van Klink JMM, et al. Gestational age at birth and outcome in monochorionic twins with different types of selective fetal growth restriction: A systematic literature review. Prenat Diagn. 2022;42(9):1094-110.
33. Quintero R, Kontopoulos E, Williams ME, Sloop J, Vanderbilt D, Chmait RH. Neurodevelopmental outcome of monochorionic twins with selective intrauterine growth restriction (SIUGR) type II: laser versus expectant management. J Matern Fetal Neonatal Med. 2021;34(10):1513-21.
34. Rustico MA, Consonni D, Lanna M, Faiola S, Schena V, Scelsa B, et al. Selective intrauterine growth restriction in monochorionic twins: changing patterns in umbilical artery Doppler flow and outcomes. Ultrasound Obstet Gynecol. 2017;49(3):387-93.
35. Ishii K, Murakoshi T, Takahashi Y, Shinno T, Matsushita M, Naruse H, et al. Perinatal outcome of monochorionic twins with selective intrauterine growth restriction and different types of umbilical artery Doppler under expectant management. Fetal Diagn Ther. 2009;26(3):157-61.
36. Colmant C, Lapillonne A, Stirnemann J, Belaroussi I, Leroy-Terquem E, Kermovant-Duchemin E, et al. Impact of different prenatal management strategies in short- and long-term outcomes in monochorionic twin pregnancies with selective intrauterine growth restriction and abnormal flow velocity waveforms in the umbilical artery Doppler: a retrospective observational study of 108 cases. BJOG. 2021;128(2):401-9.
37. Weisz B, Hogen L, Yinon Y, Gindes L, Shrim A, Simchen M, et al. Perinatal outcome of monochorionic twins with selective IUGR compared with uncomplicated monochorionic twins. Twin Res Hum Genet. 2011;14(5):457-62.
38. Sobhani NC, Sparks TN, Gosnell KA, Rand L, Gonzalez JM, Feldstein VA. Outcomes of Monochorionic, Diamniotic Twin Pregnancies with Prenatally Diagnosed Intertwin Weight Discordance. Am J Perinatol. 2021;38(7):649-56.
39. Prasad S, Beg S, Badran D, Masciullo L, Huddy C, Khalil A. Neurodevelopmental outcome in complicated twin pregnancy: prospective observational study. Ultrasound Obstet Gynecol. 2024;63(2):189-97.
40. Hillman SC, Morris RK, Kilby MD. Co-twin prognosis after single fetal death: a systematic review and meta-analysis. Obstet Gynecol. 2011;118(4):928-40.
41. Inklaar MJ, van Klink JM, Stolk TT, van Zwet EW, Oepkes D, Lopriore E. Cerebral injury in monochorionic twins with selective intrauterine growth restriction: a systematic review. Prenat Diagn. 2014;34(3):205-13.
42. Ishii K, Murakoshi T, Sago H. Adverse outcome in monochorionic twins with selective intrauterine fetal growth restriction in the presence of abnormal umbilical artery Doppler and severe oligohydramnios. J Obstet Gynaecol Res. 2012;38(10):1271.
43. Shanahan MA, Bebbington MW. Monochorionic Twins: TTTS, TAPS, and Selective Fetal Growth Restriction. Clin Obstet Gynecol. 2023;66(4):825-40.
44. Mustafa HJ, Javinani A, Heydari MH, Aghajani F, Saldana AV, Rohita DK, et al. Perinatal Outcomes of Monochorionic Twin Pregnancies with Selective Fetal Growth Restriction According to Umbilical Artery Dopplers and Fetal intervention: a Systematic Review and Meta-analysis. PREPRINT (Version 1) available at Research Square. 2024.
45. Quintero RA, Bornick PW, Morales WJ, Allen MH. Selective photocoagulation of communicating vessels in the treatment of monochorionic twins with selective growth retardation. Am J Obstet Gynecol. 2001;185(3):689-96.
46. Ishii K, Nakata M, Wada S, Murakoshi T, Sago H. Feasibility and preliminary outcomes of fetoscopic laser photocoagulation for monochorionic twin gestation with selective intrauterine growth restriction accompanied by severe oligohydramnios. J Obstet Gynaecol Res. 2015;41(11):1732-7.
47. Miyadahira MY, Brizot ML, Carvalho MHB, Biancolin SE, Machado RCA, Krebs VLJ, et al. Type II and III Selective Fetal Growth Restriction: Perinatal Outcomes of Expectant Management and Laser Ablation of Placental Vessels. Clinics (Sao Paulo). 2018;73:e210.
48. Nassr AA, Hessami K, Corroenne R, Sanz Cortes M, Donepudi R, Espinoza J, et al. Outcome of laser photocoagulation in monochorionic diamniotic twin pregnancy complicated by Type-II selective fetal growth restriction. Ultrasound Obstet Gynecol. 2023;62(3):369-73.
49. Peeva G, Bower S, Orosz L, Chaveeva P, Akolekar R, Nicolaides KH. Endoscopic Placental Laser Coagulation in Monochorionic Diamniotic Twins with Type II Selective Fetal Growth Restriction. Fetal Diagn Ther. 2015;38(2):86-93.
50. Uribe KA, Birk A, Shantz C, Miller JL, Kush ML, Olson S, et al. Resolution of selective fetal growth restriction after laser surgery for twin-to-twin transfusion syndrome can be predicted by predisease growth discordance. Ultrasound Obstet Gynecol. 2025;65(1):47-53.
51. Ortiz JU, Guggenberger J, Graupner O, Ostermayer E, Kuschel B, Lobmaier SM. The Outcome after Laser Therapy of Monochorionic Twin Pregnancies Complicated by Twin-Twin Transfusion Syndrome with Coexistent Selective Fetal Growth Restriction.

J Clin Med. 2024;13(8):2432.
52. D'Antonio F, Marinceu D, Prasad S, Eltaweel N, Khalil A. Outcome following laser surgery of twin-twin transfusion syndrome complicated by selective fetal growth restriction: systematic review and meta-analysis. Ultrasound Obstet Gynecol. 2023;62(3):320-7.
53. Parra-Cordero M, Bennasar M, Martínez JM, Eixarch E, Torres X, Gratacós E. Cord Occlusion in Monochorionic Twins with Early Selective Intrauterine Growth Restriction and Abnormal Umbilical Artery Doppler: A Consecutive Series of 90 Cases. Fetal Diagn Ther. 2016;39(3):186-91.
54. Rahimi-Sharbaf F, Shirazi M, Golshahi F, Salari Z, Haghiri M, Ghaemi M, Feizmahdavi H. Comparison of Prenatal and Neonatal Outcomes of Selective Fetal Growth Restriction in Monochorionic Twin Pregnancies with or Without Twin-to-Twin Transfusion Syndrome After Radiofrequency Ablation. Iran J Med Sci. 2022;47(5):433-9.
55. Evans MI, Johnson MP, Quintero RA, Fletcher JC. Ethical issues surrounding multifetal pregnancy reduction and selective termination. Clin Perinatol. 1996;23(3):437-51.
56. Valsky DV, Eixarch E, Martinez JM, Crispi F, Gratacós E. Selective intrauterine growth restriction in monochorionic twins: pathophysiology, diagnostic approach and management dilemmas. Semin Fetal Neonatal Med. 2010;15(6):342-8.
57. Javinani A, Papanna R, Van Mieghem T, Moldenhauer JS, Johnson A, Lopriore E, et al. Selective termination: a life-saving procedure for complicated monochorionic gestations. J Perinat Med. 2024;53(3):305-10.
58. Chen L, Zhou W, Zhang Y, Zhao W, Wen H. Natural evolution and risk factors for adverse outcome in selective intrauterine growth restriction under expectant management: A retrospective observational study. Int J Gynaecol Obstet. 2023;162(2):569-77.
59. Khalil A, Liu B. Controversies in the management of twin pregnancy. Ultrasound Obstet Gynecol. 2021;57(6):888-902.
60. American College of Obstetricians and Gynecologists Committee on Practice Bulletins-Obstetrics; Society for Maternal-Fetal Medicine; ACOG Joint Editorial Committee. ACOG Practice Bulletin #56: Multiple gestation: complicated twin, triplet, and high-order multifetal pregnancy. Obstet Gynecol. 2004;104(4):869-83.
61. Kilby MD, Bricker L, Royal College of Obstetricians and Gynaecologists. Management of Monochorionic Twin Pregnancy Green-Top Guideline No. 51 (2024 Partial Update). BJOG. 2025;132(6):e98-e129.
62. Khalil A, Prasad S, Woolfall K, Mitchell TK, Kirkham JJ, Yaghi O, et al. FERN: is it possible to conduct a randomised controlled trial of intervention or expectant management for early-onset selective fetal growth restriction in monochorionic twin pregnancy - protocol for a prospective multicentre mixed-methods feasibility study. BMJ Open. 2024;14(8):e080021.
63. Ashcroft R, Woolfall K, Prasad S, Khalil A. Ethical considerations of a randomised controlled trial of fetal intervention versus expectant management in monochorionic twin pregnancies with early-onset selective fetal growth restriction. BJOG. 2025;132(6):694-7.
64. Mitchell TK, Popa M, Ashcroft RE, Prasad S, Sharp A, Carnforth C, FERN study team, et al. Balancing key stakeholder priorities and ethical principles to design a trial comparing intervention or expectant management for early-onset selective fetal growth restriction in monochorionic twin pregnancy: FERN qualitative study. BMJ Open. 2024;14(8):e080488.
65. Khalil A, Thilaganathan B. Selective fetal growth restriction in monochorionic twin pregnancy: a dilemma for clinicians and a challenge for researchers. Ultrasound Obstet Gynecol. 2019;53(1):23-25.
66. Kanokpongsakdi S. Pre-operative diagnosis of alive twin tubal pregnancy. Siriraj Med J. 2020;62(2):71-72.